

ERASMUS UNIVERSITY ROTTERDAM

ECONOMETRICS & MANAGEMENT SCIENCE

THESIS QUANTITATIVE FINANCE

Comparing the Block Maxima and Peak over Threshold
method in quantifying risk under serial dependence

Author:

M.V. NUIS

Supervisor:

C. ZHOU

Student Number:

361830

Second Assessor:

Abstract

This thesis compares the Block Maxima and Peak over Threshold methods in estimating the Value-at-Risk, for portfolios constructed from assets with different levels of serial dependence, volatility clustering and cross-sectional dependence. The serial dependence is modeled via an ARMA-GARCH process with volatility clustering, while the cross-sectional dependence is modeled by a Clayton copula. The results show that the Peak over Threshold outperforms the Block Maxima for lower levels of serial dependence. For higher levels of serial dependence, especially after introducing volatility clustering, the Block Maxima is the superior method. The presence of cross-sectional dependence has no significant effect on either method. The back-testing result of estimating the Value-at-Risk on a portfolio consisting of European stocks and bonds is in favor of the Block Maxima method.

Keywords: Peak over Threshold, Block Maxima, Value-at-Risk, ARMA, GARCH, Clayton copula, serial dependence, RMSE

Contents

1	Introduction	2
2	Literature	6
3	Methodology	9
3.1	Value-at-Risk	9
3.2	Extreme Value Theory	9
3.3	Block Maxima	13
3.4	Peak over Threshold	18
3.5	Simulation Setup	21
3.6	Simulation Evaluation	24
3.7	Financial Application Evaluation	25
4	Empirical Data	26
4.1	Preliminary	26
4.2	Descriptive Statistics	28
5	Simulation	30
5.1	The choice of k	30
5.2	Serial dependence: ARMA	32
5.3	Volatility Clustering: GARCH	36
5.4	Cross-sectional dependence: Clayton copula	40
6	Financial Application	45
7	Conclusion	48
	References	51
A	Appendices	54
A.1	Maximum Domain of Attraction Examples	54
A.2	Slowly and regularly varying functions	55
A.3	Tables and Graphs	56

1 Introduction

A major aspect of quantitative risk management focuses on measuring risk. Over the years, this has resulted in the development of a range of risk measures. The focus of this paper is primarily on the Value-at-Risk (VaR). The VaR measure is widely accepted within the banking industry as the preferred method for quantifying market risk. It plays an important role in the Basel Accords because the capital requirements of the banks are dependent on market risk. The accuracy of the VaR estimation is of great importance: an overestimation of the risk can lead to unnecessarily large capital allocations which could have been used elsewhere, while an underestimation could lead to extreme losses or even bankruptcy. However, during the financial crisis of 2008, it became apparent that this popular risk measure was not without flaws. As with many risk measures, the calculation of the VaR is based on assumptions which are often invalid with financial data. Another point of criticism is that the VaR is not able to implement other risk factors that influence the market risk, such as liquidity, cash flow, counter-party and political risk. Hence, improving the estimation of the VaR is not only relevant from an academic standpoint, but is also valuable to the financial industry.

This paper will calculate the VaR for a diversified investment portfolio in European stocks and bonds. However, this portfolio contains serial dependence, which is generally the case for financial returns, and violates one of the assumptions used in calculating the VaR: that the observed data are independent and identically distributed (IID). The existing methods for calculating the VaR are analyzed and compared after allowing for serial dependence. The comparison of the traditional VaR and the VaR after correcting for serial dependency is particularly interesting in times of extreme values, such as the 2008 financial crisis.

Extreme Value Theory (EVT) has become increasingly popular in financial risk management because it only focuses on the distribution of the tail rather than the whole distribution. Within EVT, the two dominant methods to estimate tail probabilities are the Block Maxima (BM) and the Peak over Threshold (POT) approach. Both methods attempt to derive the limiting distribution of extreme values, but they differ in how the

extreme values are chosen. The BM method divides the sample set into blocks of equal size and only considers the maximum values of these blocks, whereas the POT method only uses the extreme values that exceed a certain threshold. Both the BM and POT methods provide ways to infer high quantiles of the original data sample using the estimated distribution of the tails. However, one of the assumptions involved in estimating the VaR using the classical POT or BM method is that the data sample is IID or exhibits weak dependence.

Various studies have analyzed the application of the POT or BM method on serially dependent observations to estimate the tail distributions and calculate the VaR. It has become apparent that both methods are able to deal with the serial dependency, albeit with both advantages and disadvantages. Drees (2003) demonstrated that the POT can still be used in the same approach as in the IID case to estimate the VaR when dealing with a serially dependent data sample and is therefore straightforward to implement. However, the estimates usually bear a higher asymptotic variance. The estimation of the VaR with serially dependent data can also be achieved using the BM method. In contrast to the POT method, the asymptotic properties of the estimators actually remain valid as the block maxima itself is arguably IID. However, McNeil (1998) showed that estimating the VaR using BM requires the additional step of estimating the extremal index first. The extremal index is a parameter that characterizes the serial dependence as it indicates the clustering of extreme values; see Leadbetter (1983), for example.

Theoretically, it seems that the advantages and disadvantages of using the POT and BM approaches to estimate the VaR under serially correlated data are roughly balanced. This conjecture needs to be proven, hence the following research question:

“Which method is empirically the most appropriate for estimating high quantiles under serial dependence?”

This research paper compares the BM and POT methods and aims to determine which method is the most appropriate for estimating high quantiles under serial dependence. The research is based on a simulation study and an empirical study. We begin with the simula-

tion in order to fully analyze the performance of both methods on different levels of serial dependence. The data is generated using a Monte Carlo simulation in which the level of serial dependence is controlled. The simulation stays close to the empirical application by generating two time-series resembling stock and bond returns, respectively. We first simulate two Autoregressive Moving Average (ARMA) processes to mimic the univariate return series of the stock and bond returns, each containing serial dependence. We then use a Generalized Autoregressive Conditional Heteroskedasticity (GARCH) model for the innovations of each time-series to allow for the volatility clustering that is often present in financial returns. On each given day, the pair of innovations from the two time-series, are simulated from a Clayton copula model to allow for cross-sectional dependence. This allows us to incorporate conditional tail dependency, which is in line with the joint distribution of the returns of a stock and bond portfolio. The BM and POT methods are then applied to estimate the 99.99% VaR of the portfolio which invests in the two return series with equal weighting. To estimate the VaR at such a high probability level, it is necessary to estimate the risk measures using EVT because a non-parametric estimation is not possible. The estimated VaR for every simulation sample is then compared with the true VaR which is obtained via a pre-simulation. To evaluate the BM and POT methods for each risk measure estimate, the root mean squared error (RMSE) and root mean squared percentage error (RMSPE) are calculated over the simulated samples.

In the empirical study, we apply the same BM and POT methods as in the simulation study to an investment portfolio that closely resembles the typical portfolio of a large bank. To evaluate the VaR estimates, we use the binomial method; see Christoffersen (1998). The binomial method is based on the number of observations that exceed the estimated VaR. Under the null hypothesis, the number of observations exceeding the 99.99% VaR follows a binomial distribution where the probability of success equals 0.01%.

For the empirical application, we consider an investment portfolio consisting of the STOXX Europe 600 index and the Barclays Euro Aggregate Treasury Total Return Index, to represent the stock and bond markets respectively. The data consists of daily observations starting from January 1, 2000 until December 31, 2017. This period is interesting as it contains two major financial crises: the burst of the dot-com bubble and the 2008

global financial crisis.

The simulation application revealed that for lower levels of serial dependence, the BM method is more accurate than POT when excluding volatility clustering and cross-sectional dependence. However, the POT method ultimately outperformed the BM method for extreme levels of serial dependence. Introducing volatility clustering had a major negative impact on both methods: a clear linear trend in error could be seen when the level of volatility clustering was increased. However, the POT method seemed more affected at high levels of volatility clustering than the BM method. Cross-sectional dependence had no visible effect on estimating the VaR for either method. The financial application demonstrated that both methods were fairly comparable in terms of coverage and that both methods failed to reject the null hypothesis under the binomial method.

The remainder of this paper is structured as follows. Section 2 discusses the current literature. The methodology is outlined in section 3, where the POT and BM methods are discussed and the simulation setup is described. Section 4 closely examines the empirical data. The results of the simulation are considered and outlined in Section 5. The performance of both methods in the financial application is analyzed and discussed in Section 6, before Section 7 concludes the research.

2 Literature

EVT is a field of research within statistics that primarily focuses on the stochastic behavior of extreme values in a process. The history of EVT dates all the way back to Bernoulli in 1709 as demonstrated by Kotz and Nadarajah (2000). Over the years, EVT has evolved and currently relies mainly on two distinct methods to model the distribution of extreme values: the BM method and the POT method. Of the two, the BM method has been established for longer. Fundamental to the BM method is the probability theory of maxima, and this needs to be discussed first. It was first mentioned by Fisher and Tippett (1928), who indicated that the limiting behavior of maxima can be described by a set of three extreme value distributions: the Gumbel, Fréchet and the inverse Weibull distributions.

Denote X_1, \dots, X_n as the IID observations with cumulative distribution function (CDF) F and $M_n = \max(X_1, \dots, X_n)$. Then, assume that

$$\Pr\left(\frac{M_n - b_n}{a_n} \leq x\right) = F^n(a_n x + b_n) \rightarrow H(x), \quad (1)$$

for some constants a_n and b_n as $n \rightarrow \infty$. Similar to the Central Limit Theorem, the normalized maxima converge to the distribution H . The Extremal Types Theorem (Fisher and Tippett (1928); Gnedenko (1943)) states that the limit distribution H can only be one of the following types:

$$\begin{aligned} \text{Type I:} \quad & H(x) = \exp(-\exp(-x)), \quad \text{for } x \in \mathbb{R}, \\ \text{Type II:} \quad & H(x) = \begin{cases} 0 & \text{if } x < 0, \\ \exp(-x^{-a}) & \text{if } x \geq 0, \end{cases} \\ \text{Type III:} \quad & H(x) = \begin{cases} \exp(-(-x)^a) & \text{if } x < 0, \\ 1 & \text{if } x \geq 0, \end{cases} \end{aligned}$$

where for type II and III it holds that $a > 0$. These three types are referred to as the Gumbel, Fréchet and the inverse Weibull distributions, respectively. Gnedenko (1943) shows that these three CDFs can be generalized into one distribution function, which is

called the Generalized Extreme Value (GEV) distribution, see equation (4) below. Hence, the maxima obtained from a sample of observations approximately follow the GEV distribution, and the type of distribution is dependent on the shape parameter ξ .

The BM method naturally follows the limit behavior of maxima. The block maxima are constructed by dividing the sample of observations into k blocks. They approximately follow the GEV distribution, and can therefore be used to estimate the shape, scale and location parameters. The most popular methods of estimating the parameters of the GEV distribution are the maximum likelihood (ML) estimation by Prescott and Walden (1980) and the probability weighted moments (PWM) by Hosking, Wallis, and Wood (1985). More recently, Bücher and Segers (2018) derived the ML estimators of the Fréchet distribution and established the consistency and asymptotic normality. After fitting the GEV distribution to the block maxima using ML, the obtained parameters are used to estimate high quantiles of the block maxima.

McNeil (1998) demonstrates that the relation between the high quantile of the block maxima, sometimes referred to as the return level, and a high quantile of the observations depends only on the probability level and the block size of the block maxima. In the same paper, the estimation of high quantiles on serially dependent data is analyzed. The BM method can still be applied directly to the serially dependent case, but the relation between the quantile of the block maxima and the quantile of the original observations breaks down. This is due to the extremal index parameter, which indicates the degree of clustering of extreme values; see Leadbetter (1983) for a more detailed theoretical interpretation. The relation between the high quantiles of the block maxima and the high quantiles of the observations also depends on this extremal index. Hence, the extremal index needs to be estimated first in order to obtain a high quantile of serially dependent data. The estimation of the extremal index under stationary and weak dependence has been performed by Hsing (1993) and Smith and Weissman (1994). More recently, Berghaus and Bücher (2018) provided an improved version of the ML estimator suggested by Northrop (2015), by incorporating sliding block maxima.

The POT method has recently gained significant popularity over the BM method. The

POT differs from the BM method in the way that the extreme values (from which we try to obtain the limiting distribution) are chosen. The POT only considers those extreme values that exceed a certain threshold. One of its advantages, which has been mentioned repeatedly, for example Ferreira and De Haan (2015) and the references thereafter, is the fact that the POT method uses all of the extreme values. As the BM method only considers the maximum in a range of values, it may waste extreme values. This feature is even more strongly present in the case of non-IID data, as extreme values are usually more clustered together. Assume $X - u$ to be the excess losses. Then, using the general rules of conditional probability, the distribution of the excess losses can be described as $F_u(x) = P(X - u \leq x | X > u) = \frac{F(x+u) - F(u)}{1 - F(u)}$. If and only if the distribution of the observations, F , is in the maximum domain of attraction of the GEV distribution, then it follows that the excess distribution function F_u can be approximated by the Generalized Pareto Distribution (GPD); see equation (7). The theorem behind this relation is derived from Balkema and De Haan (1974) and Pickands (1975). Hence, the excess losses above a high threshold approximately follow the GPD distribution. The shape parameter in the GPD distribution is identical to the shape parameter of the GEV distribution.

As with the BM method, the most important estimators for estimating the parameters of the GPD distribution are the ML and PWM estimators, which are both discussed in Hosking and Wallis (1987). Smith (1987) extensively investigated the tail estimation based on IID data and has derived the theoretical properties of the ML estimator based on POT. High quantiles of the data can then be estimated through the estimated parameters of the GPD and the inverse CDF. When the limit of the maxima is of type II, another applicable method to estimate the shape parameters is the Hill estimator, by Hill (1975). As the data is now considered to be heavy-tailed, the tails approximately follow the Pareto distribution, and the VaR can be estimated by extrapolating a less extreme quantile to a high quantile using the reciprocal of the shape parameter. Both VaR estimators are described by McNeil, Frey, Embrechts, et al. (2005). In the case of non-IID data, Drees (2003) has demonstrated that the derived methods can still be used. However, the asymptotic variance is different from, and usually higher than, the IID case. Drees (2003) also provides a theoretical estimator for the asymptotic variance.

3 Methodology

3.1 Value-at-Risk

Before discussing the BM and POT methods in further detail, a formal definition of the VaR is required. The VaR is a quantitative risk measure that is usually applied on the loss distribution. In probabilistic terms, the VaR can be interpreted as the quantile of this loss distribution. A comprehensive definition is given by McNeil et al. (2005) as follows:

Definition 1. (*Value-at-Risk*). *Given some confidence level $p \in (0, 1)$. The VaR of the losses at the confidence interval p is given by the smallest number l such that the probability that the loss L exceeds l is no larger than $(1 - p)$. Formally,*

$$VaR_p = \inf\{l \in \mathbb{R} : P(L > l) \leq 1 - p\} = \inf\{l \in \mathbb{R} : F_L(l) \geq p\}. \quad (2)$$

It is common to use high values for p such as $p = 0.95$ or $p = 0.99$. The focus of this paper lies in extreme values and inferring high quantiles using EVT. Therefore, the confidence level of interest throughout this paper is chosen to be $p = 0.9999$. The major drawback of the VaR as a risk measure is that the VaR does not provide any information about the extreme losses that occur with a probability of less than $1 - p$.

3.2 Extreme Value Theory

It is essential to discuss the probability theory behind the convergence of maxima before deriving the estimators in the BM method. Assume a set of IID random variables denoted as X_1, X_2, \dots with distribution function F and define the maximum as $M_n = \max(X_1, \dots, X_n)$. The EVT considers the limiting distribution of M_n . Assume that with normalizing constants a_n and b_n , M_n converge in distribution as $n \rightarrow \infty$, i.e.

$$\lim_{n \rightarrow \infty} P\left(\frac{M_n - b_n}{a_n} \leq x\right) = \lim_{n \rightarrow \infty} F^n(a_n x + b_n) = H(x), \quad (3)$$

where $H(x)$ is a non-degenerate distribution function. Here, a non-degenerate distribution function is a limiting distribution that is not concentrated on a single point. If condition (3) holds, then F is said to be in the maximum domain of attraction of H , which can be written as $F \in MDA(H)$. In a similar manner as the Central Limit Theorem for averages, the Extremal Types Theorem for maxima of Fisher and Tippett (1928) and

Gnedenko (1943) states that in case the distribution of a normalized maximum converges, the limiting distribution has to be one of a particular class of distributions.

Theorem 1. (Fisher-Tippett, Gnedenko). *If $F \in MDA(H)$ for some non-degenerate distribution function H , then H must be a GEV distribution defined as*

$$H_\xi(x) = \begin{cases} \exp\left(- (1 + \xi x)^{-\frac{1}{\xi}}\right) & \text{for } \xi \neq 0, \\ \exp(-\exp(-x)) & \text{for } \xi = 0 \end{cases} \quad (4)$$

where $1 + \xi x > 0$. A three-parameter family is obtained by defining $H_{\xi,\mu,\sigma}(x) := H_\xi\left(\frac{x-\mu}{\sigma}\right)$ where $\sigma > 0$ and $\mu, \xi \in \mathbb{R}$. The parameters μ , σ and ξ are referred to as the location, scale and shape parameters, respectively. Two examples of obtaining the GEV are provided in Appendix A.1, with F following the exponential distribution and the Pareto distribution. Depending on the value of ξ , the distribution H_ξ defines a type of distribution. There are three possible states of ξ , each of which correspond to one of the three types of extreme value distributions. Figure 1 illustrates the three different extreme value distribution families for which it holds that:

- $\xi = 0$: Gumbel or type I extreme value distribution
- $\xi > 0$: Fréchet or type II extreme value distribution
- $\xi < 0$: Weibull or type III extreme value distribution.

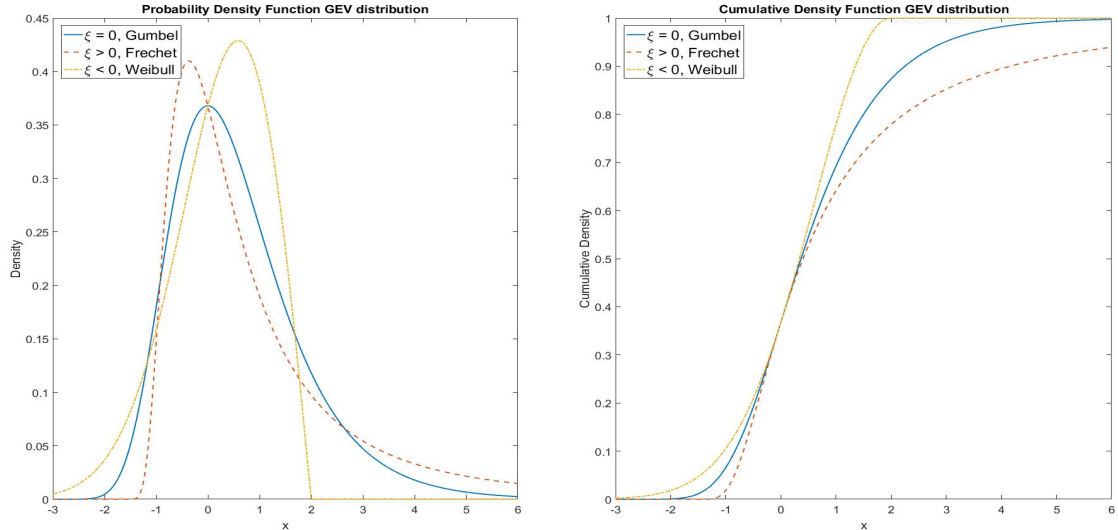


Figure 1: The probability density function (PDF) and CDF for three different values of ξ and $\mu = 0$ and $\sigma = 1$. The solid line corresponds to $\xi = 0$ (Gumbel); the dashed line $\xi = 0.5$ (Fréchet); and the dotted-dashed line $\xi = -0.5$ (Weibull).

When $F \in MDA(G)$ with G the Weibull distribution, we say that F is in the maximum domain of attraction of the Weibull distribution. The same definition holds for the Gumbel and Fréchet domains. The distributions that are in the maximum domain of attraction of the Weibull distribution are considered short-tailed distributions with a finite right endpoint, denoted by $x_F = \sup\{x \in \mathbb{R} : F(x) < 1\}$. This class of distributions is usually not that interesting when quantifying financial risk, as the distribution of losses is often considered heavy-tailed. Both the Gumbel and Fréchet distributions are heavy-tailed distributions with infinite right endpoints. However, the class of distributions that is in the maximum domain of attraction of the Gumbel distribution can have either infinite or finite right endpoints. Within the Gumbel domain there are many distributions; for example, the normal, lognormal, gamma and chi-squared distributions. The Fréchet distribution has a slower decay of the right tail than the Gumbel distribution, and in its maximum domain of attraction are heavy-tailed distributions with infinite right endpoints, for example the Pareto distribution. These distributions are also known as the power-tailed distributions and are often the preferred choice for modeling financial losses.

In order to derive the estimators under the POT, it is essential to establish the probability theory used to model the tail distribution. Let the losses X be a random variable

with possibly unknown distribution function F such that $F(x) = P(X \leq x)$. We then define the CDF $F_u(x)$ for the excess losses $X - u$, given that the losses exceed the threshold u as

$$\begin{aligned} F_u(x) &= P(X - u \leq x | X > u) \\ &= \frac{F(x + u) - F(u)}{1 - F(u)}, \end{aligned} \tag{5}$$

for $0 \leq x < x_F - u$, where $x_F \leq \infty$ is the right endpoint of F . The theorem of Pickands-Balkema-de Haan, derived in Balkema and De Haan (1974) and Pickands (1975), states that the distributions for which normalized maxima converge to a GEV distribution establish a set of distributions for which the excess distribution converges to the GPD whenever the threshold u is increased.

Theorem 2. (Pickands-Balkema-de Haan). *It is possible to obtain a positive measurable function $\sigma(u)$, such that*

$$\lim_{u \rightarrow x_F} \sup_{0 \leq x < x_F - u} |F_u(x) - G_{\sigma(u), \xi}(x)| = 0, \tag{6}$$

if and only if $F \in MDA(H_\xi)$ with $\xi \in \mathcal{R}$.

Here, $G_{\sigma, \xi}$ is the GPD and is defined as

$$G_{\sigma, \xi}(x) = \begin{cases} 1 - (1 + \xi \frac{x}{\sigma})^{-\frac{1}{\xi}} & \text{for } \xi \neq 0, \\ 1 - e^{-\frac{x}{\sigma}} & \text{for } \xi = 0, \end{cases} \tag{7}$$

where $\sigma > 0$ and $\xi \in \mathbb{R}$. It also holds that $x \geq \mu$ when $\xi \geq 0$ and $\mu \leq x \leq -\frac{\sigma}{\xi}$ when $\xi \leq 0$. Again, the parameters σ and ξ are referred to as the scale,= and shape parameters, respectively. The parameter ξ is equal to the shape parameter of the GEV. Figure 2 displays the GPD distribution for different values of the scale and shape parameters.

Among others, De Haan and Ferreira (2006) show that equation (6) further implies that

$$\lim_{u \rightarrow x_F} F_u\left(\frac{x}{\sigma(u)}\right) = G_{1, \xi}(x) \iff F \in MDA(H_\xi). \tag{8}$$

In addition, Gnedenko (1943) demonstrates that when the observations are approximately heavy-tailed distributed, the following relation holds

$$F \in MDA(H_{\xi>0}) \iff \bar{F}(x) = x^{-\frac{1}{\xi}}L(x), \quad (9)$$

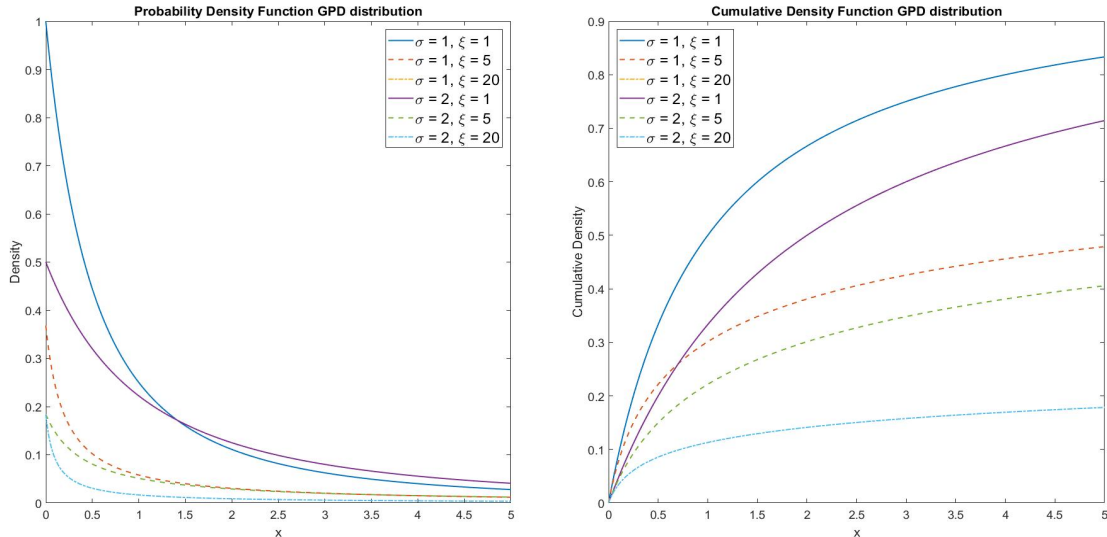


Figure 2: The PDF and CDF for three different values of ξ and two different values of σ .

where $L(x)$ is a slowly varying function. The definitions of slowly and regularly varying functions can be found in Appendix A.2. The decay of the tails is a power function in which the rate of decay, denoted by $\frac{1}{\xi}$, is often referred to as the tail index of the distribution. De Haan and Ferreira (2006) also show that if F belongs to the maximum domain of attraction of the Fréchet distribution, then for $\sigma(u) = \xi u$ equation (9) is equivalent to

$$\lim_{u \rightarrow \infty} F_u \left(\frac{x}{\sigma(u)} \right) = G_{1,\xi}(x) \iff \lim_{u \rightarrow \infty} \frac{1 - F(ux)}{1 - F(x)} = x^{-\frac{1}{\xi}}. \quad (10)$$

3.3 Block Maxima

This section first examines the BM method for the IID case, before the theory is extended to serially dependent data. The BM method has been fundamental and is considered to be one of the oldest models within EVT.

In order to estimate the parameters, the BM method divides the data with total number of observations N into k equally sized blocks, each containing n observations. Taking

the maximum of each block generates a new sample that contains extreme values. Define the sample of block maxima formally as $\mathbf{M}_n = \{M_{n,1}, \dots, M_{n,k}\}$ where $M_{n,i}$ denotes the i th block maximum. Then, the block maxima approximately follow a GEV distribution $H_{\xi,\mu,\sigma}$. The choice of block size, n , and the corresponding number of blocks, k , have a significant impact when estimating the parameters of the GEV distribution. A large block size leads to a more accurate approximation of the block maxima distribution by a GEV following the limit relation. Consequently, the parameter estimates have a lower bias. Meanwhile, adopting a large k increases the number of block maxima. As a result, the estimated parameters have a low variance. A visual interpretation of the BM method is presented in Figure 3.

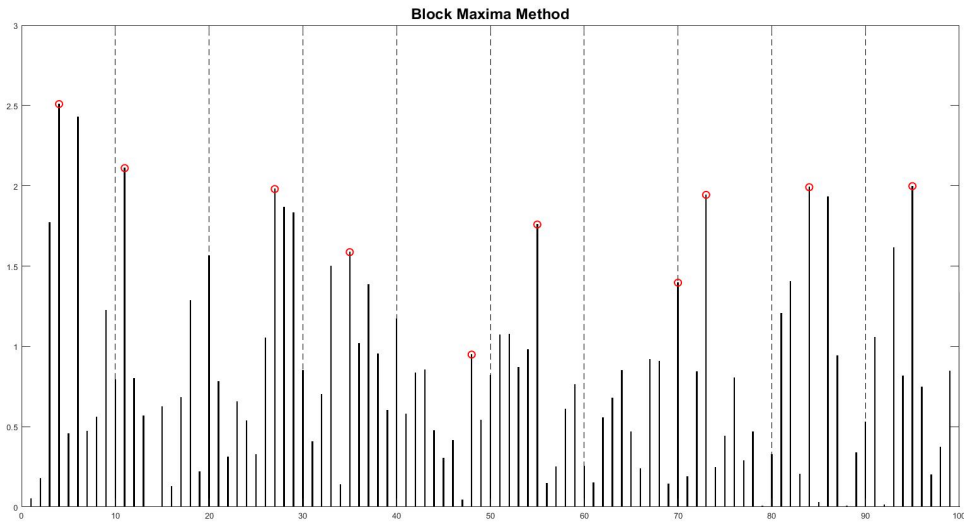


Figure 3: Visual interpretation of the BM method. The total number of observations N equals 100 and is divided into $k = 10$ blocks of $n = 10$ observations where only the maximum values per block size are considered.

To estimate the parameters of the GEV distribution, either of the following two estimators is generally used: the ML estimators, see Prescott and Walden (1980) and Bücher and Segers (2018); and the PWM estimators, see Hosking and Wallis (1987) and Ferreira and De Haan (2015). In this study we use ML both in the BM and POT approaches in order to make a fair comparison. The aim of this paper is to infer high quantiles on financial losses containing serial dependence. Mandelbrot (1963) argued that financial losses are heavy-tailed and provided the evidence in a later publication, see Mandelbrot (1997). Therefore, since financial losses are known to be heavy-tailed, we restrict the

research to the class of Fréchet distributions, or equivalently $\xi > 0$. This paper adopts the estimators derived in Bücher and Segers (2018), where the Fréchet distribution is used and the location parameter is set to zero. Here, we first explain the application of the ML estimators for the Fréchet distribution in detail.

The CDF of the Fréchet distribution can be obtained via the GEV distribution (4) by using $\xi > 0$ and $y = 1 + \xi x$, and is defined as

$$F_\xi(y) = \begin{cases} \exp\left(-y^{-\frac{1}{\xi}}\right) & \text{for } y > 0, \\ 0 & \text{for } y \leq 0 \end{cases} \quad (11)$$

We focus on the two-parameter Fréchet distribution, similar to Bücher and Segers (2018), which is obtained by $F_{\xi,\sigma}(y) := F_\xi\left(\frac{y}{\sigma}\right)$ and with CDF

$$F_{\xi,\sigma}(y) = \exp\left(-\left(\frac{y}{\sigma}\right)^{-\frac{1}{\xi}}\right) \quad \text{for } y > 0. \quad (12)$$

The PDF can be obtained by taking the first order derivative of the CDF.

$$\begin{aligned} f_{\xi,\sigma}(y) &= \frac{\delta F_{\xi,\sigma}(y)}{\delta y} \\ &= \frac{1}{\xi\sigma} \left(\frac{y}{\sigma}\right)^{-\frac{1}{\xi}-1} \exp\left(-\left(\frac{y}{\sigma}\right)^{-\frac{1}{\xi}}\right). \end{aligned} \quad (13)$$

Let $y = (y_1, \dots, y_k) \in (0, \infty)^k$ be a sample which the Fréchet distribution is to be fitted. Then the log-likelihood can be derived as

$$\begin{aligned} l(\xi, \sigma; y_1, \dots, y_n) &= \sum_{i=1}^k \ln(f_{\xi,\sigma}(y_i)) \\ &= -k(\ln(\xi) + \ln(\sigma)) - \sigma^{\frac{1}{\xi}} \sum_{i=1}^k y_i^{-\frac{1}{\xi}} - \left(\frac{1}{\xi} + 1\right) \left(\sum_{i=1}^k \ln(y_i) - k \ln(\sigma)\right). \end{aligned} \quad (14)$$

The ML estimators $\hat{\xi}$ and $\hat{\sigma}$ are obtained by maximizing (14) to the respective parameter. Bücher and Segers (2018) derived the ML estimators for the shape and scale parameters, and established the consistency and asymptotic normality for the ML estimators for both IID and strictly stationary time-series. The ML estimators for the scale parameter σ and

shape parameter ξ are obtained as follows:

$$\hat{\sigma} = \left(\frac{1}{k} \sum_{i=1}^k y_i^{-\frac{1}{\hat{\xi}}} \right)^{-\hat{\xi}}, \quad (15)$$

where $\hat{\xi}$ is the unique solution of $\Psi_k(\xi|y) = 0$, with $\Psi_k(\xi|y)$ defined as

$$\Psi_k(\xi|y) = \xi + \frac{\frac{1}{k} \sum_{i=1}^k y_i^{-\frac{1}{\xi}} \ln(y_i)}{\frac{1}{k} \sum_{i=1}^k y_i^{-\frac{1}{\xi}}} - \frac{1}{k} \sum_{i=1}^k \ln(y_i). \quad (16)$$

If $\xi > 0$, the block maxima \mathbf{M}_n approximately follow the Fréchet distribution. The parameters can be estimated by replacing the sample vector y by the block maxima in the above derived estimators. After obtaining parameter estimates, we estimate the quantiles of the block maxima M_n by inverting the CDF and using the ML parameters.

The relation between the VaR of the block maxima, which is sometimes referred to as the return level, and the VaR of the original observations is demonstrated by McNeil (1998). Because the VaR of the block maxima is a quantile on extreme values, it is therefore a high quantile of the original data. When the data are IID, the probability level corresponding to the VaR of the block maxima can then be calculated as

$$\Pr(M_n < VaR_p) = \left(\Pr(X < VaR_p) \right)^n = p^n. \quad (17)$$

That is, the VaR is a quantile of the block maxima with probability level p^n . Therefore, by using the inverse of equation (12) and parameter estimates (15) and (16) we can estimate the VaR as

$$\widehat{VaR}_p = \hat{\sigma} (-\ln(p^n))^{-\hat{\xi}}. \quad (18)$$

When moving away from IID data and allowing for serial dependence, the convergence of the maxima follows a GEV distribution raised to the power θ as illustrated by McNeil (1998):

$$\lim_{n \rightarrow \infty} P \left(\frac{\tilde{M}_n - b_n}{a_n} \leq x \right) = H^\theta(x), \quad (19)$$

where we use \tilde{M}_n to indicate that the data contains serial dependence and where θ in $(0, 1]$ is the so-called extremal index. Assuming that the maxima \tilde{M}_n is obtained from a stationary series with the same distribution function F as in the IID case (M_n), the

distribution of $H_\xi^\theta(x)$ is of the same type as $H_\xi(x)$ with the exact same ξ parameter. However, the location and scale parameters are different in this case. The extremal index is an important parameter that measures the degree of clustering of extremes in a stationary process.

McNeil (1998) states that for large n and $u = a_n x + b_n$ it now holds that $P(M_n \leq u) \approx P^\theta(\tilde{M}_n \leq u) = F^{n\theta}(u)$. Hence, for large values of u , the probability distribution of the maximum of n observations from the time-series with extremal index θ can be approximated by the distribution of the maximum of $n\theta < n$ observations from the associated IID time-series. The term $n\theta$ is often associated with counting the number of roughly independent clusters of observations in n observations. The extremal index θ is also known as the reciprocal of the mean cluster size.

Due to the serial dependence, the relation between the VaR of the block maxima and the VaR of the original observations changes, and are now dependent on the extremal index. As demonstrated by McNeil (1998), equations (17) and (18) now become

$$\Pr(M_n < VaR_p) = \left(\Pr(X < VaR_p)\right)^{n\theta} = p^{n\theta}, \quad (20)$$

and

$$\widehat{VaR}_p = \hat{\sigma} \left(-\ln(p^{n\hat{\theta}})\right)^{-\hat{\xi}}. \quad (21)$$

When dealing with serial dependence, we first need to estimate the extremal index. Berghaus and Bücher (2018) have recently analyzed estimators for the extremal index based on disjoint and sliding block maxima. They derived the asymptotic normality and revealed that the sliding block estimator outperforms other block estimators. Hence, we will adopt the sliding block estimators as proposed by Berghaus and Bücher (2018):

$$\hat{\theta}_n^{(1),sl} = \left(\frac{1}{k} \sum_{i=1}^k \hat{Z}_{n,i}^{sl}\right)^{-1}, \quad \hat{\theta}_n^{(2),sl} = \left(\frac{1}{k} \sum_{i=1}^k \hat{Y}_{n,i}^{sl}\right)^{-1}, \quad (22)$$

where

$$\hat{Z}_{n,i}^{sl} = n \left(1 - \hat{W}_{n,i}^{sl}\right) \quad \text{and} \quad \hat{Y}_{n,i}^{sl} = -n \log \left(\hat{W}_{n,i}^{sl}\right)$$

with

$$\hat{W}_{n,i}^{sl} = \hat{F}_n \left(M_{n,i}^{sl}\right).$$

Here, \hat{F}_n is the empirical CDF of the observations X_1, \dots, X_N . The sliding block maxima are obtained by dividing the sample of observations into $N - n + 1$ blocks of length n , such that $M_{n,i}^{sl} = \max(X_i, \dots, X_{i+n-1})$ for $t = 1, \dots, N - n + 1$.

To summarize, when dealing with IID data, the VaR can be estimated using equation (18). Here, the relation between the quantiles of the block maxima and the quantiles of the original observations, and the estimated scale and shape parameters are used. These parameters are often estimated using either ML or PWM estimators. In this paper we obtain the ML parameters with equations (15) and (16). If the data is a strictly stationary time-series then the scale parameter may change, but the shape parameter is exactly the same. The relation between the quantiles of the block maxima and the quantiles of the original observations now depends on the extremal index. Under serial dependence, the VaR estimator now changes to equation (21) using equation (22) to estimate the extremal index.

3.4 Peak over Threshold

A major disadvantage of the BM method is that it potentially neglects extreme values in the tails. This is because only the maximum of a group of data is used to estimate the GEV distribution. The existence of serial dependency within the data magnifies this shortcoming. This gave rise to the POT, another often-used method in EVT, which considers those extreme observations that exceed a certain threshold, as illustrated in Figure 4. This section begins by discussing the theory of the POT method in the IID case. Subsequently, the IID assumption is relaxed and the differences are analyzed.

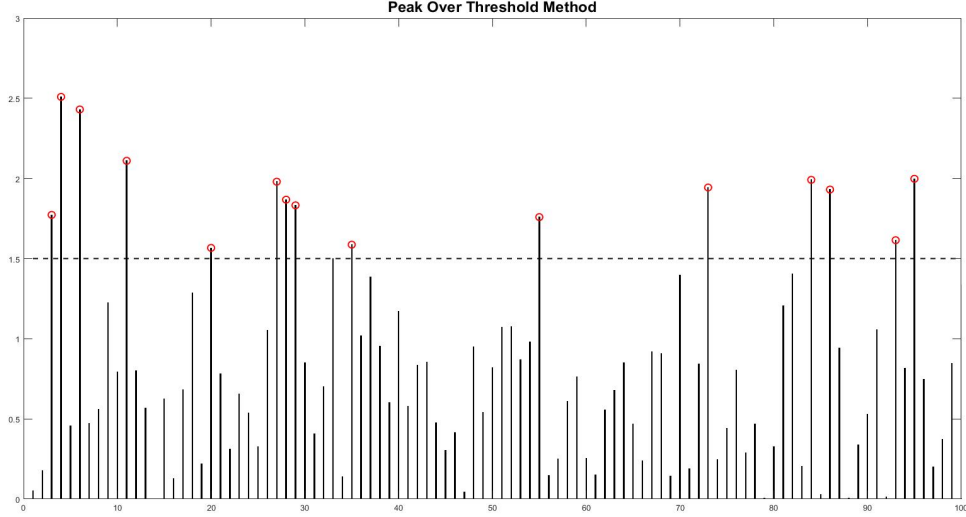


Figure 4: Visual interpretation of the POT method. Only those values exceeding the threshold of 1.5 are considered.

We start by deriving the VaR estimators in the general case $\xi \in \mathbb{R}$ after which the theory is extended to derive the estimators in the case $\xi > 0$. Using the rules for probabilities for a random variable X and threshold u such that $x \geq u$,

$$\begin{aligned}
 \bar{F}(x) &= P(X > u)P(X > x|X > u) \\
 &= \bar{F}(u)P(X - u > x - u|X > u) \\
 &\approx \bar{F}(u)G_{\mu,\sigma,\xi}(x - u) \\
 &\approx \bar{F}(u)\left(1 + \xi \frac{x - u}{\sigma}\right)^{-\frac{1}{\xi}}.
 \end{aligned} \tag{23}$$

The k excess losses can be obtained as $\{X_{N-i,N} - X_{N-k,N}\}_{i=0}^{k-1}$, where $X_{j,N}$ is the j -th element in the order statistics $X_{1,N} \leq \dots \leq X_{N,N}$. Hence, it holds that the threshold $u = X_{N-k,N}$. An estimator for the tail probabilities can then be constructed as proposed by Smith (1987). Multiple estimation techniques are available for obtaining the estimated parameters of the GPD model, for example ML or PWM estimators. Given that we obtained the estimators for the scale and shape parameters $\hat{\sigma}$ and $\hat{\xi}$ by fitting the GPD to excess losses over threshold $X_{N-k,N}$ and using the empirical estimator $\frac{k}{N}$ for $\bar{F}(X_{N-k,N})$ with k , the number of observations exceeding the threshold $X_{N-k,N}$, this results in the following estimator:

$$\hat{F}(x) = \frac{k}{N} \left(1 + \hat{\xi} \frac{x - X_{N-k,N}}{\hat{\sigma}}\right)^{-\frac{1}{\hat{\xi}}} \quad \text{for } x \geq X_{N-k,N}. \quad (24)$$

As the VaR is simply a quantile of the distribution, it can be obtained by inverting the CDF. By applying this to the estimator of the CDF of the excess losses, we derive the estimator for the VaR, the $(1 - p_n)$ quantile of X as

$$\widehat{VaR}_{p_n} = F^{-1}(1 - p_n) = X_{N-k,N} + \frac{\hat{\sigma}}{\hat{\xi}} \left(\left(\frac{k}{N(1 - p_n)} \right)^{\hat{\xi}} - 1 \right). \quad (25)$$

We assumed the observations to be of a heavy-tailed distribution or equivalently $\xi > 0$, as this is a stylized fact of financial returns. In chapter 3.2 we demonstrated that the distribution of the observations is therefore in the maximum domain of attraction of the Fréchet distribution. Consequently, the ratio of the exceedances and the threshold, $\frac{X}{u} | X > u$, approximately follows $\bar{F}(x) = x^{-\frac{1}{\xi}}$ when $u \rightarrow \infty$. The exceedance ratio can then be fitted to the Pareto distribution, which is defined as

$$H_{\xi}(x) = 1 - x^{-\frac{1}{\xi}}. \quad (26)$$

Hence, the tail distribution can be approximated as

$$\bar{F}(x) \approx \bar{F}(u) \left(\frac{x}{u} \right)^{-\frac{1}{\xi}}. \quad (27)$$

Another conventional method for estimating ξ which utilizes the heavy-tailed distribution, is the Hill estimator, proposed by Hill (1975). The formula for the Hill estimator is given by

$$\hat{\xi}_{k,N}^{(H)} = \frac{1}{k} \sum_{j=1}^k \ln X_{N-j+1,N} - \ln X_{N-k,N}. \quad (28)$$

The difficulty in using the Hill estimator lies in choosing k , as it needs to hold that $k \rightarrow \infty$ and $\frac{k}{N} \rightarrow 0$ as $N \rightarrow \infty$. The choice of k is often based on the analysis of so-called Hill plots. Thereby, the estimates of ξ are plotted against the different values for k , and the value for u is chosen wherever the estimations become stable. This method has obvious drawbacks; most importantly, it is difficult to implement in an automated fashion. Hence, a statistical or data-driven selection criterion is needed. Danielsson, Ergun, de Haan, and de Vries (2016), recently proposed a selection method that minimizes the maximum distance between the fitted Pareto type tail and the observed quantile.

As ξ can be estimated by the Hill estimator (28), and again substituting the empirical estimator $\frac{k}{N}$ for $\bar{F}(u)$, the standard form of the Hill tail estimator is as follows:

$$\hat{F}(x) = \frac{k}{N} \left(\frac{x}{X_{N-k,N}} \right)^{-\frac{1}{\hat{\xi}^{(H)}}}. \quad (29)$$

Consequently, the VaR estimator is derived by inverting equation (29)

$$\widehat{VaR}_{p_n} = X_{N-k,N} \left(\frac{k}{N(1-p_n)} \right)^{\hat{\xi}_{k,N}^{(H)}}. \quad (30)$$

The limiting distribution of a range of estimators has been thoroughly researched mostly in the IID case, notably by Dekkers, Einmahl, and De Haan (1989) and de Haan and Rootzén (1993). It is demonstrated that the limiting distribution converges to the normal distribution

$$\frac{\sqrt{k}}{\log\left(\frac{k}{Np_n}\right)} \left(\frac{\widehat{VaR}_{p_n}}{VaR_{p_n}} - 1 \right) \xrightarrow{d} \mathcal{N}(\lambda, \sigma^2) \quad \text{as } N \rightarrow \infty. \quad (31)$$

Whenever the data is no longer IID and serial dependence is relevant, the estimator still holds if the serial dependence is weak. Drees (2003) demonstrates that the asymptotic variance is different and usually higher under serial dependence.

3.5 Simulation Setup

The simulation uses a general framework similar to that of the application. The goal of the simulation setup is to generate multiple scenarios in which the levels of autocorrelation, volatility clustering and tail dependence between two series are controlled with a single model. The model is first explained stepwise, before each component is explained in further detail. All of the components are then combined into a single model, which parameters and the way they will be used are finally discussed.

First, the returns of two different series are simulated using an ARMA model, of which the innovations are generated by a GARCH model. The parameters of the ARMA-GARCH model of each series are set independently. The ARMA structure will be the main contributor for generating serially dependent data. The serial dependence can be controlled by both the AR and MA terms. The AR term enables the direct incorporation

of the dependence of the lagged observations on the current observations. Meanwhile, the MA term indirectly models the dependence between observations via the unobserved shocks. By assuming that the unobserved shocks follow a GARCH process instead of a white noise process, the level of volatility clustering within each series can be controlled. For each series, the GARCH innovations are assumed to follow a white noise process with the standard normal distribution. Nevertheless, the cross-sectional dependence between the two GARCH innovation processes is assumed to follow a Clayton copula. Finally, the portfolio is obtained as a weighted average of the two simulated series as follows: $X_t = wX_{t,1} + (1 - w) X_{t,2}$.

The ARMA(1,1)-GARCH(1,1) model used for each series $j = 1, 2$ is defined by

$$\begin{aligned}
X_{t,j} &= c_j + \varepsilon_{t,j} + \phi_j X_{t-1,j} + \pi_j \varepsilon_{t-1,j}, \\
\varepsilon_{t,j} &= \sigma_{t,j} Z_{t,j}, \\
\sigma_{t,j}^2 &= \omega_j + \alpha_j \varepsilon_{t-1,j}^2 + \beta_j \sigma_{t-1,j}^2 \quad \text{with } \alpha + \beta < 1, \\
Z_{t,j} &\sim \mathcal{N}(0, 1),
\end{aligned} \tag{32}$$

where the copula of $(Z_{t,1}, Z_{t,2})$ follows the Clayton copula. The conditional variance is denoted by σ_t^2 and the parameters ϕ_i , π_i , α_i and β_i are the coefficients of the AR, MA, innovations and conditional variance terms, respectively.

Before proceeding to the implementation of the Clayton copula, a general definition of a copula now provided.

Definition 2. *A d -dimensional copula is a joint cumulative distribution function on $[0, 1]^d$ with standard uniform marginal distributions.*

Theorem 3. (Sklar) *Let F be a joint distribution with marginals F_1, \dots, F_d . Then there exists a copula $C(x_1, \dots, x_d)$ such that $F(x_1, \dots, x_d) = C(F_1(x_1), \dots, F_d(x_d))$. Conversely, if C is a copula and F_1, \dots, F_d are univariate distributions, then F is a joint distribution with marginals F_1, \dots, F_d .*

The bivariate-Clayton copula is an Archimedean copula that allows a non-zero level of lower tail dependency between two series. This tail dependency lies in the negative tail, corresponding to extreme losses, and the advantage of the Clayton copula is that the

level of dependence can be set by a single parameter, often denoted as θ . The bivariate Clayton copula is given by

$$C_{\theta}^{Cl}(u_1, u_2) = \left(u_1^{-\theta^{Cl}} + u_2^{-\theta^{Cl}} - 1 \right)^{-\frac{1}{\theta^{Cl}}} \quad \text{for } 0 < \theta^{Cl} < \infty. \quad (33)$$

Whenever $\theta^{Cl} \rightarrow 0$ we approach the independence copula, and when $\theta^{Cl} \rightarrow \infty$ we approach full dependency.

To combine all of the different components in the simulation model, we derived the following algorithm to obtain a single set of simulated data.

Algorithm 1. (Data Generating Process)

1. Generate two uniformly distributed series from the Clayton copula. Draw two independent uniform random variables $(U_{t,1}, V_{t,2})$ and set:

$$U_{t,2} = \left[U_{t,1}^{-\theta^{Cl}} \left(v_2^{-\frac{\theta^{Cl}}{(1+\theta^{Cl})}} - 1 \right) + 1 \right]^{-\frac{1}{\theta^{Cl}}}. \quad (34)$$

2. Convert the $(U_{t,1}, U_{t,2})$ to standard normal marginals using the inverse of the standard normal CDF:

$$Z_{t,1} = \Phi^{-1}(U_{t,1}) \quad \text{and} \quad Z_{t,2} = \Phi^{-1}(U_{t,2}). \quad (35)$$

The simulated standard normal variables $Z_{t,1}$ and $Z_{t,2}$ have lower tail dependency but are both IID series.

3. Use $(Z_{t,1}, Z_{t,2})$ to simulate two series from the ARMA(1,1)-GARCH(1,1) model for $j = 1, 2$:

$$\begin{aligned} X_{t,j} &= c_j + \varepsilon_{t,j} + \phi_j X_{t-1,j} + \pi_j \varepsilon_{t-1,j}, \\ \varepsilon_{t,j} &= \sigma_{t,j} Z_{t,j} \\ \sigma_{t,j}^2 &= \omega_j + \alpha_j \varepsilon_{t-1,j}^2 + \beta_j \sigma_{t-1,j}^2. \end{aligned} \quad (36)$$

4. Obtain the simulated time-series by calculating the weighted average:

$$X_t = w X_{t,1} + (1 - w) X_{t,2}. \quad (37)$$

For every specification of the parameters, one sample with sample size 1,000,000 is obtained to calculate the true VaR, and 1,000 samples with sample size 2,000 are generated to compare the two methods to estimate the VaR. Every sample uses a burn-in sample size of 1,000 data points. The true VaR is then estimated as the empirical quantile from the larger sample.

The set of models is divided into two groups: the first group depends on only one ARMA-GARCH model by setting $w = 1$ and $z_{t,1} \sim \mathcal{N}(0, 1)$; while the second group uses the Clayton copula to introduce tail dependency, and the two time-series are combined by setting $w = 0.5$.

3.6 Simulation Evaluation

In the simulation application it is possible to obtain the true VaR. Hence, the VaR estimates are evaluated by calculating the root mean squared error (RMSE) and root mean squared percentage error (RMSPE). After obtaining $m = 1,000$ VaR estimates per simulation model, as described in section 4.4, the RMSE and RMSPE can be calculated as

$$RMSE = \sqrt{\frac{\sum_{i=1}^m \left(\widehat{VaR}_{p_n} - VaR_{p_n} \right)^2}{m}}, \quad (38)$$

$$RMSPE = \sqrt{\frac{\sum_{i=1}^m \left(\frac{\widehat{VaR}_{p_n}}{VaR_{p_n}} - 1 \right)^2}{m}}. \quad (39)$$

For both the POT and BM methods, the RMSE is calculated using the same true VaR. For a given specification of parameters, we can directly compare the performance of the two methods using the RMSE. However, since the scale of the true VaR will differ across different specifications of parameters, it is not possible to make a comparison across these specifications using the RMSE. The RMSPE is based on the percentage deviation and will therefore be used to compare the two methods at different parameter specifications.

3.7 Financial Application Evaluation

In the financial application the VaR is estimated on a stock-bond portfolio consisting of 4,550 observations using both methods. Since the underlying data generating process is unknown, we cannot evaluate the VaR estimates by comparing them to the true VaR. The VaR estimates are now evaluated using the binomial method as demonstrated by Christoffersen (1998). The VaR will be estimated on a sub-sample of the data containing 3,550 observations. This leaves the test sample with 1,000 observations, denoted by W . The probability level of 99.99% used in the simulation application is therefore not appropriate to accurately evaluate the VaR estimates. Hence, we propose the use of three probability levels, $p_n = 99\%$, $p_n = 99.5\%$ and $p_n = 99.99\%$, which correspond to the VaR levels for banks and insurance companies. The binomial method is based on the unconditional coverage of the risk measure. The unconditional coverage can be seen as the empirical probability of exceeding the estimated VaR, $a = \frac{V}{W}$, with V the number of observations exceeding the VaR estimate. By definition, the unconditional coverage should equal the confidence level of the VaR. Assuming the confidence level p_n , then the probability of observing V exceptions in a testing sample of sample size W should equal the binomial PDF under the null hypothesis

$$\Pr(V = x) = \binom{W}{x} p_n^x (1 - p_n)^{W-x}. \quad (40)$$

A likelihood ratio test statistic is performed to test whether the unconditional coverage is equal to p_n . The test statistic can be calculated by

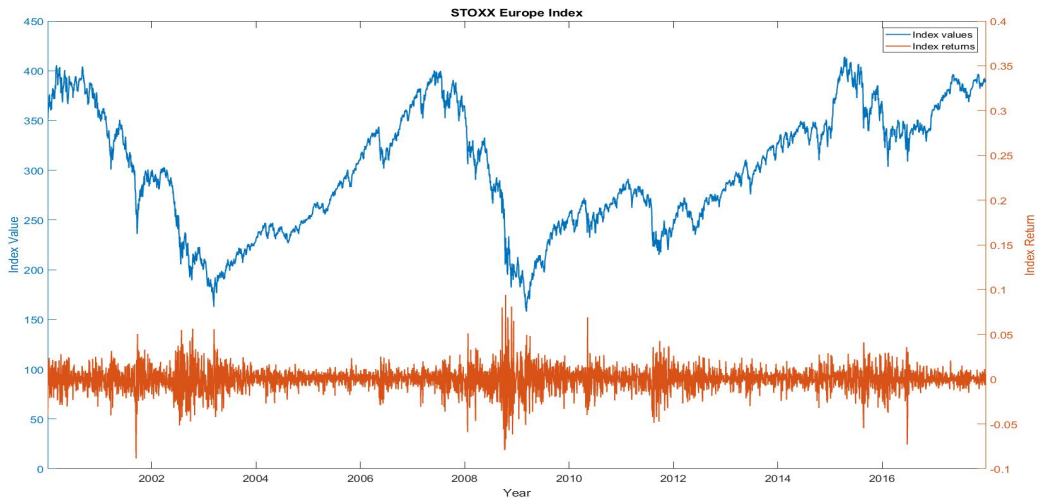
$$LR_{uc} = 2 \left[\ln \left(a^V (1 - a)^{W-V} \right) - \ln \left(p_n^V (1 - p_n)^{W-V} \right) \right] \sim \chi^2(1). \quad (41)$$

4 Empirical Data

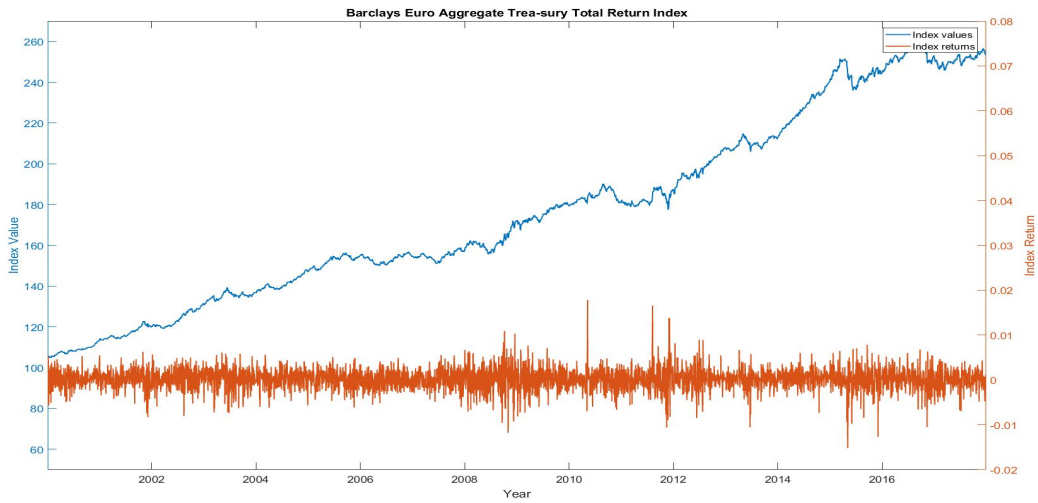
4.1 Preliminary

The empirical analysis focuses on a diversified portfolio of European markets. We setup a hypothetical portfolio investing 70% in stocks and 30% in bonds. The STOXX Europe 600 index, which holds 600 European companies, is used to represent the European stock market. The index represents large, medium and small capitalization companies in 17 European countries that account for approximately 90% of the free-float market capitalization of the European stock market. The Barclays Euro Aggregate Treasury Total Return Index is used to represent the European bond market. This bond index contains 372 fixed-income securities, which are from 13 different countries and are weighted by their market value. The data are obtained from Bloomberg Financial Markets and contain daily observations from 1 January, 2000 to 31 December, 2017, providing 4,550 observations for each index. The index values are converted to daily returns by $r_t = \log(I_t/I_{t-1})$, where I_t is the index value at time t . Figure 5 illustrates the index levels and returns of the stock index, bond index and the stock-bond portfolio, respectively.

(a) STOXX Europe Index



(b) Barclays Euro Aggregate Treasury Total Return Index



(c) Portfolio returns with allocation of 70% stocks and 30% bonds.

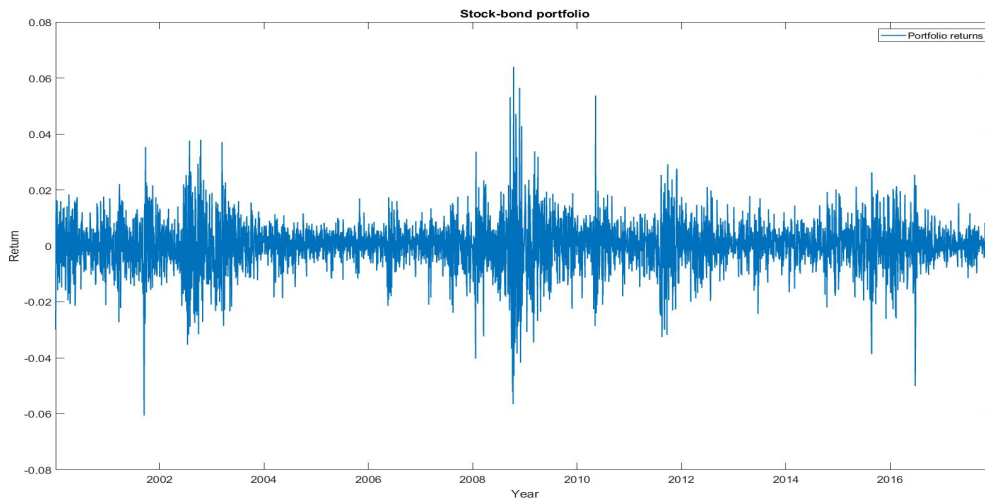


Figure 5: Index levels and returns for the stock index, the bond index and the portfolio.

The period from the beginning of 2000 to the end of 2017 is of interest because it contains two major events: the burst of the dot-com bubble in 2000 and the global financial crisis of 2008. Both events are represented by a large spike in volatility which, as expected, is more prominent in the stock index than the bond index. Even though the portfolio is well-diversified, with positions in 600 different stocks and 372 fixed-income securities, there is still a clear indication of volatility clustering.

4.2 Descriptive Statistics

The statistical properties of the empirical data need to be analyzed in further detail. Descriptive statistics are outlined in Table 1. As expected from differences in the nature of stocks and fixed-income securities, the standard deviation of the stock index is almost six times as high as that of the bond index. The returns of both indices are well-centered around zero, as indicated by the mean and median. For both indices the skewnesses are negative and with kurtosises higher than 3, that of the normal distribution. It is common for financial securities to have more extreme losses than extreme profits, as reflected by the negative skewness. The stylized fact of more extreme values than the normal distribution, and hence the notion of fatter tails, is captured by the high values of kurtosis. Formally, we reject that each series follows a normal distribution by the Jarque-Bera test. As the chosen portfolio is a weighted average between the stock and bond indices, the values of the statistical properties lie between those of the stock and bond indices.

Table 1: Descriptive statistics of the stock index, bond index and portfolio returns.

Return Series	# Obs	Min.	Max.	Mean	Median	Std. Dev	Skewness	Kurtosis	Jarque-Bera
STOXX 600	4549	-0.0886	0.0941	0.0000	0.0003	0.0124	-0.2125	8.5901	0.0000
Barclays Bond	4549	-0.0152	0.0178	0.0002	0.0002	0.0023	-0.1371	6.5306	0.0000
Portfolio	4549	-0.0606	0.0640	0.0000	0.0002	0.0086	-0.2023	8.4798	0.0000

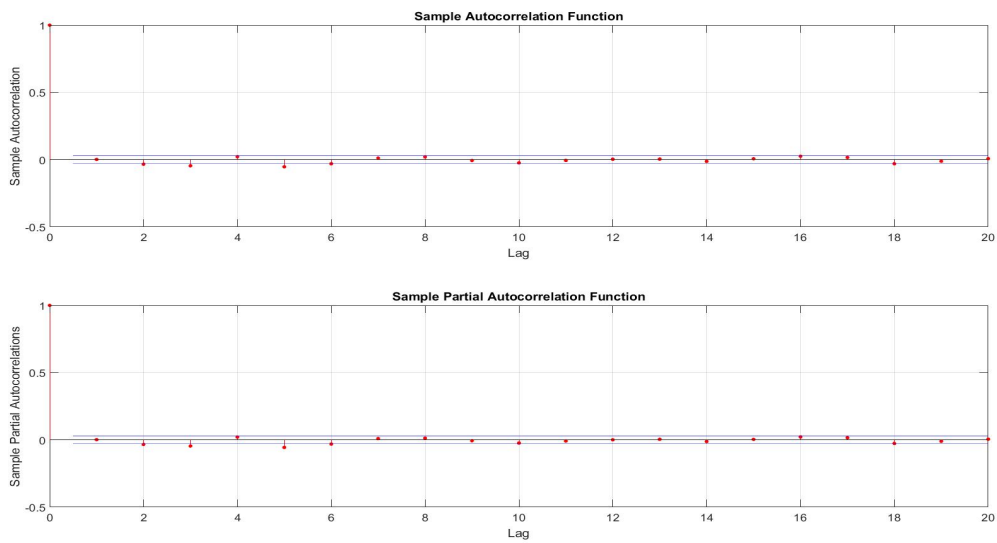
The results of the Ljung-Box test can be found in Table 2, and provide a more in-depth analysis of the serial dependency. Furthermore, Figure 6 presents autocorrelation and partial autocorrelation plots of the portfolio returns and the squared portfolio returns. The Ljung-Box Q-test indicates that for all returns series, the null hypothesis of independently distributed data can be rejected at a 5% significance level. These results are further supported by the correlation plots of the portfolio returns. For both the autocorrelation and partial autocorrelation there are multiple lags with significant correlation, most notably at lags 2, 3, 5 and 6. The correlation plots of the squared portfolio returns exhibit a strong significant autocorrelation. This confirms the presence of volatility clustering.

Table 2: Ljung-Box Q-test results.

Return Series	Test-statistic	Critical value	p -value
STOXX 600	54.02	31.41	0.0006
Barclays Bond	41.39	31.41	0.0033
Portfolio	49.81	31.41	0.0002
Squared Portfolio	3940.17	31.41	0.0000

* Test results are based on significance level $\alpha = 5\%$ and degrees of freedom equal to number of lags selected is 20.

(a) Serial dependence analysis on the portfolio returns.



(b) Serial dependence analysis on the squared portfolio returns.

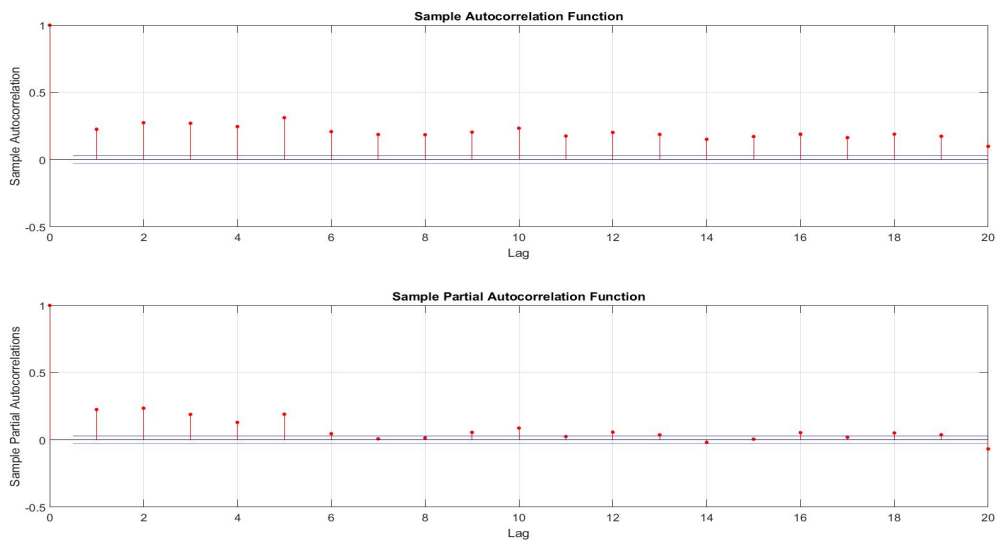


Figure 6: Sample autocorrelation and partial autocorrelation plots of the realized and squared portfolio returns.

5 Simulation

5.1 The choice of k

For the POT and BM, the number of exceedances and block maxima, respectively, have a significant impact on the accuracy on the estimations. For this reason, a number of papers report MSE of the estimated parameters for different values of k , the number of exceedances or block maxima. The simulation setup is fairly complex when considering at the number of parameters alone. Hence, the impact of k is analyzed for the IID and highly serial dependent case as a preliminary step. In the IID case the series are simulated from a Student's t-distribution with four degrees of freedom. For the serial dependent case, an ARMA process with $\phi_1 = 0.95$, $\pi_1 = 0$ and a Student's t-distribution with four degrees of freedom for the innovations are used to simulate the series. All other model parameters are set to zero. The number of simulations and VaR probability level are setup in the same way as in the simulation setup. For both the POT and BM methods we choose k that minimizes the MSE; k is then fixed across the different simulation models. The MSE is decomposed into the variance and squared bias and plotted against different values of k in Figure 7 for the POT method, and Figure 8 for the BM method.

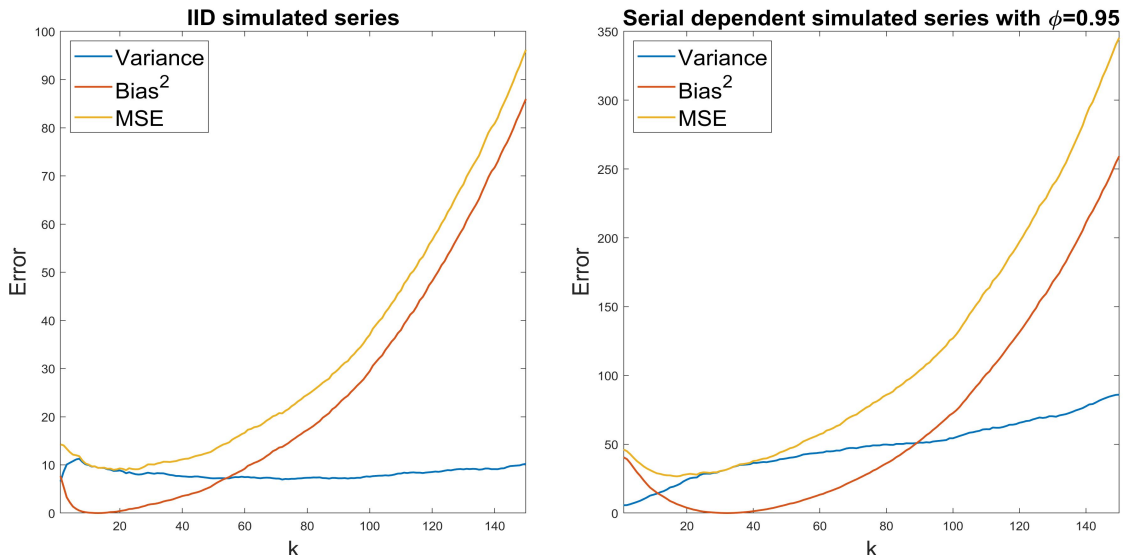


Figure 7: Decomposition of the MSE into variance and squared bias for the POT method.

In the IID case for the POT method, the MSE seems to reach its minimum at $k = 22$ and rises for high values of k . The variance remains relatively constant; consequently,

the increase in MSE is almost completely caused by the increase in squared bias. When examining the POT method for serially dependent series, the behavior of the squared bias is similar to that of the IID case. However, the variance is no longer constant and shows a clear trend. This is in line with the findings of Drees (2003) that the asymptotic variance is higher under serial dependence. Interestingly, the minimum MSE is obtained at $k = 17$, which is close to the IID case. For this reason, the value of k is fixed at 20 across the different simulation models.

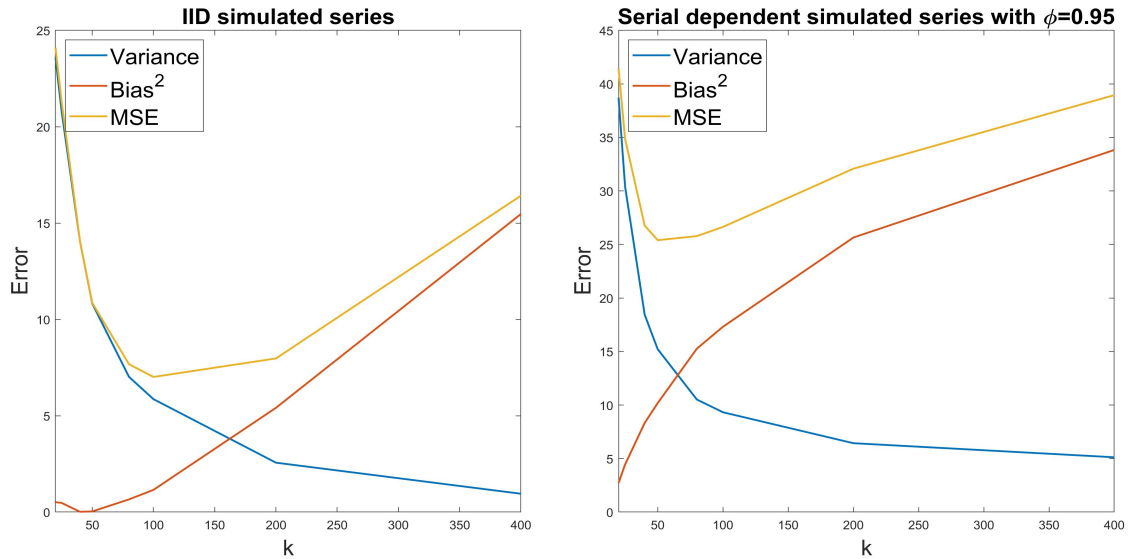


Figure 8: Decomposition of the MSE into variance and squared bias for BM method.

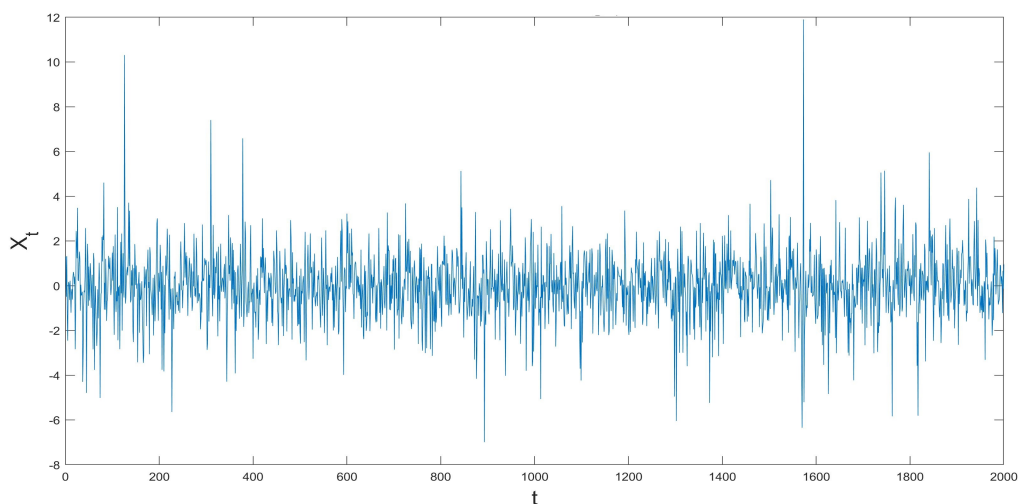
Figure 8 displays the variance and squared bias for the BM method. In the IID case, the minimum MSE is obtained around $k = 100$ and the difference of the variance and squared bias is clear. The squared bias is very low for small values of k and increases as k increases. Contrarily, the variance is large for small values of k and decreases as k increases. The effect of k on the squared bias and variance confirms the theory discussed in **3.3**. Introducing serial dependence shows that the minimum MSE lies around $k = 50$. In contrast to the POT method, the behavior of the squared bias for different values of k changes. The squared bias shows a much faster decrease as k increases, and the variance still decreases as k increases. The optimal k is much smaller than in the IID case, but the difference in MSE between $k = 50$ and $k = 100$ is quite small. Therefore, the value of k is fixed at 100 across the different simulation models.

5.2 Serial dependence: ARMA

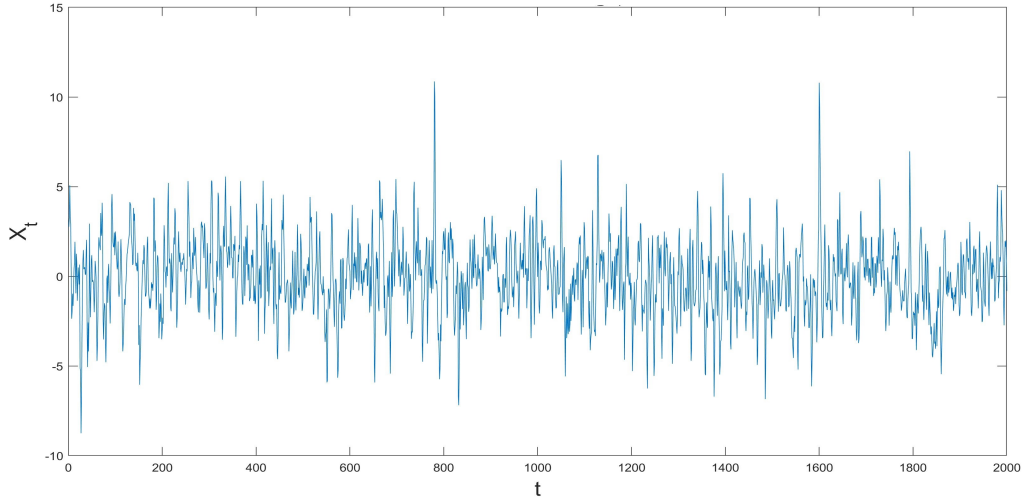
The simulation is divided into three groups to assess the performance of the POT and BM methods, which are discussed below. With the ARMA model the effect of serial dependence is highlighted. By extending the model with GARCH innovations, we can verify the estimation performance of the POT and BM methods in the presence of volatility clustering. In the same way, the impact of cross-sectional dependence in the tail on estimating the VaR is discussed by using the Clayton copula.

To analyze the serial dependence, the ARMA model defined by equation (36) is used. As the GARCH innovations and the cross-sectional dependence are not yet considered, we set the parameters to $w_1 = 1$, $w_2 = 0$, $\alpha_1 = 0$ and $\beta_1 = 0$. The innovations follow the Student's t-distribution with four degrees of freedom, $z_{t,1} \sim t(4)$, as this ensures fat tails, or equivalently $\xi > 0$. The level of serial dependence is controlled via the parameters ϕ_1 and π_1 . We set up a grid with the values of ϕ_1 and π_1 ranging from 0 to 0.95, with a step size of 0.05. Hence, this also includes the IID case whenever $\phi_1 = 0$ and $\pi_1 = 0$. Figure 9 displays three randomly chosen simulated time-series, in increasing order of serial dependence. The observed outliers are a confirmation of fat tails or $\xi > 0$, due to the Student's t distributed innovations.

(a) Simulated series with $\phi_1 = 0.1$ and $\pi_1 = 0.1$.



(b) Simulated series with $\phi_1 = 0.5$ and $\pi_1 = 0.5$.



(c) Simulated series with $\phi_1 = 0.9$ and $\pi_1 = 0.9$.

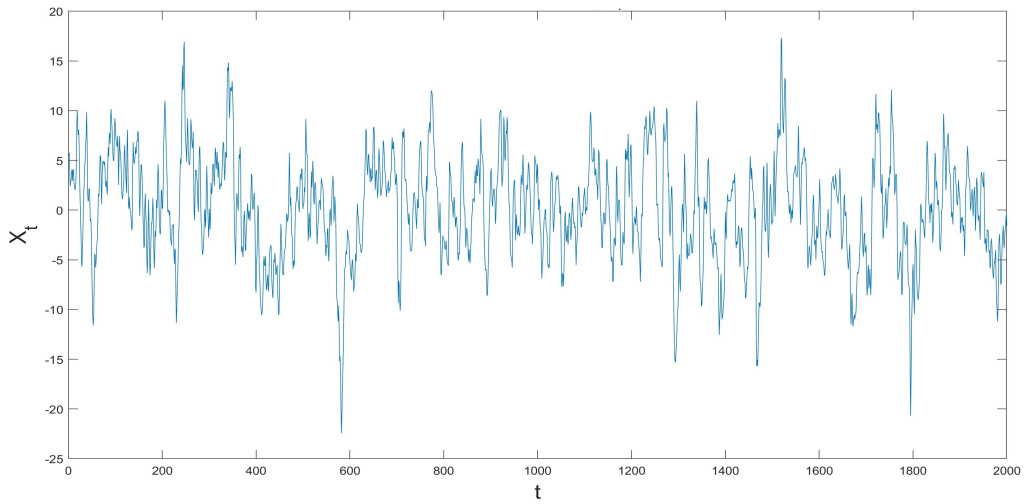
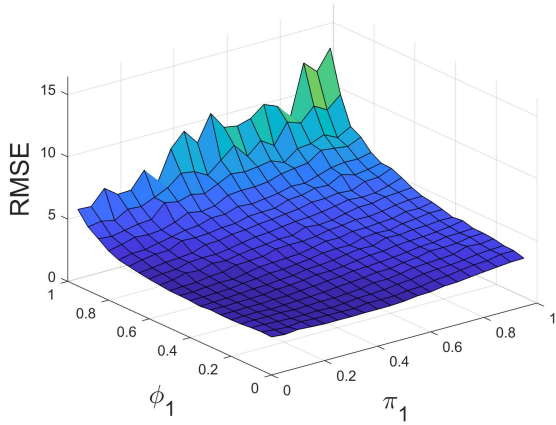


Figure 9: A random simulated series for three levels of serial dependency.

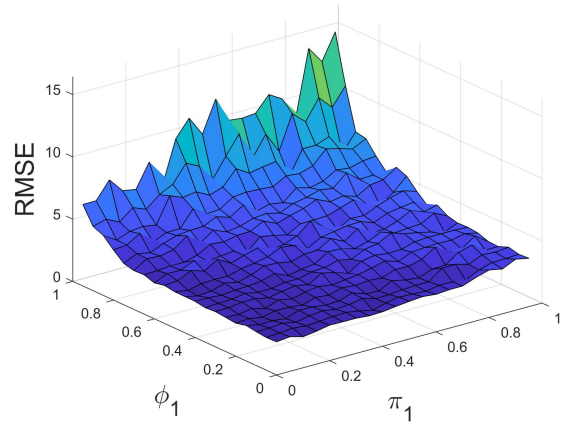
In total, the grid of different values for ϕ_1 and π_1 contains 400 combinations. For each combination, $m = 1,000$ time-series are simulated and the VaR is estimated using the POT and BM method, see equations (30) and (21) respectively. The evaluation metrics RMSE and RMSPE, see equations (38) and (39) respectively, are then calculated and the results are displayed in Figure 10. For the BM method, we use $\hat{\theta}_n^{(2),sl}$ in equation (22) to estimate the extremal index, as this estimator was found to always outperform $\hat{\theta}_n^{(1),sl}$. For three different values of π_1 , the comparison of the POT and BM methods are displayed in Figure 11 by comparing the ratio of the RMSPE.

In the IID case, the BM method estimates the VaR more accurately than the POT method. Ferreira and De Haan (2015) demonstrated that the POT is often more efficient than the BM method, when the number of exceedances are larger than the number of blocks. Furthermore, they wrote that for large sample sizes, the performances of the POT and BM method are comparable. This is in line with our findings, as the number of exceedances is not larger than the number of blocks. When comparing the RMSE across both methods, as shown in Figures 10 (a) and (b), both methods perform very similarly across different ϕ_1 and π_1 . The RMSE for the POT method is smoother than for the BM method across various values of ϕ_1 and π_1 . Both methods decrease in accuracy whenever the serial dependence increases, with the maximum RMSE obtained when $\phi_1 \rightarrow 1$ and $\pi_1 \rightarrow 1$. In Figure 11, we observe that the POT method almost always outperforms the BM method for $\phi_1 < 0.8$. However, at all three levels of π_1 , the BM method performs better than the POT method for $\phi_1 > 0.85$.

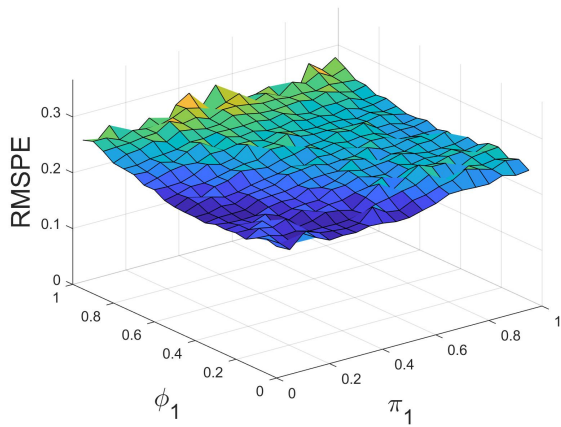
(a) RMSE - POT



(b) RMSE - BM (2)



(c) RMSPE - POT



(d) RMSPE - BM (2)

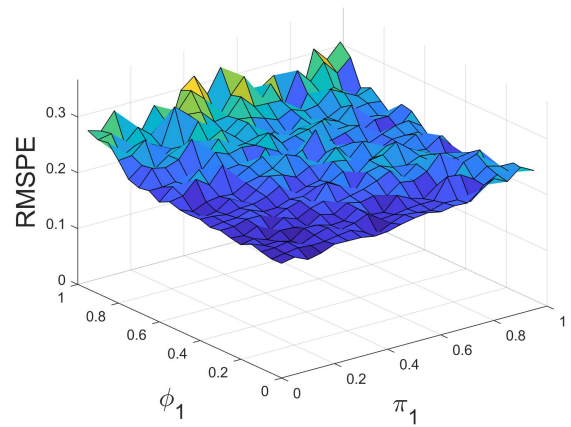


Figure 10: Surface plots of evaluation metrics RMSE and RMSPE for increasing ϕ_1 and π_1 .

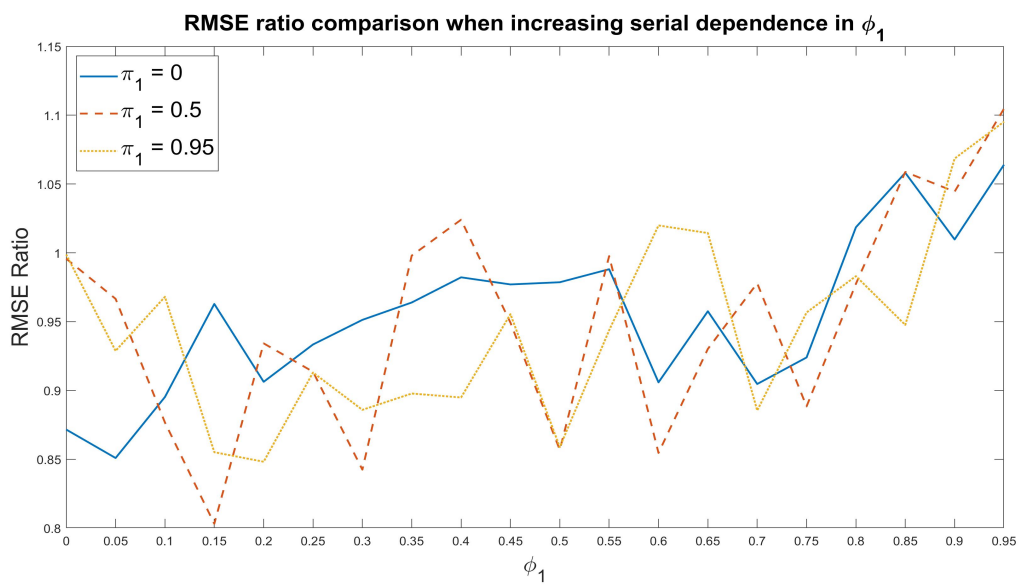


Figure 11: Comparison of the RMSE ratio for increasing ϕ_1 at three levels of π_1 .

Both methods show an increase in RMSE as ϕ_1 and π_1 increases. The reduction in the RMSE is stronger for higher ϕ_1 than π_1 , especially for the POT method. One reason for this could be that ϕ_1 contributes directly to the serial dependence via the lagged values, whereas π_1 achieves this indirectly via the lagged innovations. Hence, the level of serial dependence is more affected by the parameter ϕ_1 than π_1 which leads to decrease in performance as indicated by the RMSE. To compare the performance across different parameter specifications, the RMSPE shown in Figures 10 (c) and (d) and Figure 12 demonstrates that performance decreases as the level of serial dependence increases. Here, the BM method has much lower RMSPE values when ϕ_1 is lower, and higher RMSPE values than those of the POT when ϕ_1 is higher.

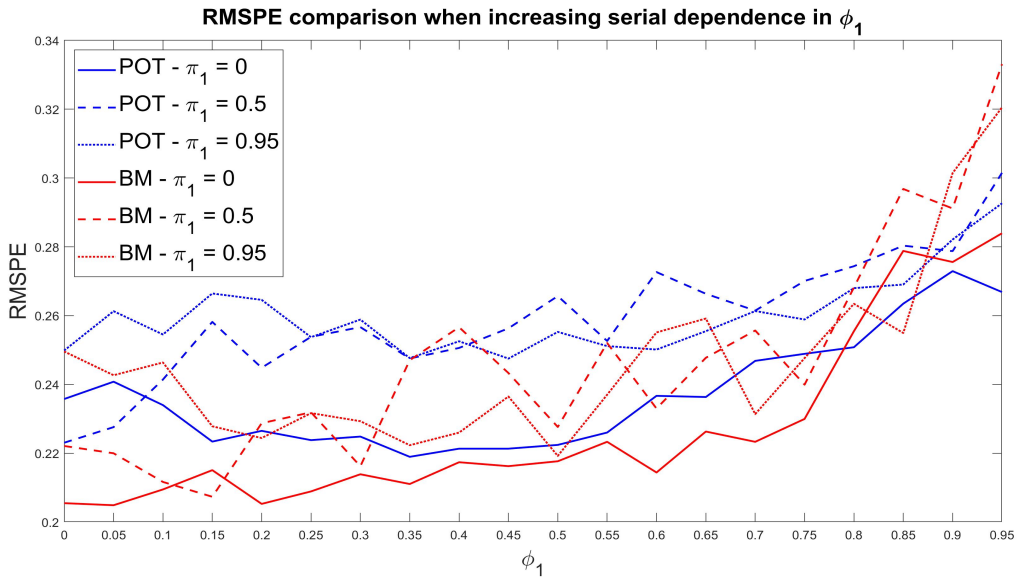


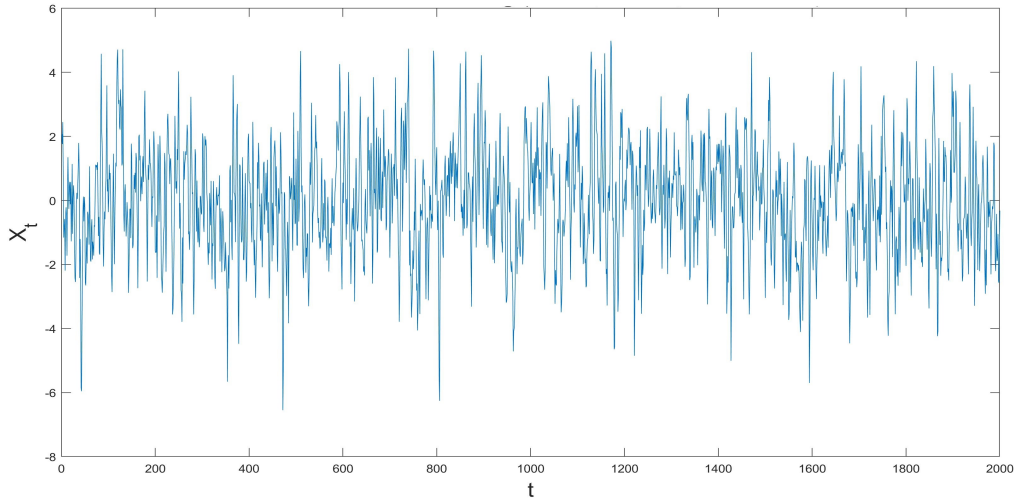
Figure 12: Comparison of the RMSPE for increasing ϕ at three levels of θ .

5.3 Volatility Clustering: GARCH

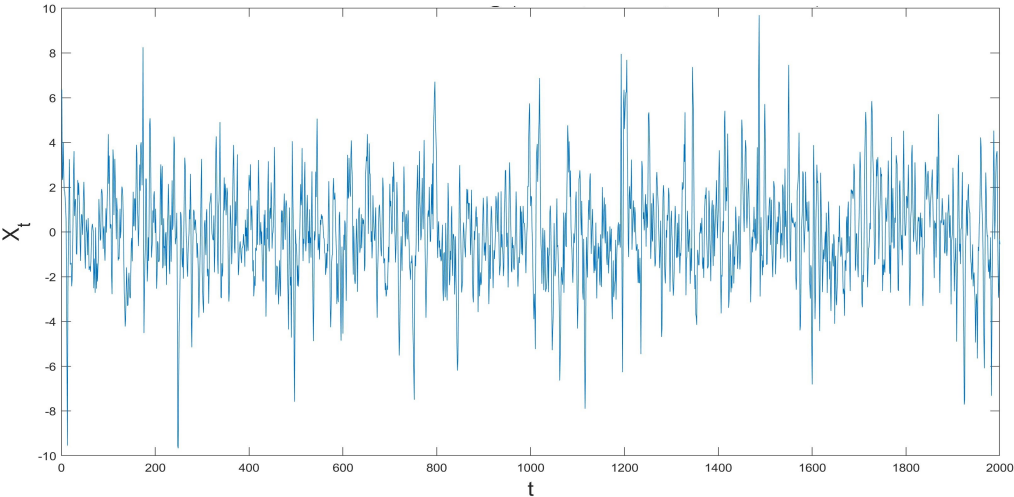
The simulation model is further extended to allow for innovations of the ARMA model follow a GARCH model. The cross-sectional dependence is not yet considered, hence we set the parameter of equation (36) as $w_1 = 0$. Again, $z_{t,1} \sim t(4)$ to ensure heavy tails. The parameters ϕ_1 and π_1 determine the level of serial dependence and the volatility clustering is controlled via α_1 and β_1 . Similarly to the ARMA models, we compose a grid with values for α_1 and β_1 ranging from 0 to 0.95 and with step size 0.05. Ignoring the case $\alpha_1 = \beta_1 = 0$ and taking the parameter restriction $\alpha_1 + \beta_1 < 1$ into account, results

in 209 parameter combinations. Increasing levels of $\alpha_1 + \beta_1$ indicates an increasing level of volatility clustering. We analyze five levels of serial dependence via the ARMA process by setting the parameters $\phi_1 = \pi_1 \in (0.1, 0.3, 0.5, 0.7, 0.9)$. Combining the ARMA models with the GARCH models results in a total of 1,045 different model specifications. Three randomly selected simulated time-series with an increasing level of volatility clustering are displayed in Figure 13.

(a) Simulated series with $\phi_1 = 0.5, \pi_1 = 0.5, \alpha_1 = 0.1$ and $\beta_1 = 0.1$.



(b) Simulated series with $\phi_1 = 0.5, \pi_1 = 0.5, \alpha_1 = 0.25$ and $\beta_1 = 0.25$.



(c) Simulated series with $\phi_1 = 0.5$, $\pi_1 = 0.5$, $\alpha_1 = 0.45$ and $\beta_1 = 0.45$.

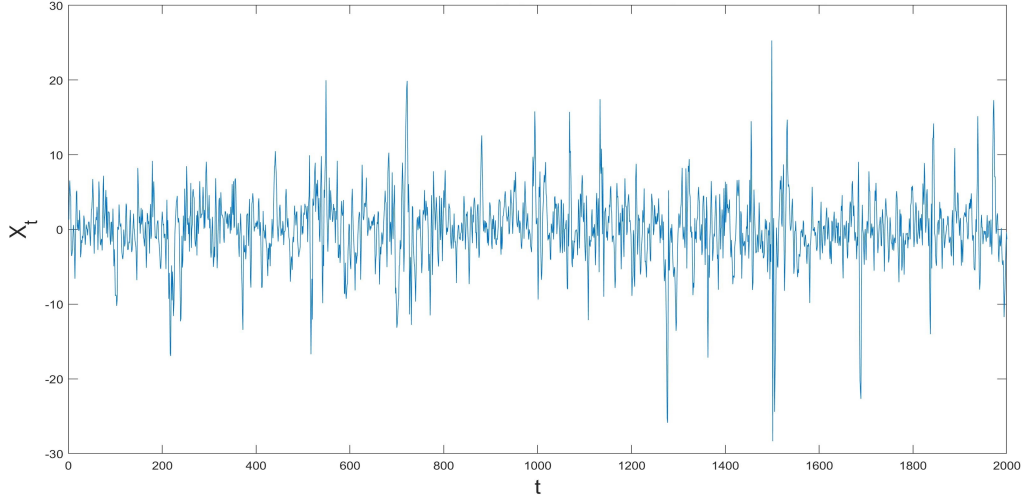
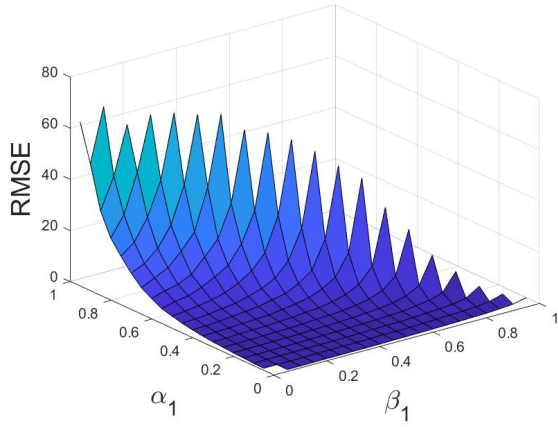


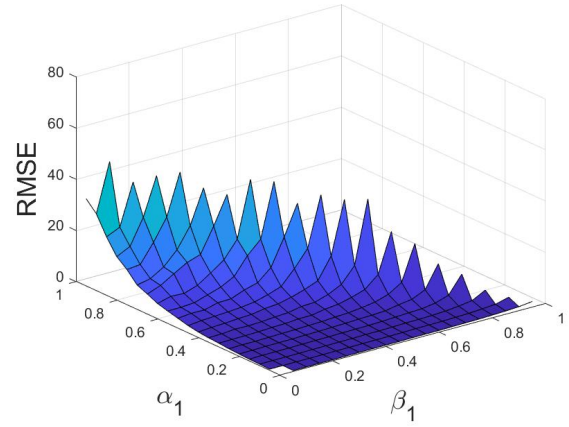
Figure 13: A random simulated series for three levels of volatility clustering.

The calculated RMSE and RMSPE for all possible combinations of α_1 and β_1 and with $\phi_1 = \pi_1 = 0.5$ are displayed in Figure 14. The graphs containing the results for the remaining four levels of serial dependence can be found in the Appendix, Figures 25 - 28. Comparing the POT and BM methods in terms of RMSE values, as shown in Figures 14 (a) and (b), indicates that the BM method is better overall. In Figure 15 the ratio of the RMSPE is plotted against α_1 with $\beta_1 = 0$ and three levels of serial dependence. For $\phi_1 = \pi_1 = 0.9$, the POT and BM methods leads to almost identical RMSE. For the other two levels of serial dependence the BM method has a lower RMSE than the POT method. The difference in performance between the POT and BM methods is higher as the level of volatility increases. The true VaR increases substantially when the level of volatility clustering increases. One potential reason for that is the fact that increasing the volatility clustering leads to more extreme values. To compare the performance across different levels of volatility clustering, we consider the RMSPE displayed in Figures 14 (c) and (d) and Figure 16. As the level of volatility clustering increases, the RMSPE increases. Overall, increasing the volatility clustering has a greater impact on the performance than increasing the serial dependence in the ARMA setup.

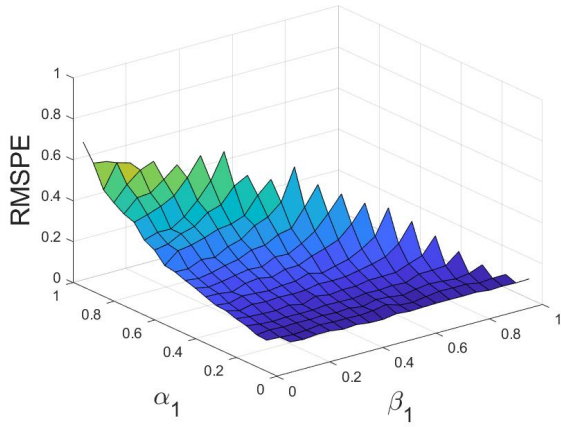
(a) RMSE - POT



(b) RMSE - BM (2)



(c) RMSPE - POT



(d) RMSPE - BM (2)

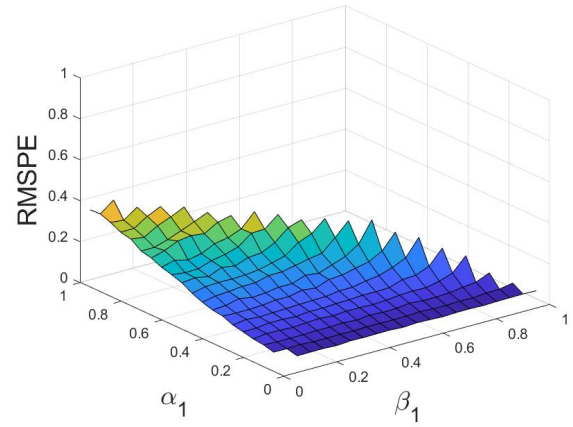


Figure 14: Surface plots of the evaluation metrics RMSE and RMSPE for increasing α_1 and β_1 with $\phi_1 = \pi_1 = 0.5$.

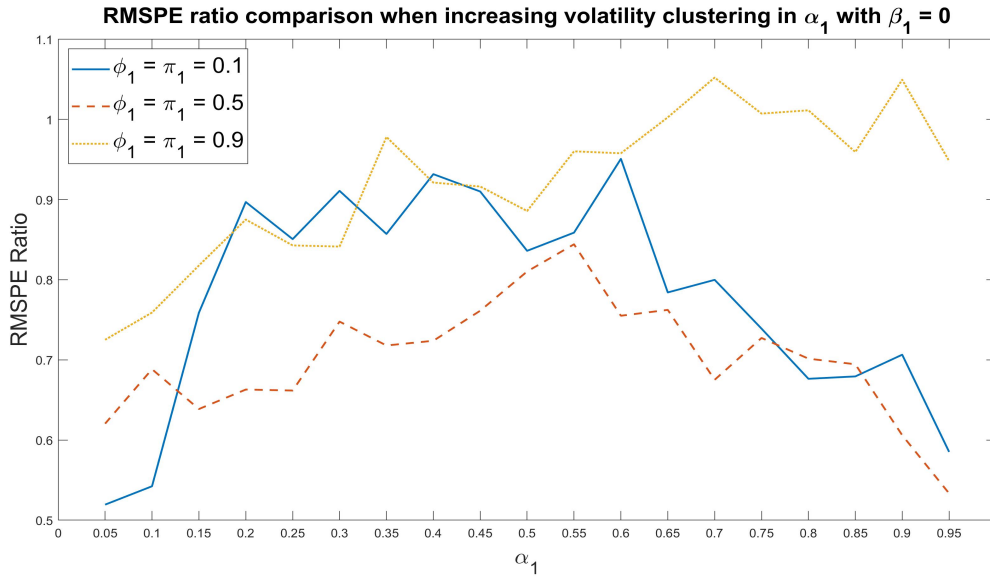


Figure 15: Comparing the RMSPE ratio for increasing α_1 at three levels of serial dependence and $\beta_1 = 0$.

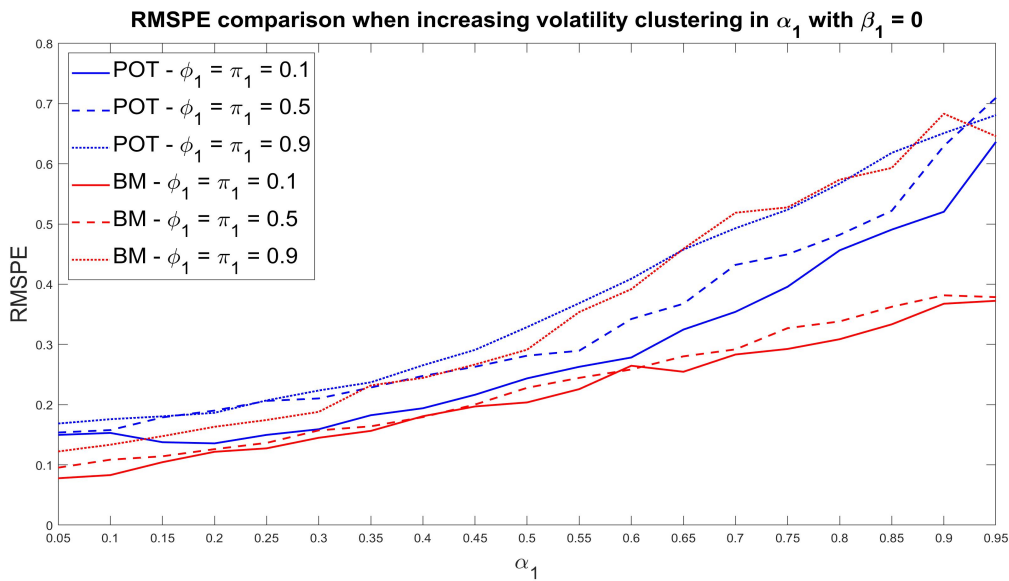


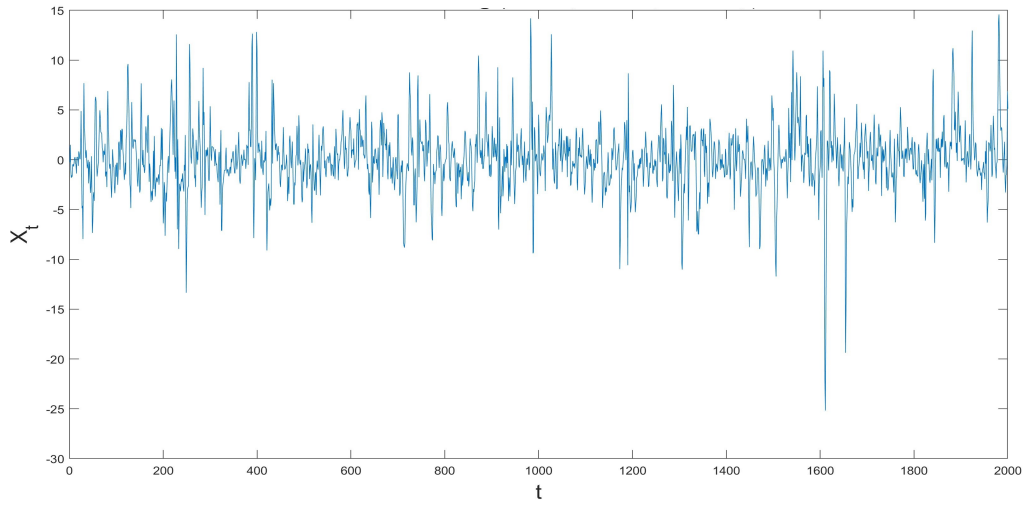
Figure 16: Comparing the RMSPE for increasing α at three levels of serial dependence and $\beta = 0$.

5.4 Cross-sectional dependence: Clayton copula

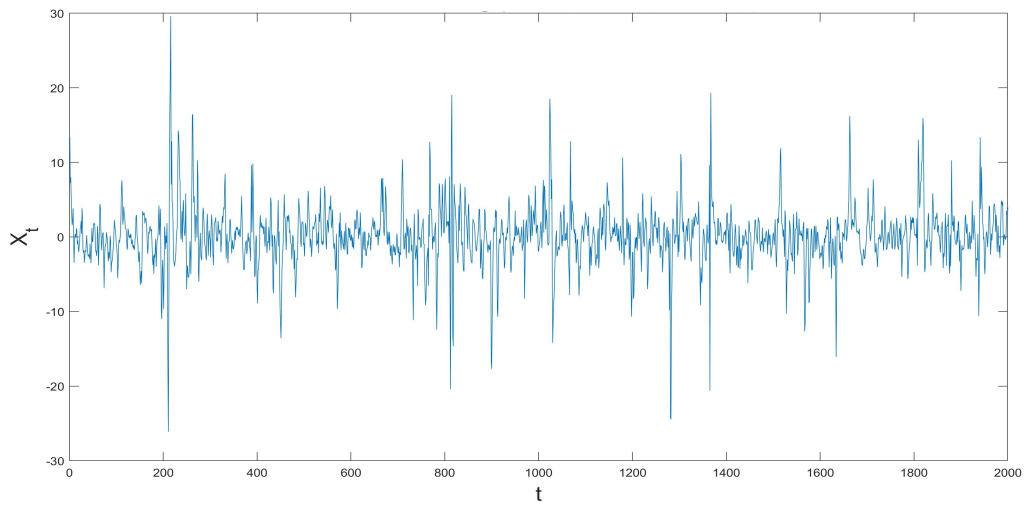
The simulation model is now extended once more to incorporate cross-sectional dependence and is fully derived in Algorithm 1. A univariate time-series is obtained as the equally weighted average of two series, each simulated using the ARMA-GARCH model

described previously. However, it now holds that $j \in (1, 2)$ and the joint distribution of $z_{t,1}$ and $z_{t,2}$ can be described by a Clayton copula. The level of tail dependence between $z_{t,1}$ and $z_{t,2}$ is set via the parameter θ^{Cl} , where we let $\theta^{Cl} \in (1, 2, \dots, 9, 10)$. We again consider five levels of serial dependence with $\phi_j = \pi_j \in (0.1, 0.3, 0.5, 0.7, 0.9)$ and 19 levels of volatility clustering with $\alpha_j \in (0.05, 0.10, \dots, 0.90, 0.95)$ and $\beta_j = 0$. This results in a total of 900 models with different parameter specifications. Three randomly selected simulated time-series with different levels of cross-sectional dependence are displayed in Figure 17.

(a) Simulated series with $\phi = 0.5$, $\pi = 0.5$, $\alpha = 0.5$, $\beta = 0$ and $\theta^{Cl} = 1$.



(b) Simulated series with $\phi = 0.5$, $\pi = 0.5$, $\alpha = 0.5$, $\beta = 0$ and $\theta^{Cl} = 6$.



(c) Simulated series with $\phi = 0.5$, $\pi = 0.5$, $\alpha = 0.5$, $\beta = 0$ and $\theta^{Cl} = 10$.

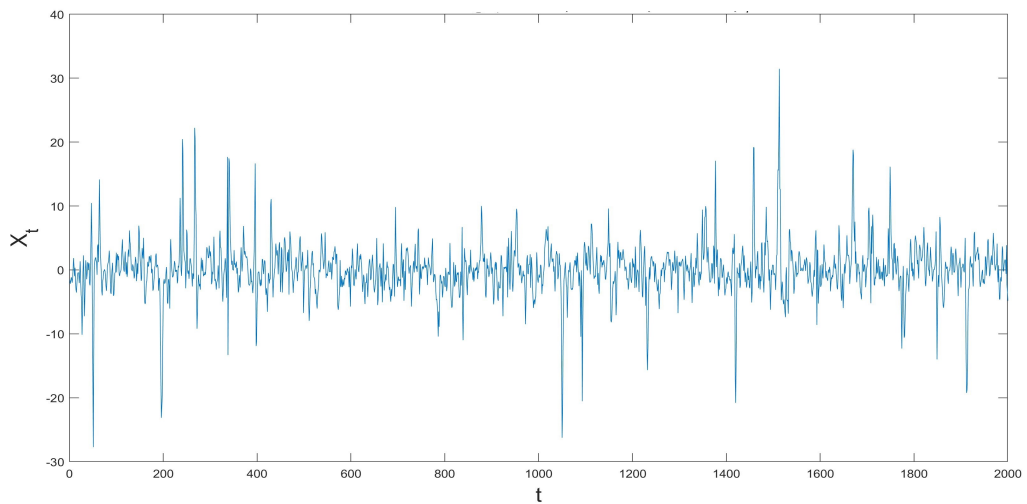


Figure 17: A random simulated series for three levels of cross-sectional dependency.

We now compare the POT method and the BM method by examining the results of the RMSE and the RMSPE ratio, displayed in Figures 18 (a) and (b) and Figure 19, respectively. We observe that the BM method performance better than the POT method. However, increasing the level of cross-sectional dependence does not lead to an increase in the RMSE for either method.

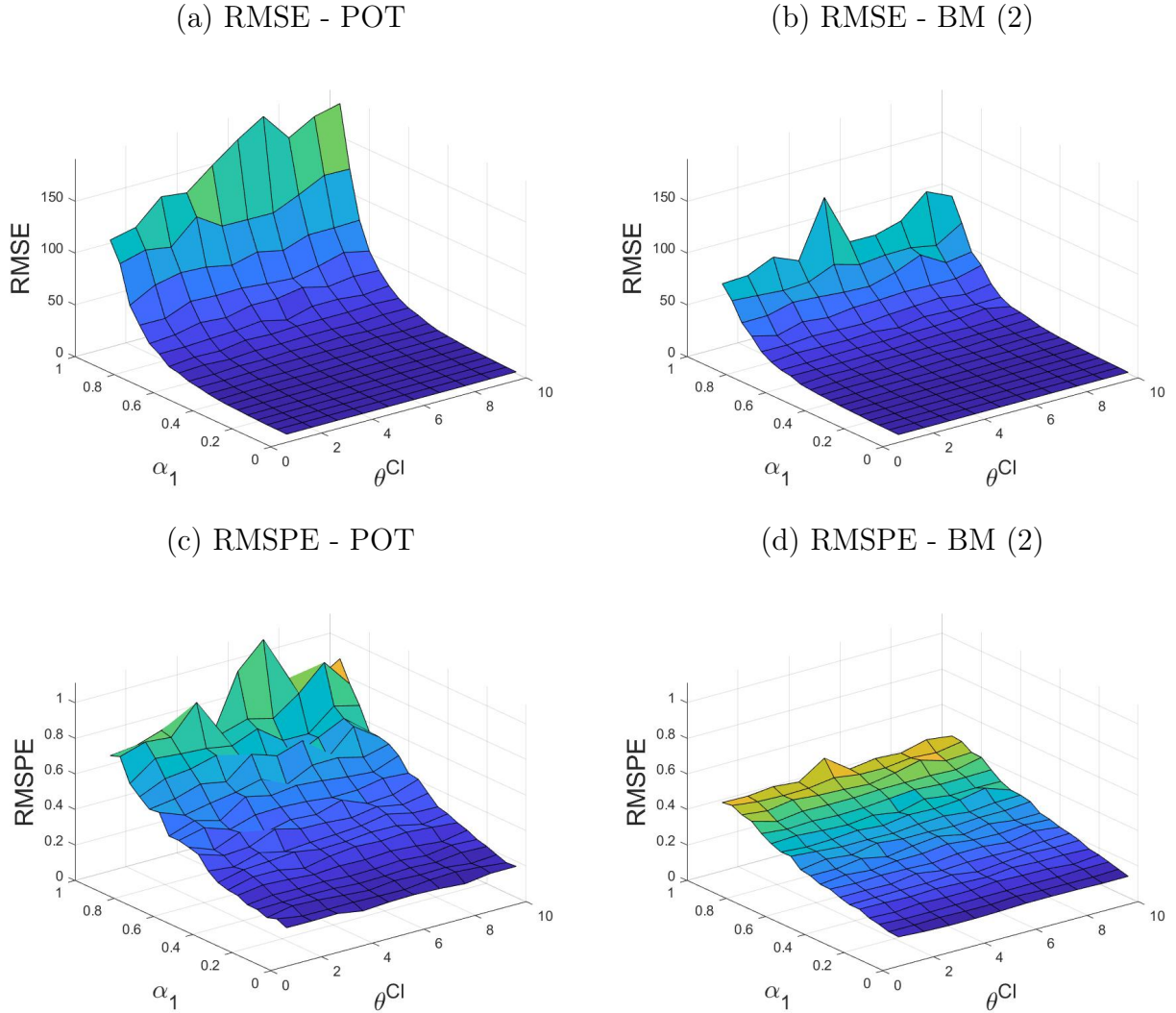


Figure 18: Surface plots of the evaluation metrics RMSE and RMSPE for increasing α and θ^{Cl} and with ϕ and π set to 0.5.

Across different levels of cross-sectional dependence, the performance of both methods is rather constant, as indicated by the RMSPE in Figure 20. We can conclude that the existence of cross-sectional dependence affect neither the performance of the POT nor that of the BM method. The fact that the BM method performed better than the POT method, as indicated by the RMSE, can therefore entirely explained by the level of serial dependence and more prominently by the level of volatility clustering. The other surface

plots of the RMSE and RMSPE for different model specifications can be found in the Appendix Figures 30 - 33.

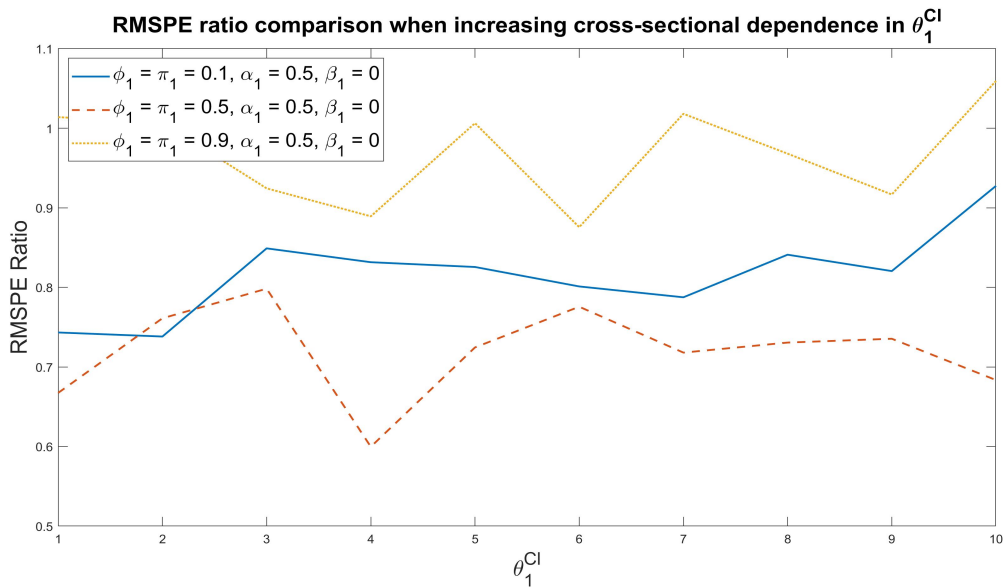


Figure 19: Comparing the RMSPE ratio for increasing θ^{Cl} at three levels of serial dependence and $\alpha = 0.5$ and $\beta = 0$.

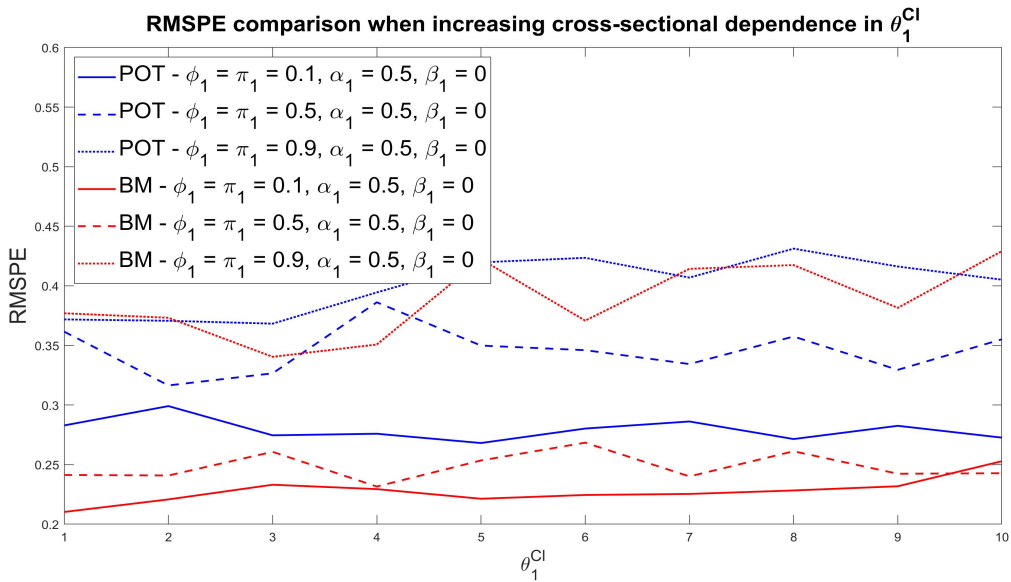


Figure 20: Comparison of the RMSPE for increasing θ^{Cl} at three levels of serial dependence and $\alpha = 0.5$ and $\beta = 0$.

6 Financial Application

The POT and BM methods are applied in the financial application to estimate the 99%, 99.5% and 99.9% VaR on a stock-bond portfolio. The VaR estimates are evaluated by using the binomial method of Christoffersen (1998). The portfolio returns consist of 4,550 daily observations and are split into a training and a test sample. The training sample contains the first 3,550 observations and are used to estimate the VaR using both methods. Meanwhile, the last 1,000 observations are used as the test sample. The estimated parameters of the POT and BM method that are used to estimate the VaR are provided in Table 4. For the POT method the high quantile estimator only depends on the shape parameter ξ and the intermediate quantile whereas for the BM method, the high quantile estimator depends on the θ and σ parameters as well. Comparing the estimated value of the shape parameter, $\hat{\xi}$, the POT and BM method resulted in similar values with 0.1974 and 0.1966, respectively. This is in line with the fact that the distribution of financial losses is heavy-tailed. The extremal index is estimated as $\hat{\theta} = 0.4412$, which indicates that the financial losses contain clusters with an average cluster size of 2.2665. The sample size is essentially reduced to $n\hat{\theta} = 3,550 * 0.4412 \approx 1566$ of roughly independent clusters of observations.

Table 3: Estimated parameters of the POT and BM method.

	POT	BM
$\hat{\xi}$	0.1974	0.1966
$\hat{\theta}$		0.4412
$\hat{\sigma}$		0.0182

The effect of k , the number of exceedances or blocks in the POT and BM method, respectively, on the 99% quantile estimation is displayed in Figure 21. The value of k is chosen as $k = 20$ and $k = 100$ for the POT and BM method, respectively. For the POT method, the quantile estimate convergences as the number of exceedances increases. For small values of k , the estimator suffers from the small estimation sample which results in an estimated quantile that lies far from the empirical quantile. The BM method shows a different pattern with no clear convergence as the number of blocks increases. However,

the number of blocks does not influence the estimated quantile much.

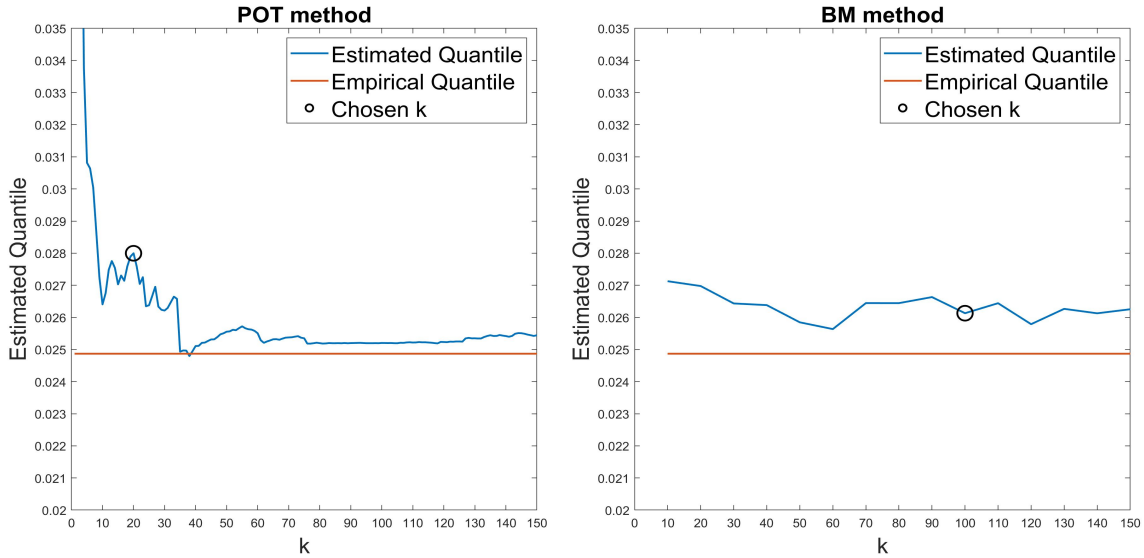


Figure 21: Estimated 99% VaR for increasing values in k .

The binomial method might not be suitable for assessing the $VaR_{0.99}$ on a test sample of size 1,000. Whenever the empirical number of exceedances equals the expected number of exceedances of 1, the test statistic will be equal to zero. Therefore, $VaR_{0.99}$ is not backtested and only the VaR estimates are provided. Tables 4, 5 present the results for the $VaR_{0.99}$ and $VaR_{0.995}$, respectively.

Table 4: Results of estimating the $VaR_{0.99}$.

	POT		BM	
Est. VaR	0.0280		0.0261	
	Training Sample	Test Sample	Training Sample	Test Sample
99% Quantile	0.0249	0.0204	0.0249	0.0204
Exceedances	27 (0.0076)	2 (0.002)	34 (0.0096)	3 (0.003)
LR statistic	2.2361	9.6267	0.0641	6.8255
p -value	0.1348	0.0019	0.8002	0.0090

Considering the results in Table 4, the $VaR_{0.99}$ is estimated as 0.0280 and 0.0261 by POT and BM, respectively, on the training sample. These are very close to the empirical 99% quantile of 0.0249. Comparing the POT and BM methods for the test sample, we

observe that the number of exceedances for POT equals 2, and for BM equals 3. The values within the brackets correspond with the empirical probability a^* . However, the expected number of exceedances is 10 and is far off. The POT method has a test statistic of 9.6267 and the null hypothesis is rejected at a 5% confidence level. With one additional observation exceeding the estimated VaR, the BM method has a test statistic of 6.8255 and the null hypothesis is also rejected at a 5% confidence level. Both methods reject the null hypothesis because there are not enough exceedances. However, as the BM method does have more exceedances than the POT method, we can conclude that the BM method performs better because it yields a lower point estimate, albeit not convincingly. Notice that the empirical 99% quantile of the test sample is much lower than that of the training sample, which leads to fewer exceedances. As the VaR is estimated on the training sample, the estimated VaR lies closer to the empirical quantile of the training sample than that of the test sample for both methods. Consequently, applying the binomial test on the training sample results in a higher coverage, as indicated by the test statistic and p -values.

Table 5: Results of estimating the $VaR_{0.995}$.

	POT		BM	
Est. VaR	0.0321		0.0325	
	Training Sample	Test Sample	Training Sample	Test Sample
99.5% Quantile	0.0317	0.0256	0.0317	0.0256
Exceedances	16 (0.0045)	2 (0.002)	15 (0.0042)	2 (0.002)
LR statistic	0.1784	2.3439	0.4505	2.3439
p -value	0.6728	0.1258	0.5021	0.1258

Similar to the result for $VaR_{0.99}$, the $VaR_{0.995}$ estimates are close to the empirical 99.5% quantile. The number of exceedances in the test sample, 2, is exactly the same for the POT as for the BM method. Therefore, the test statistic and p -values are also identical. Neither the POT nor the BM method reject the null hypothesis at a 5% confidence level. Figures 22 and 23 display the coverage of the $VaR_{0.99}$ estimates on the training and test sample, respectively. The $VaR_{0.999}$ estimates of the POT and BM method equals 0.0441 and 0.0512, respectively. The POT estimates is closer to the empirical quantile of 0.0444 but this is not meaningful as empirical quantile may not be an accurate estimate

for such a high level of probability.

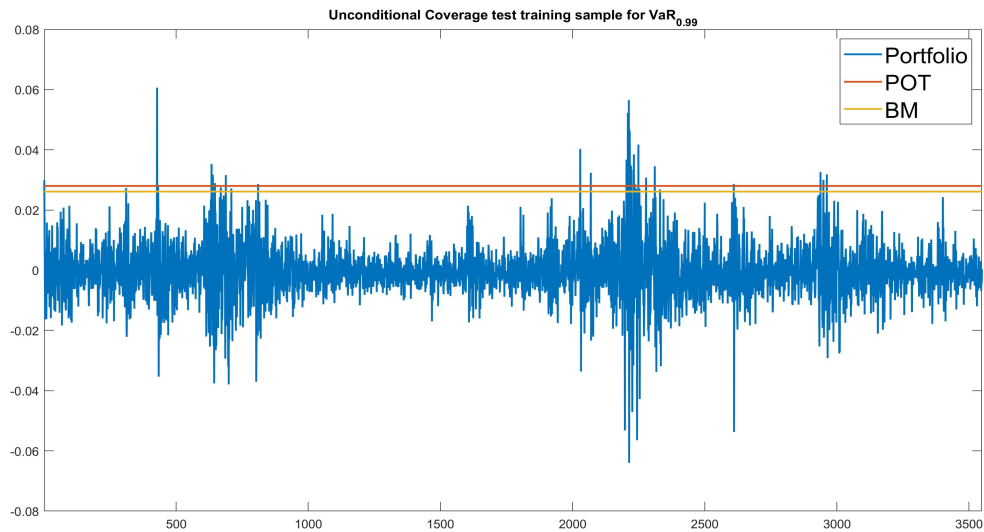


Figure 22: Unconditional coverage of the POT and BM methods for the $VaR_{0.99}$ estimate on the training sample.

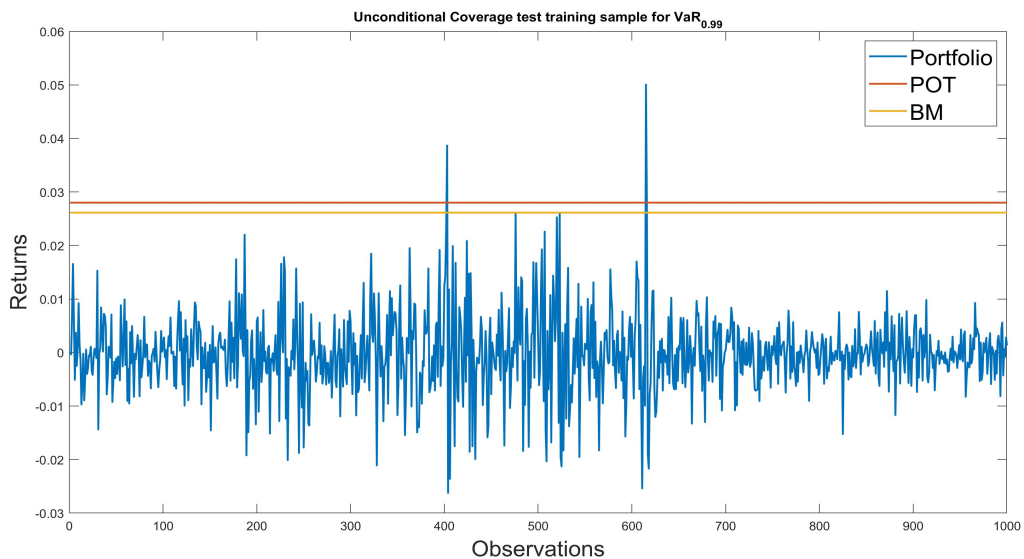


Figure 23: Unconditional coverage of the POT and BM methods for the $VaR_{0.99}$ estimate on the test sample.

7 Conclusion

In this research we analyze and compare the POT and BM methods for estimating the VaR of a strictly stationary time-series. In a simulation setup, we examine the effects of

serial dependence, volatility clustering and cross-sectional dependence on the estimation of the VaR. We then estimate the VaR on a stock-bond portfolio in a financial application, where the POT and BM methods are compared by backtesting the conditional coverage.

Firstly, comparing the POT and BM methods in estimating the VaR on serially dependent observations, the BM method outperforms the POT method for lower levels of serial dependence, particularly for the IID case. When the serial dependence was considerably elevated, the POT method estimates the VaR more accurately than the BM method. When comparing the RMSPE, it became evident that an increase in serial dependence has a greater negative impact on the BM method. Secondly, introducing volatility clustering has a larger negative effect on both the POT and BM methods. The POT method performs worse at higher levels of volatility clustering and was outperformed by the BM method in terms of the RMSE. Furthermore, increasing the volatility clustering showed a trend in the RMSPE: at the maximum level of volatility clustering, the RMSPE was over five times higher than the RMSPE without volatility clustering. Finally, the POT method performs better than the BM method across different models when allowing for cross-sectional dependence. Nevertheless, the level of cross-sectional dependence does not influence the performance much as indicated by the RMSPE.

The financial application shows that the BM method performed slightly better than the POT method in the out-of-sample backtest when estimating the $VaR_{0.99}$. Both methods reject the null hypothesis but the BM method has a smaller test statistic than the POT method. This result is in line with our findings in the simulation setup that the BM method is better when the level of serial dependence is not extremely high. The results for $VaR_{0.995}$ show that the BM and POT method both do not reject the null hypothesis and the performance of each method is exactly equal. Hence, we can not conclude which method performs better. Overall, by combining the results of the simulation and financial application we conclude that the BM method empirically outperforms the POT method for IID or low levels serial dependent observations. For extremely high levels of serial dependence, the POT method is better than the BM method.

This study makes some arbitrary assumptions hence leaves room for potential future

research. Firstly, the value of k is kept constant across different simulation models. Alternatively, one may optimize k for different levels of serial dependence, volatility clustering or cross-sectional dependence. Accordingly, it would be interesting to investigate how the two methods compare when both are optimized for the parameter k . Secondly, the degrees of freedom in the Student's t-distribution used as the stochastic part in the simulation setup is set to 4. Different degrees of freedom or strength of decay in heavy-tailed distributions as indicated by the tail index might lead to other results.

References

- Balkema, A. A., & De Haan, L. (1974). Residual life time at great age. *The Annals of Probability*, 2(5), 792–804.
- Berghaus, B., & Bücher, A. (2018). Weak convergence of a pseudo maximum likelihood estimator for the extremal index. *The Annals of Statistics*, 46(5), 2307–2335.
- Bücher, A., & Segers, J. (2018). Maximum likelihood estimation for the fréchet distribution based on block maxima extracted from a time series. *Bernoulli*, 24(2), 1427–1462.
- Christoffersen, P. F. (1998). Evaluating interval forecasts. *International Economic Review*, 39(4), 841–862.
- Danielsson, J., Ergun, L., de Haan, L., & de Vries, C. (2016). Tail index estimation: Quantile driven threshold selection.
- De Haan, L., & Ferreira, A. (2006). *Extreme value theory: an introduction*. Springer Science & Business Media.
- de Haan, L., & Rootzén, H. (1993). On the estimation of high quantiles. *Journal of Statistical Planning and Inference*, 35(1), 1–13.
- Dekkers, A. L., Einmahl, J. H., & De Haan, L. (1989). A moment estimator for the index of an extreme-value distribution. *The Annals of Statistics*, 17(4), 1833–1855.
- Drees, H. (2003). Extreme quantile estimation for dependent data, with applications to finance. *Bernoulli*, 9(4), 617–657.
- Ferreira, A., & De Haan, L. (2015). On the block maxima method in extreme value theory: Pwm estimators. *The Annals of Statistics*, 43(1), 276–298.
- Fisher, R. A., & Tippett, L. H. C. (1928). Limiting forms of the frequency distribution of the largest or smallest member of a sample. In *Mathematical proceedings of the cambridge philosophical society* (Vol. 24, pp. 180–190).
- Gnedenko, B. (1943). Sur la distribution limite du terme maximum d’une serie aleatoire. *Annals of Mathematics*, 44(3), 423–453.

- Hill, B. M. (1975). A simple general approach to inference about the tail of a distribution. *The Annals of Statistics*, 3(5), 1163–1174.
- Hosking, J. R., & Wallis, J. R. (1987). Parameter and quantile estimation for the generalized pareto distribution. *Technometrics*, 29(3), 339–349.
- Hosking, J. R., Wallis, J. R., & Wood, E. F. (1985). Estimation of the generalized extreme-value distribution by the method of probability-weighted moments. *Technometrics*, 27(3), 251–261.
- Hsing, T. (1993). Extremal index estimation for a weakly dependent stationary sequence. *The Annals of Statistics*, 21(4), 2043–2071.
- Kotz, S., & Nadarajah, S. (2000). *Extreme value distributions: theory and applications*. World Scientific.
- Leadbetter, M. R. (1983). Extremes and local dependence in stationary sequences. *Probability Theory and Related Fields*, 65(2), 291–306.
- Mandelbrot, B. (1963). New methods in statistical economics. *Journal of Political economy*, 71(5), 421–440.
- Mandelbrot, B. (1997). The variation of certain speculative prices. In *Fractals and scaling in finance* (pp. 371–418). Springer.
- McNeil, A. J. (1998). *Calculating quantile risk measures for financial return series using extreme value theory* (Tech. Rep.). ETH Zurich.
- McNeil, A. J., Frey, R., Embrechts, P., et al. (2005). *Quantitative risk management: Concepts, techniques and tools* (Vol. 3). Princeton university press Princeton.
- Northrop, P. J. (2015). An efficient semiparametric maxima estimator of the extremal index. *Extremes*, 18(4), 585–603.
- Pickands, J. (1975). Statistical inference using extreme order statistics. *The Annals of Statistics*, 3(1), 119–131.
- Prescott, P., & Walden, A. (1980). Maximum likelihood estimation of the parameters of the generalized extreme-value distribution. *Biometrika*, 67(3), 723–724.

Smith, R. L. (1987). Estimating tails of probability distributions. *The Annals of Statistics*, 15(3), 1174–1207.

Smith, R. L., & Weissman, I. (1994). Estimating the extremal index. *Journal of the Royal Statistical Society. Series B (Methodological)*, 56(3), 515–528.

A Appendices

A.1 Maximum Domain of Attraction Examples

Recalling the rate of convergence for maxima follows

$$\lim_{n \rightarrow \infty} P \left(\frac{M_n - b_n}{a_n} \leq x \right) = \lim_{n \rightarrow \infty} F^n(a_n x + b_n) = H(x), \quad (42)$$

two examples are constructed for the underlying distributions: exponential and Pareto.

Exponential distribution

Assume the underlying distribution to be exponential with distribution function $F(x) = 1 - \exp(-\beta x)$ for $\beta > 0$ and $x \geq 0$, then the limiting distribution of maxima can directly be calculated by choosing the normalizing constants $a_n = \frac{1}{\beta}$ and $b_n = \frac{\ln(n)}{\beta}$. It holds that

$$\begin{aligned} F^n(a_n x + b_n) &= F^n \left(\frac{x}{\beta} + \frac{\ln(n)}{\beta} \right), \\ F^n(a_n x + b_n) &= \left(1 - \frac{1}{n} \exp(-x) \right)^n, \quad x \geq -\ln(n), \end{aligned} \quad (43)$$

$$\lim_{n \rightarrow \infty} F^n(a_n x + b_n) = \exp(-\exp(-x)), \quad x \in \mathbb{R}.$$

Hence, we conclude that $F \in MDA(H_0)$.

Pareto distribution

Assume the underlying distribution to be Pareto with parameters α and k and distribution function $F(x) = 1 - \left(\frac{k}{k+x}\right)^\alpha$ for $\alpha > 0$, $k > 0$ and $x \geq 0$, then the limiting distribution of maxima can directly be calculated by choosing the normalizing constants $a_n = k \frac{n^{\frac{1}{\alpha}}}{\alpha}$ and $b_n = kn^{\frac{1}{\alpha}} - k$. It holds that

$$\begin{aligned} F^n(a_n x + b_n) &= F^n \left(k \frac{n^{\frac{1}{\alpha}}}{\alpha} x + \left(kn^{\frac{1}{\alpha}} - k \right) \right), \\ F^n(a_n x + b_n) &= \left(1 - \frac{1}{n} \left(1 + \frac{x}{\alpha} \right)^{-\alpha} \right)^n, \quad 1 + \frac{x}{\alpha} \geq n - \frac{1}{\alpha}, \\ \lim_{n \rightarrow \infty} F^n(a_n x + b_n) &= \exp \left(- \left(1 + \frac{x}{\alpha} \right)^{-\alpha} \right), \quad 1 + \frac{x}{\alpha} > 0, \end{aligned} \quad (44)$$

Hence, we conclude that $F \in MDA \left(H_{\frac{1}{\alpha}} \right)$.

A.2 Slowly and regularly varying functions

Slowly varying functions

A positive, Lebesgue-measurable function L on $(0, \infty)$ is slowly varying at ∞ if

$$\lim_{x \rightarrow \infty} \frac{L(ux)}{L(x)} = 1, u > 0. \quad (45)$$

Regularly varying functions

A positive, Lebesgue-measurable function J on $(0, \infty)$ is regularly varying at ∞ with index $\rho \in \mathcal{R}$ if

$$\lim_{x \rightarrow \infty} \frac{J(ux)}{J(x)} = u^\rho, u > 0. \quad (46)$$

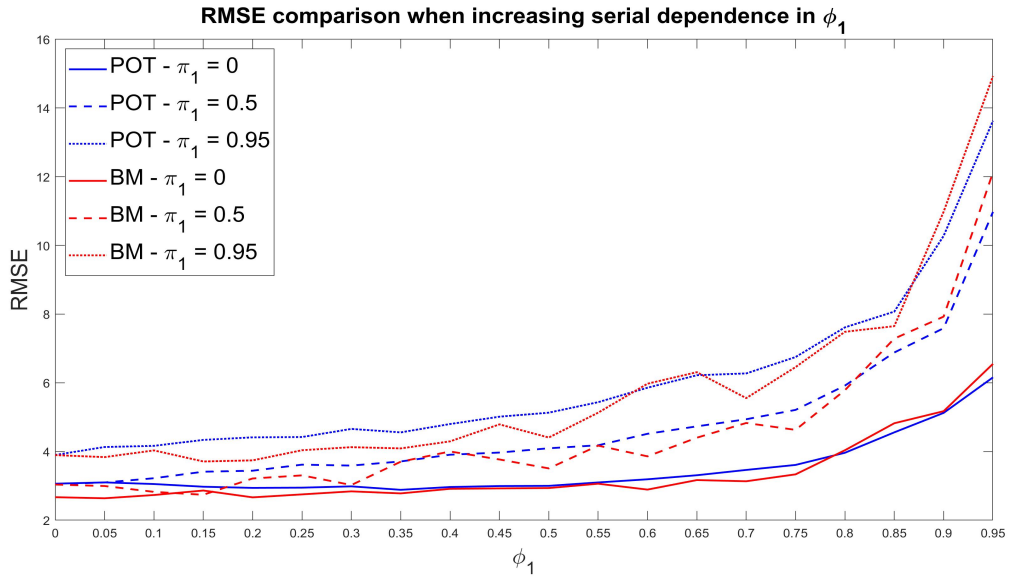
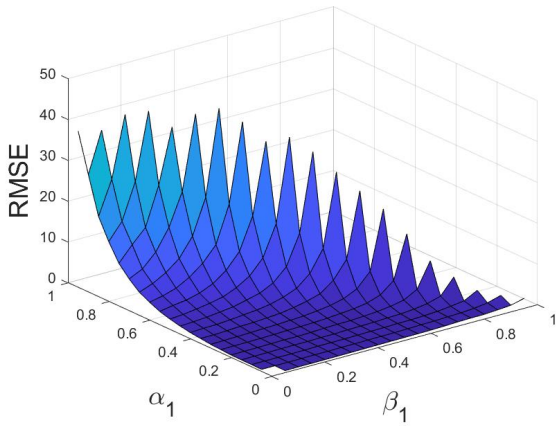


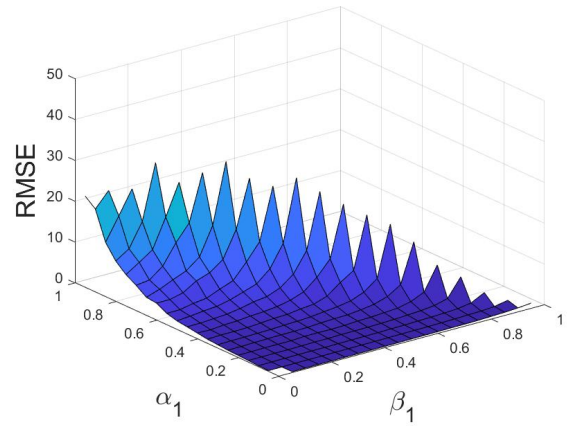
Figure 24: Comparison of the RMSE for increasing ϕ at three levels of π .

(a) RMSE - POT

(b) RMSE - BM (2)



(c) RMSPE - POT



(d) RMSPE - BM (2)

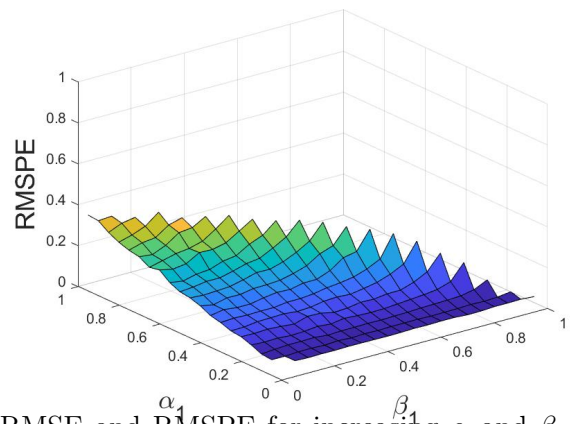
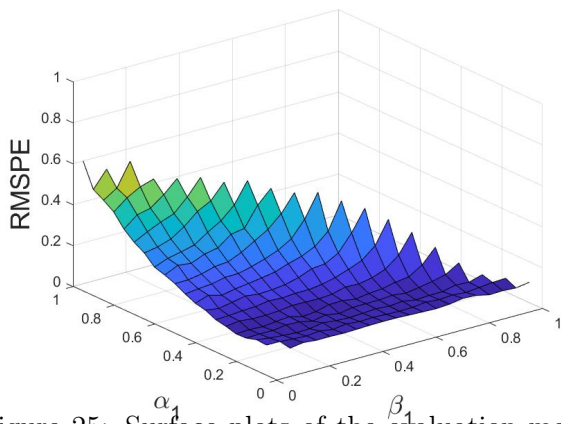
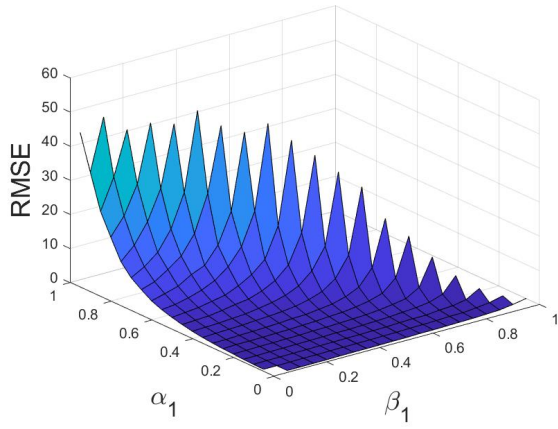
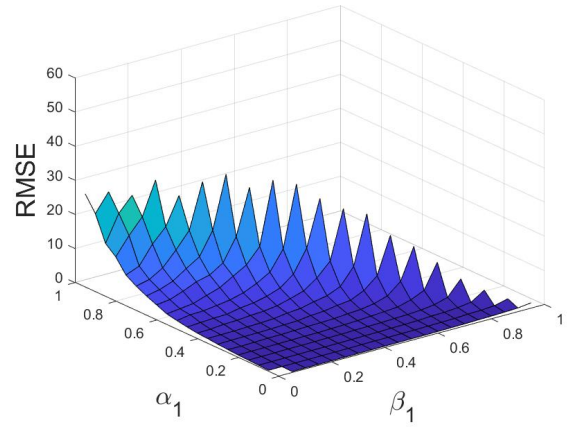


Figure 25: Surface plots of the evaluation metrics RMSE and RMSPE for increasing α and β with $\phi = \theta = 0.1$.

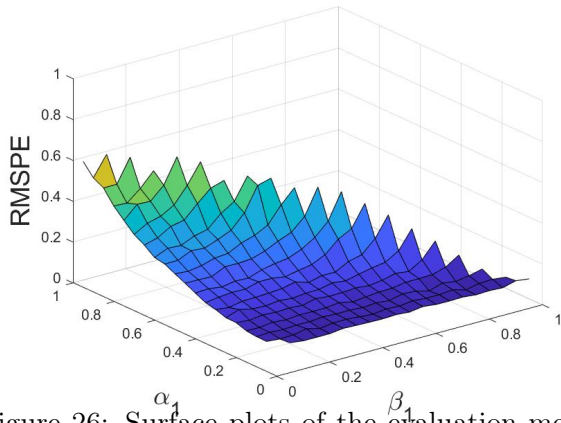
(a) RMSE - POT



(b) RMSE - BM (2)



(c) RMSPE - POT



(d) RMSPE - BM (2)

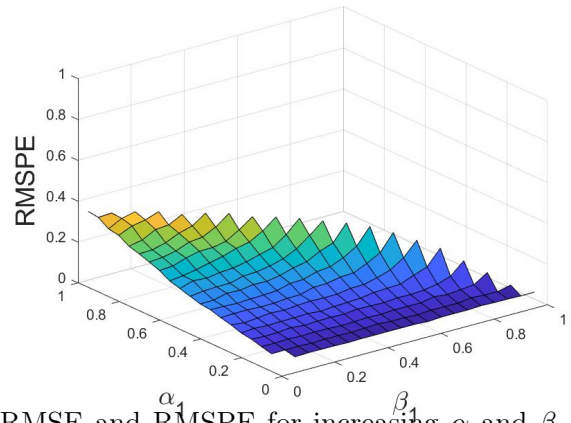
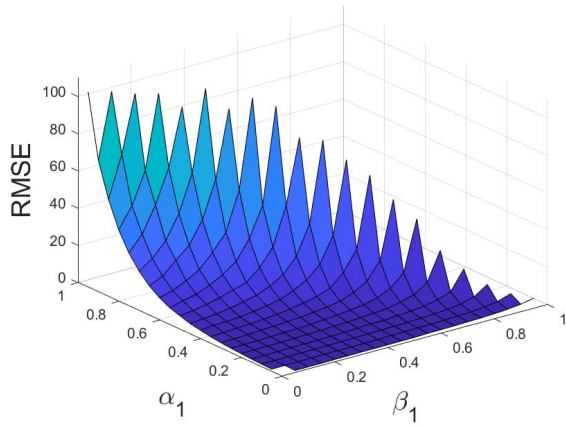
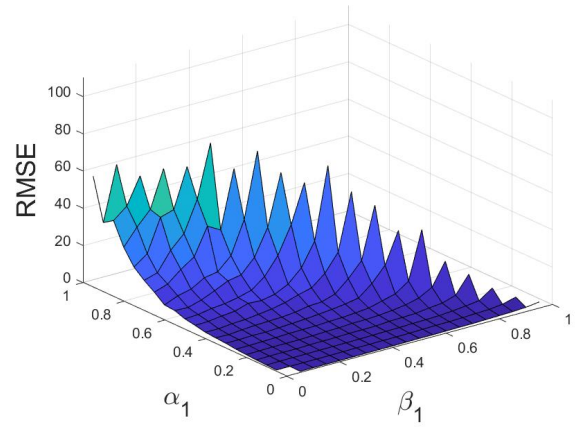


Figure 26: Surface plots of the evaluation metrics RMSE and RMSPE for increasing α and β with $\phi = \theta = 0.3$.

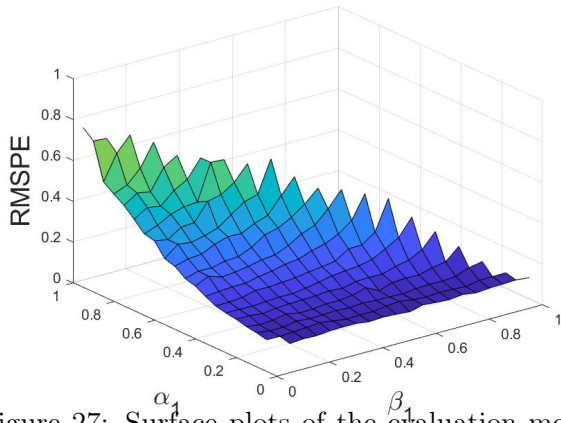
(a) RMSE - POT



(b) RMSE - BM (2)



(c) RMSPE - POT



(d) RMSPE - BM (2)

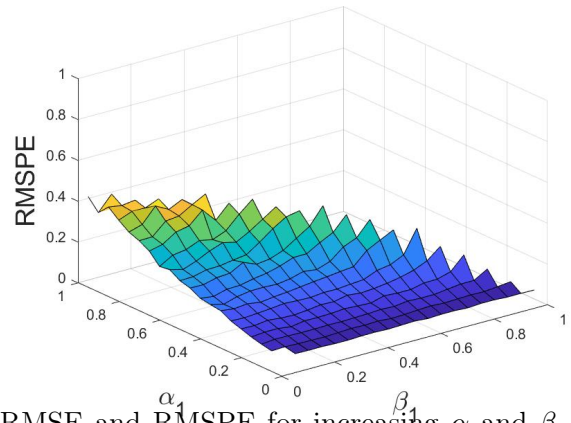
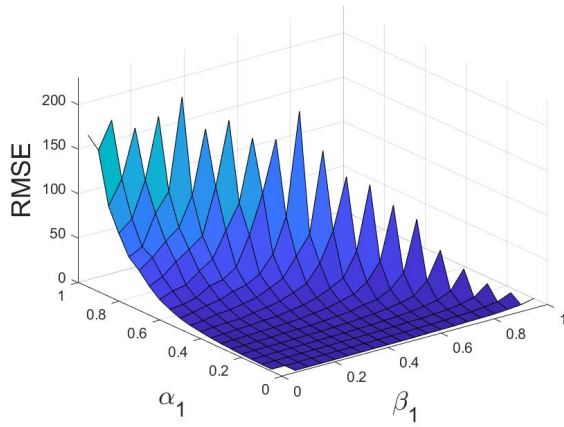
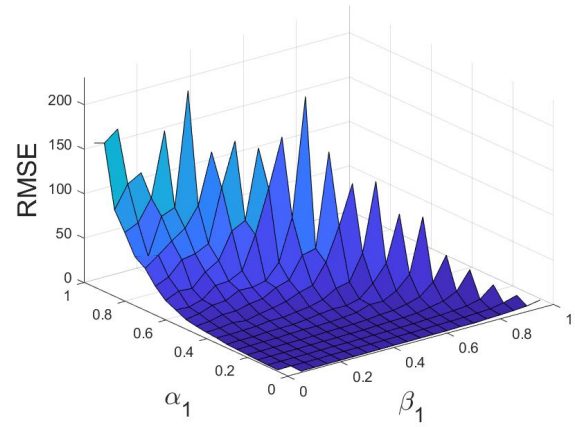


Figure 27: Surface plots of the evaluation metrics RMSE and RMSPE for increasing α and β with $\phi = \theta = 0.7$.

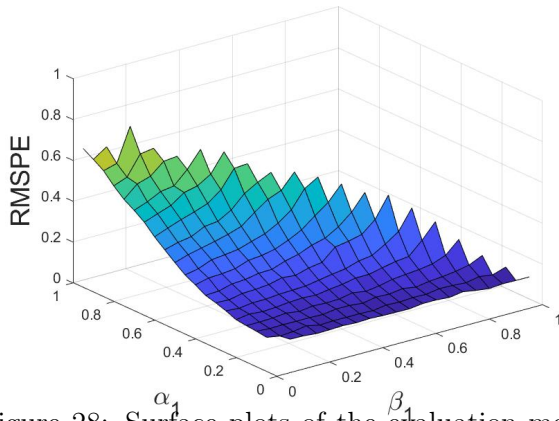
(a) RMSE - POT



(b) RMSE - BM (2)



(c) RMSPE - POT



(d) RMSPE - BM (2)

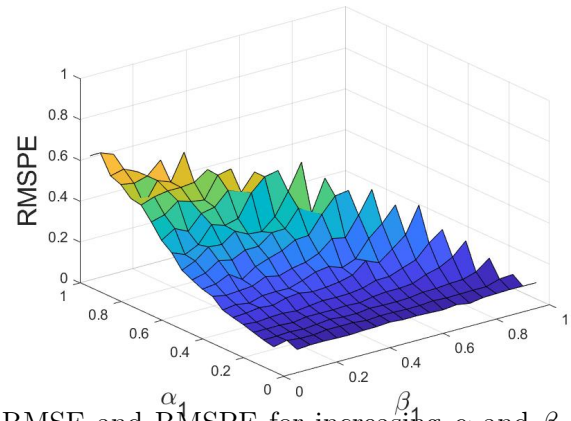


Figure 28: Surface plots of the evaluation metrics RMSE and RMSPE for increasing α and β with $\phi = \theta = 0.9$.

Comparison when increasing volatility clustering in α

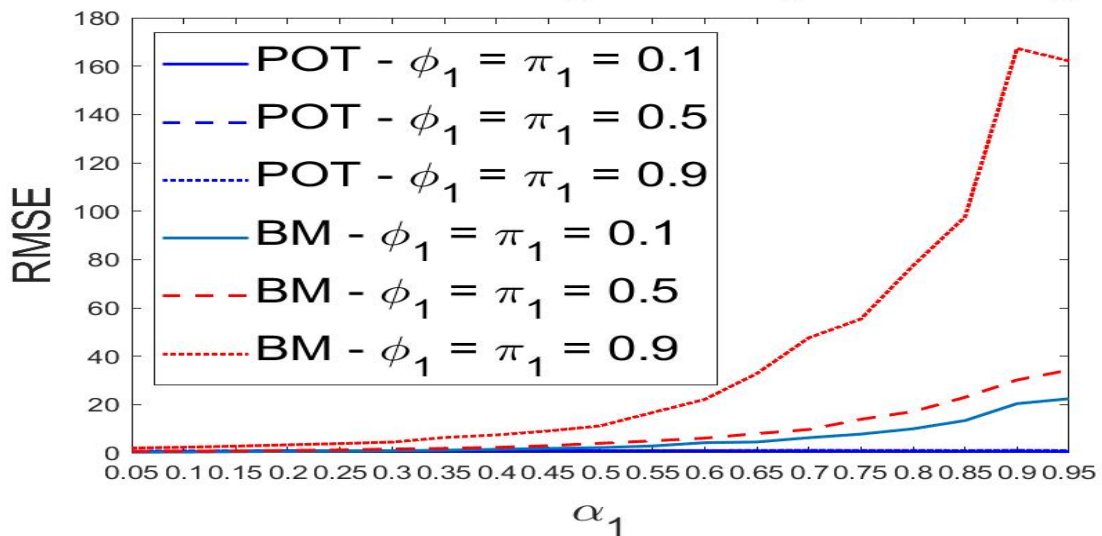


Figure 29: Comparing the RMSE for increasing α at three levels of serial dependence and $\beta = 0$.

Table 12: The RMSE of the POT method on ARMA-GARCH model with $\phi = \theta = 0.1$

ARIMA-GARCH		Beta																			
		0.00	0.05	0.10	0.15	0.20	0.25	0.30	0.35	0.40	0.45	0.50	0.55	0.60	0.65	0.70	0.75	0.80	0.85	0.90	0.95
Alpha	0.00		0.55	0.60	0.59	0.61	0.62	0.65	0.69	0.72	0.75	0.77	0.80	0.84	0.92	1.06	1.14	1.16	1.37	1.64	2.46
	0.05	0.59	0.61	0.61	0.61	0.66	0.64	0.70	0.71	0.75	0.78	0.81	0.87	0.97	1.02	1.16	1.26	1.50	1.95	2.89	
	0.10	0.64	0.62	0.62	0.62	0.66	0.73	0.73	0.75	0.81	0.88	0.91	1.02	1.03	1.17	1.35	1.73	2.16	3.87		
	0.15	0.63	0.66	0.68	0.75	0.77	0.74	0.84	0.83	0.95	1.01	1.10	1.25	1.34	1.63	2.11	3.06	6.85			
	0.20	0.69	0.73	0.74	0.81	0.87	0.85	0.93	1.08	1.17	1.21	1.41	1.64	2.05	2.71	4.46	10.57				
	0.25	0.83	0.91	0.93	0.97	1.05	1.16	1.23	1.34	1.52	1.80	2.06	2.58	3.70	6.34	16.91					
	0.30	1.00	1.07	1.15	1.23	1.38	1.47	1.64	1.79	2.15	2.61	3.41	4.91	8.31	22.74						
	0.35	1.28	1.31	1.45	1.64	1.73	1.93	2.18	2.70	3.38	4.32	6.74	11.01	26.91							
	0.40	1.58	1.78	1.82	2.08	2.40	2.72	3.23	4.10	5.40	8.13	13.39	31.21								
	0.45	2.03	2.21	2.45	2.85	3.24	4.02	4.84	6.43	9.54	16.86	35.95									
	0.50	2.60	2.87	3.30	3.85	4.52	5.91	7.89	11.43	18.93	39.25										
	0.55	3.34	3.91	4.35	5.20	6.60	9.01	12.74	20.56	37.98											
	0.60	4.44	5.12	6.13	7.92	10.46	14.13	23.19	42.48												
	0.65	5.75	6.98	8.79	11.36	15.94	24.60	45.50													
	0.70	7.87	9.42	12.65	17.84	25.70	43.85														
	0.75	10.52	14.23	17.55	27.06	40.39															
	0.80	14.71	18.79	27.64	44.03																
	0.85	19.71	27.98	42.93																	
0.90	28.85	38.83																			
0.95	38.31																				

Table 13: The RMSE of the BM method on ARMA-GARCH model with $\phi = \theta = 0.1$

ARIMA-GARCH		Beta																			
		0.00	0.05	0.10	0.15	0.20	0.25	0.30	0.35	0.40	0.45	0.50	0.55	0.60	0.65	0.70	0.75	0.80	0.85	0.90	0.95
Alpha	0.00		0.31	0.30	0.32	0.32	0.34	0.35	0.36	0.37	0.39	0.42	0.44	0.48	0.51	0.51	0.57	0.67	0.77	0.97	1.27
	0.05	0.31	0.31	0.34	0.35	0.35	0.39	0.38	0.41	0.42	0.45	0.48	0.51	0.52	0.58	0.64	0.74	0.83	1.06	1.70	
	0.10	0.35	0.38	0.42	0.43	0.45	0.43	0.47	0.50	0.53	0.55	0.60	0.65	0.74	0.82	0.96	1.14	1.65	3.31		
	0.15	0.48	0.48	0.50	0.49	0.53	0.60	0.58	0.69	0.69	0.72	0.78	0.90	1.07	1.27	1.61	2.49	6.91			
	0.20	0.62	0.63	0.68	0.68	0.66	0.85	0.88	0.81	0.90	1.09	1.16	1.39	1.60	2.32	3.78	9.54				
	0.25	0.71	0.74	0.84	0.89	0.95	0.95	1.04	1.24	1.39	1.45	1.81	2.29	3.29	5.31	14.93					
	0.30	0.91	0.98	1.00	1.08	1.13	1.30	1.41	1.60	1.96	2.29	2.85	4.09	6.57	18.99						
	0.35	1.10	1.27	1.25	1.32	1.57	1.81	1.93	2.37	2.66	3.75	6.21	8.29	21.01							
	0.40	1.48	1.40	1.70	1.81	2.13	2.33	2.69	3.35	4.52	7.20	10.84	23.38								
	0.45	1.85	1.91	2.09	2.32	2.84	3.57	3.97	5.24	7.72	12.63	26.21									
	0.50	2.18	2.45	2.83	3.08	3.79	4.85	5.96	8.74	14.09	29.30										
	0.55	2.87	2.88	3.54	3.94	5.28	6.49	10.19	14.27	27.00											
	0.60	4.22	4.22	5.01	7.04	8.15	10.50	17.00	28.64												
	0.65	4.51	5.59	7.04	8.34	10.86	17.72	32.48													
	0.70	6.29	6.72	9.21	14.07	18.09	29.50														
	0.75	7.78	9.88	12.10	19.22	26.86															
	0.80	9.95	12.07	17.85	31.38																
	0.85	13.39	18.97	24.73																	
0.90	20.38	24.04																			
0.95	22.42																				

Table 14: The RMSPE of the POT method on ARMA-GARCH model with $\phi = \theta = 0.1$

ARIMA-GARCH		Beta																			
		0.00	0.05	0.10	0.15	0.20	0.25	0.30	0.35	0.40	0.45	0.50	0.55	0.60	0.65	0.70	0.75	0.80	0.85	0.90	0.95
Alpha	0.00		0.14	0.15	0.14	0.14	0.14	0.14	0.15	0.15	0.15	0.14	0.14	0.14	0.14	0.15	0.15	0.14	0.14	0.14	0.15
	0.05	0.15	0.15	0.14	0.14	0.15	0.14	0.15	0.14	0.14	0.14	0.14	0.14	0.15	0.14	0.15	0.14	0.15	0.16	0.16	
	0.10	0.15	0.14	0.14	0.13	0.14	0.15	0.14	0.14	0.14	0.15	0.14	0.15	0.14	0.14	0.14	0.16	0.15	0.17		
	0.15	0.14	0.14	0.14	0.15	0.15	0.13	0.15	0.13	0.15	0.15	0.15	0.15	0.15	0.16	0.17	0.18	0.22			
	0.20	0.14	0.14	0.14	0.14	0.15	0.13	0.14	0.16	0.16	0.15	0.16	0.16	0.18	0.19	0.23	0.30				
	0.25	0.15	0.16	0.15	0.15	0.16	0.16	0.16	0.16	0.17	0.18	0.18	0.19	0.22	0.27	0.36					
	0.30	0.16	0.16	0.17	0.17	0.18	0.18	0.18	0.18	0.19	0.21	0.23	0.26	0.31	0.42						
	0.35	0.18	0.17	0.19	0.20	0.19	0.19	0.20	0.22	0.24	0.25	0.29	0.37	0.47							
	0.40	0.19	0.22	0.20	0.21	0.22	0.23	0.24	0.26	0.28	0.31	0.37	0.50								
	0.45	0.22	0.22	0.23	0.24	0.25	0.26	0.28	0.31	0.35	0.42	0.54									
	0.50	0.24	0.24	0.26	0.27	0.28	0.31	0.35	0.39	0.44	0.53										
	0.55	0.26	0.29	0.28	0.31	0.33	0.37	0.39	0.48	0.55											
	0.60	0.28	0.30	0.32	0.33	0.38	0.42	0.48	0.58												
	0.65	0.32	0.34	0.36	0.40	0.46	0.49	0.57													
	0.70	0.35	0.39	0.42	0.44	0.51	0.58														
	0.75	0.40	0.45	0.46	0.51	0.57															
	0.80	0.46	0.51	0.54	0.56																
	0.85	0.49	0.53	0.65																	
0.90	0.52	0.60																			
0.95	0.64																				

Table 15: The RMSPE of the BM method on ARMA-GARCH model with $\phi = \theta = 0.1$

ARIMA-GARCH		Beta																			
		0,00	0,05	0,10	0,15	0,20	0,25	0,30	0,35	0,40	0,45	0,50	0,55	0,60	0,65	0,70	0,75	0,80	0,85	0,90	0,95
Alpha	0,00	0,08	0,08	0,08	0,08	0,08	0,08	0,08	0,08	0,08	0,08	0,08	0,08	0,08	0,08	0,07	0,08	0,08	0,08	0,08	0,08
	0,05	0,08	0,08	0,08	0,08	0,08	0,08	0,08	0,08	0,08	0,08	0,08	0,08	0,08	0,08	0,08	0,08	0,08	0,09	0,09	
	0,10	0,08	0,09	0,09	0,09	0,09	0,09	0,09	0,09	0,09	0,09	0,09	0,09	0,10	0,10	0,10	0,10	0,12	0,12	0,15	
	0,15	0,11	0,10	0,10	0,10	0,10	0,10	0,11	0,10	0,11	0,11	0,11	0,11	0,12	0,12	0,13	0,15	0,23			
	0,20	0,12	0,12	0,12	0,12	0,11	0,14	0,13	0,12	0,12	0,13	0,13	0,14	0,14	0,16	0,19	0,26				
	0,25	0,13	0,13	0,14	0,14	0,14	0,14	0,14	0,14	0,15	0,15	0,15	0,16	0,17	0,19	0,23	0,32				
	0,30	0,15	0,15	0,15	0,15	0,15	0,16	0,16	0,16	0,18	0,18	0,19	0,21	0,24	0,35						
	0,35	0,16	0,17	0,16	0,16	0,17	0,18	0,18	0,19	0,19	0,22	0,27	0,27	0,36							
	0,40	0,18	0,17	0,19	0,19	0,20	0,20	0,20	0,22	0,24	0,28	0,30	0,37								
	0,45	0,20	0,19	0,20	0,20	0,22	0,24	0,23	0,25	0,28	0,32	0,39									
	0,50	0,21	0,21	0,22	0,22	0,24	0,26	0,26	0,30	0,33	0,40										
	0,55	0,23	0,22	0,23	0,24	0,26	0,27	0,31	0,33	0,39											
	0,60	0,27	0,25	0,26	0,30	0,30	0,31	0,35	0,39												
	0,65	0,26	0,27	0,29	0,30	0,31	0,36	0,41													
	0,70	0,29	0,28	0,31	0,35	0,36	0,39														
	0,75	0,29	0,31	0,32	0,37	0,38															
	0,80	0,31	0,32	0,35	0,41																
	0,85	0,33	0,36	0,37																	
	0,90	0,37	0,37																		
	0,95	0,37																			

Table 16: The RMSE of the POT method on ARMA-GARCH model with $\phi = \theta = 0.3$

ARIMA-GARCH		Beta																			
		0,00	0,05	0,10	0,15	0,20	0,25	0,30	0,35	0,40	0,45	0,50	0,55	0,60	0,65	0,70	0,75	0,80	0,85	0,90	0,95
Alpha	0,00	0,66	0,65	0,67	0,69	0,75	0,76	0,78	0,81	0,86	0,87	0,97	0,99	1,05	1,15	1,21	1,37	1,55	2,10	2,83	
	0,05	0,71	0,70	0,73	0,81	0,77	0,84	0,87	0,88	0,90	0,99	1,02	1,14	1,18	1,27	1,46	1,47	1,86	2,33	3,27	
	0,10	0,78	0,82	0,83	0,88	0,90	0,98	0,99	1,04	1,07	1,17	1,20	1,40	1,49	1,51	1,91	2,15	2,88	5,10		
	0,15	0,89	0,91	0,99	1,00	1,07	1,12	1,17	1,28	1,27	1,41	1,56	1,73	2,03	2,32	2,85	4,13	8,55			
	0,20	1,08	1,09	1,19	1,20	1,29	1,32	1,49	1,54	1,67	1,85	2,01	2,37	2,92	3,57	5,81	13,70				
	0,25	1,23	1,40	1,39	1,44	1,56	1,62	1,80	1,94	2,24	2,44	2,93	3,63	4,83	8,27	19,50					
	0,30	1,49	1,52	1,69	1,78	1,92	2,10	2,39	2,51	2,99	3,48	4,55	6,33	10,91	24,35						
	0,35	1,80	1,96	2,09	2,23	2,55	2,77	3,07	3,57	4,44	5,77	8,49	14,32	33,32							
	0,40	2,22	2,38	2,53	2,84	3,09	3,68	4,33	5,35	7,07	10,44	16,64	37,39								
	0,45	2,82	3,05	3,23	3,81	4,48	5,03	6,33	8,33	11,85	20,20	41,97									
	0,50	3,55	3,94	4,33	5,09	5,85	7,54	9,77	13,17	21,97	46,02										
	0,55	4,44	4,89	5,77	7,01	8,78	11,76	16,53	25,92	50,60											
	0,60	5,66	6,69	7,84	10,19	11,84	16,71	25,61	47,78												
	0,65	7,56	8,84	11,36	14,26	19,76	30,50	49,34													
	0,70	9,67	11,87	15,01	20,78	30,46	53,45														
	0,75	13,01	16,77	22,62	31,37	49,21															
	0,80	18,85	24,00	32,27	49,17																
	0,85	25,00	34,03	46,91																	
	0,90	35,13	50,26																		
	0,95	45,43																			

Table 17: The RMSE of the BM method on ARMA-GARCH model with $\phi = \theta = 0.3$

ARIMA-GARCH		Beta																			
		0,00	0,05	0,10	0,15	0,20	0,25	0,30	0,35	0,40	0,45	0,50	0,55	0,60	0,65	0,70	0,75	0,80	0,85	0,90	0,95
Alpha	0,00	0,35	0,38	0,39	0,40	0,40	0,42	0,44	0,46	0,47	0,50	0,49	0,56	0,60	0,64	0,75	0,80	0,92	1,08	1,56	
	0,05	0,42	0,44	0,46	0,45	0,49	0,50	0,51	0,55	0,61	0,59	0,63	0,63	0,73	0,77	0,84	1,07	1,16	1,42	2,42	
	0,10	0,53	0,54	0,58	0,57	0,61	0,63	0,62	0,67	0,73	0,75	0,85	0,88	0,96	1,23	1,27	1,60	2,12	4,62		
	0,15	0,67	0,66	0,69	0,77	0,74	0,80	0,84	0,86	1,00	1,04	1,09	1,26	1,36	1,61	2,13	3,21	7,56			
	0,20	0,77	0,84	0,84	0,89	0,93	1,02	0,99	1,12	1,22	1,36	1,65	1,88	2,16	3,26	4,97	12,10				
	0,25	0,99	0,93	1,05	1,17	1,18	1,32	1,44	1,53	1,64	1,99	2,23	2,83	4,06	7,31	16,41					
	0,30	1,19	1,29	1,33	1,37	1,45	1,61	1,71	2,23	2,47	3,14	3,53	5,33	8,59	19,06						
	0,35	1,50	1,55	1,58	1,74	1,84	2,05	2,64	2,93	3,85	4,55	6,10	11,02	25,27							
	0,40	1,70	1,81	2,20	2,31	2,69	2,87	3,38	4,46	5,66	8,43	12,20	26,13								
	0,45	2,10	2,38	2,59	2,67	3,50	3,91	4,82	6,17	9,22	15,81	28,93									
	0,50	2,61	3,30	3,39	3,89	4,48	5,48	7,21	9,39	14,99	33,28										
	0,55	3,20	3,65	4,09	5,50	6,75	9,09	11,21	15,18	34,25											
	0,60	4,53	4,98	6,46	8,19	9,06	11,43	18,11	31,38												
	0,65	5,79	6,55	8,00	10,62	12,96	19,72	35,32													
	0,70	7,26	8,11	10,51	14,70	19,26	32,50														
	0,75	9,13	10,56	16,22	20,08	27,66															
	0,80	13,20	18,56	22,95	32,57																
	0,85	15,60	23,64	27,13																	
	0,90	23,18	28,34																		
	0,95	27,33																			

Table 18: The RMSPE of the POT method on ARMA-GARCH model with $\phi = \theta = 0.3$

ARIMA-GARCH		Beta																			
		0,00	0,05	0,10	0,15	0,20	0,25	0,30	0,35	0,40	0,45	0,50	0,55	0,60	0,65	0,70	0,75	0,80	0,85	0,90	0,95
Alpha	0,00		0,15	0,14	0,14	0,14	0,15	0,15	0,14	0,14	0,15	0,14	0,15	0,14	0,14	0,14	0,14	0,14	0,14	0,15	0,14
	0,05	0,15	0,14	0,15	0,16	0,14	0,15	0,15	0,15	0,14	0,15	0,15	0,15	0,15	0,15	0,16	0,14	0,15	0,15	0,15	0,15
	0,10	0,15	0,15	0,15	0,15	0,15	0,16	0,16	0,16	0,15	0,16	0,15	0,17	0,16	0,14	0,17	0,16	0,17	0,18	0,17	0,18
	0,15	0,16	0,15	0,16	0,16	0,16	0,16	0,16	0,16	0,17	0,16	0,16	0,17	0,17	0,18	0,18	0,18	0,18	0,20	0,24	
	0,20	0,17	0,17	0,17	0,17	0,17	0,17	0,18	0,18	0,18	0,18	0,18	0,19	0,20	0,19	0,20	0,19	0,23	0,31		
	0,25	0,17	0,20	0,18	0,18	0,19	0,18	0,19	0,19	0,20	0,20	0,21	0,22	0,23	0,27	0,36					
	0,30	0,19	0,18	0,20	0,20	0,20	0,21	0,22	0,20	0,22	0,22	0,25	0,27	0,33	0,43						
	0,35	0,20	0,21	0,22	0,21	0,23	0,23	0,22	0,24	0,25	0,28	0,34	0,37	0,48							
	0,40	0,23	0,23	0,22	0,23	0,23	0,25	0,26	0,27	0,30	0,34	0,40	0,53								
	0,45	0,25	0,25	0,25	0,28	0,28	0,28	0,30	0,33	0,36	0,42	0,55									
	0,50	0,27	0,27	0,28	0,30	0,30	0,34	0,36	0,39	0,47	0,54										
	0,55	0,30	0,30	0,33	0,32	0,35	0,38	0,44	0,56	0,58											
	0,60	0,31	0,34	0,33	0,36	0,38	0,44	0,48	0,58												
	0,65	0,35	0,36	0,40	0,42	0,48	0,54	0,56													
	0,70	0,37	0,41	0,43	0,47	0,55	0,64														
	0,75	0,42	0,48	0,48	0,54	0,66															
	0,80	0,47	0,46	0,52	0,59																
	0,85	0,53	0,53	0,65																	
	0,90	0,56	0,66																		
	0,95	0,62																			

Table 19: The RMSPE of the BM method on ARMA-GARCH model with $\phi = \theta = 0.3$

ARIMA-GARCH		Beta																				
		0,00	0,05	0,10	0,15	0,20	0,25	0,30	0,35	0,40	0,45	0,50	0,55	0,60	0,65	0,70	0,75	0,80	0,85	0,90	0,95	
Alpha	0,00		0,08	0,08	0,08	0,08	0,08	0,08	0,08	0,08	0,08	0,08	0,08	0,08	0,08	0,08	0,08	0,08	0,08	0,08	0,08	
	0,05	0,09	0,09	0,09	0,09	0,09	0,09	0,09	0,09	0,10	0,09	0,09	0,09	0,09	0,09	0,10	0,09	0,09	0,09	0,09	0,11	
	0,10	0,10	0,10	0,10	0,10	0,10	0,10	0,10	0,10	0,10	0,10	0,11	0,10	0,10	0,12	0,11	0,12	0,12	0,12	0,17		
	0,15	0,12	0,11	0,11	0,12	0,11	0,12	0,12	0,11	0,12	0,12	0,12	0,12	0,12	0,13	0,14	0,16	0,22				
	0,20	0,12	0,13	0,12	0,13	0,13	0,13	0,12	0,13	0,13	0,13	0,15	0,15	0,15	0,18	0,20	0,27					
	0,25	0,14	0,13	0,14	0,15	0,14	0,15	0,15	0,15	0,15	0,16	0,16	0,18	0,20	0,24	0,31						
	0,30	0,15	0,15	0,15	0,15	0,15	0,16	0,16	0,18	0,18	0,19	0,19	0,22	0,26	0,33							
	0,35	0,17	0,17	0,16	0,17	0,17	0,17	0,19	0,19	0,21	0,22	0,24	0,29	0,36								
	0,40	0,17	0,17	0,19	0,19	0,20	0,20	0,21	0,23	0,24	0,27	0,29	0,37									
	0,45	0,19	0,20	0,20	0,20	0,22	0,22	0,23	0,25	0,28	0,33	0,38										
	0,50	0,20	0,22	0,22	0,23	0,23	0,24	0,26	0,28	0,32	0,39											
	0,55	0,22	0,22	0,23	0,25	0,27	0,29	0,30	0,33	0,39												
	0,60	0,25	0,25	0,27	0,29	0,29	0,30	0,34	0,38													
	0,65	0,26	0,27	0,28	0,31	0,31	0,35	0,40														
	0,70	0,28	0,28	0,30	0,33	0,34	0,39															
	0,75	0,30	0,30	0,34	0,35	0,37																
	0,80	0,33	0,36	0,37	0,39																	
	0,85	0,33	0,37	0,38																		
	0,90	0,37	0,37																			
	0,95	0,37																				

Table 20: The RMSE of the POT method on ARMA-GARCH model with $\phi = \theta = 0.5$

ARIMA-GARCH		Beta																				
		0,00	0,05	0,10	0,15	0,20	0,25	0,30	0,35	0,40	0,45	0,50	0,55	0,60	0,65	0,70	0,75	0,80	0,85	0,90	0,95	
Alpha	0,00		0,88	0,87	0,93	0,96	0,94	1,00	0,98	1,02	1,12	1,15	1,23	1,31	1,40	1,51	1,67	1,78	2,10	2,53	3,63	
	0,05	0,95	0,96	0,97	1,02	1,10	1,12	1,17	1,19	1,29	1,44	1,36	1,43	1,62	1,83	2,00	2,25	2,46	3,16	4,65		
	0,10	1,08	1,14	1,16	1,22	1,26	1,33	1,36	1,44	1,45	1,67	1,74	1,80	2,07	2,38	2,66	3,05	4,05	7,22			
	0,15	1,32	1,31	1,33	1,40	1,46	1,53	1,66	1,74	1,83	2,03	2,18	2,47	2,70	3,42	4,18	5,73	12,61				
	0,20	1,54	1,55	1,61	1,66	1,80	1,78	2,10	2,14	2,37	2,59	2,98	3,33	4,06	5,41	8,09	18,55					
	0,25	1,85	1,80	1,98	2,04	2,22	2,31	2,51	2,85	3,13	3,50	4,20	5,24	7,07	11,49	28,22						
	0,30	2,15	2,15	2,44	2,53	2,68	2,96	3,29	3,82	4,19	5,11	6,54	9,05	14,70	36,43							
	0,35	2,58	2,71	2,86	3,24	3,57	3,76	4,50	5,27	6,35	8,32	11,47	19,60	47,49								
	0,40	3,16	3,31	3,63	4,17	4,65	5,24	6,44	7,48	9,96	13,72	24,51	51,86									
	0,45	3,89	4,17	4,66	5,36	6,07	7,40	8,99	11,73	17,12	28,37	57,13										
	0,50	4,91	5,36	6,10	6,99	8,35	10,74	14,09	19,71	33,05	61,18											
	0,55	5,91	7,31	8,08	10,16	12,70	15,85	22,77	34,37	63,54												
	0,60	8,08	9,67	10,83	13,32	18,69	24,37	36,81	64,28													
	0,65	10,46	12,90	15,45	20,47	26,65	42,70	69,86														
	0,70	14,32	16,64	21,18	28,91	43,32	69,33															
	0,75	19,10	23,17	31,47	44,61	69,53																
	0,80	24,38	32,12	47,29	68,37																	
	0,85	33,11	45,35	64,11																		
	0,90	49,80	70,68																			
	0,95	64,19																				

Table 21: The RMSE of the BM method on ARMA-GARCH model with $\phi = \theta = 0.5$

ARIMA-GARCH		Beta																			
		0.00	0.05	0.10	0.15	0.20	0.25	0.30	0.35	0.40	0.45	0.50	0.55	0.60	0.65	0.70	0.75	0.80	0.85	0.90	0.95
Alpha	0.00		0.48	0.50	0.51	0.51	0.57	0.57	0.61	0.64	0.62	0.70	0.72	0.73	0.81	0.88	0.93	1.08	1.27	1.56	2.17
	0.05	0.59	0.61	0.66	0.64	0.65	0.69	0.70	0.76	0.78	0.80	0.88	0.99	1.01	1.06	1.21	1.33	1.67	2.10	3.41	
	0.10	0.75	0.73	0.77	0.79	0.85	0.87	0.94	0.93	1.08	1.06	1.16	1.38	1.38	1.52	1.79	2.32	3.08	5.79		
	0.15	0.84	0.96	0.99	0.99	1.09	1.17	1.17	1.29	1.37	1.40	1.58	1.84	2.11	2.28	3.10	4.78	11.73			
	0.20	1.02	1.08	1.21	1.27	1.26	1.45	1.47	1.65	1.78	2.02	2.17	2.44	3.42	4.13	6.49	15.15				
	0.25	1.22	1.41	1.37	1.50	1.61	1.74	1.89	2.03	2.42	2.68	3.28	4.05	5.71	8.92	22.80					
	0.30	1.62	1.65	1.72	1.86	2.13	2.24	2.68	2.68	3.68	4.25	5.51	7.19	11.67	27.08						
	0.35	1.87	2.02	2.48	2.33	2.55	3.01	3.30	4.35	4.51	6.18	8.71	14.79	39.95							
	0.40	2.30	2.73	2.94	3.34	3.56	4.48	4.90	6.16	7.75	9.72	18.15	39.11								
	0.45	2.99	3.58	3.88	4.17	4.55	5.20	6.69	8.44	14.26	20.70	40.32									
	0.50	4.04	4.61	4.48	5.95	6.05	8.15	9.51	14.10	24.96	36.05										
	0.55	5.08	5.05	5.42	7.17	8.83	11.67	18.63	23.49	45.07											
	0.60	6.19	7.66	7.27	9.01	12.55	16.31	22.87	45.31												
	0.65	8.13	10.15	13.42	16.48	18.05	27.89	38.51													
	0.70	9.77	10.82	14.10	19.45	27.65	40.98														
	0.75	14.18	14.48	22.10	30.70	47.32															
	0.80	17.40	19.88	30.10	45.33																
	0.85	23.45	25.40	42.32																	
	0.90	30.75	50.43																		
	0.95	34.34																			

Table 22: The RMSPE of the POT method on ARMA-GARCH model with $\phi = \theta = 0.5$

ARIMA-GARCH		Beta																			
		0.00	0.05	0.10	0.15	0.20	0.25	0.30	0.35	0.40	0.45	0.50	0.55	0.60	0.65	0.70	0.75	0.80	0.85	0.90	0.95
Alpha	0.00		0.15	0.15	0.15	0.15	0.14	0.15	0.14	0.14	0.15	0.14	0.15	0.15	0.15	0.15	0.14	0.14	0.14	0.14	0.14
	0.05	0.15	0.15	0.15	0.15	0.16	0.15	0.15	0.15	0.16	0.17	0.15	0.15	0.16	0.16	0.16	0.16	0.16	0.15	0.16	0.16
	0.10	0.16	0.16	0.16	0.16	0.16	0.16	0.16	0.17	0.15	0.17	0.17	0.16	0.17	0.18	0.17	0.17	0.18	0.20		
	0.15	0.18	0.17	0.17	0.17	0.17	0.17	0.17	0.17	0.18	0.18	0.18	0.18	0.18	0.20	0.20	0.21	0.26			
	0.20	0.19	0.18	0.18	0.18	0.19	0.17	0.20	0.18	0.19	0.19	0.20	0.20	0.20	0.23	0.25	0.33				
	0.25	0.21	0.19	0.20	0.20	0.20	0.20	0.20	0.21	0.21	0.21	0.23	0.24	0.26	0.31	0.40					
	0.30	0.21	0.20	0.22	0.22	0.21	0.22	0.22	0.24	0.23	0.24	0.26	0.29	0.34	0.46						
	0.35	0.23	0.23	0.22	0.24	0.25	0.24	0.26	0.26	0.29	0.31	0.33	0.39	0.48							
	0.40	0.25	0.24	0.24	0.26	0.27	0.26	0.30	0.29	0.33	0.37	0.44	0.52								
	0.45	0.26	0.25	0.27	0.28	0.30	0.32	0.33	0.36	0.38	0.46	0.56									
	0.50	0.28	0.28	0.31	0.30	0.33	0.35	0.40	0.43	0.48	0.64										
	0.55	0.29	0.34	0.35	0.37	0.40	0.40	0.43	0.51	0.57											
	0.60	0.34	0.35	0.39	0.40	0.46	0.48	0.55	0.58												
	0.65	0.37	0.39	0.39	0.43	0.49	0.57	0.70													
	0.70	0.43	0.45	0.48	0.51	0.58	0.67														
	0.75	0.45	0.51	0.52	0.57	0.62															
	0.80	0.48	0.55	0.61	0.63																
	0.85	0.52	0.64	0.62																	
	0.90	0.63	0.62																		
	0.95	0.71																			

Table 23: The RMSPE of the BM method on ARMA-GARCH model with $\phi = \theta = 0.5$

ARIMA-GARCH		Beta																			
		0.00	0.05	0.10	0.15	0.20	0.25	0.30	0.35	0.40	0.45	0.50	0.55	0.60	0.65	0.70	0.75	0.80	0.85	0.90	0.95
Alpha	0.00		0.08	0.08	0.08	0.08	0.09	0.08	0.09	0.09	0.08	0.09	0.08	0.08	0.08	0.08	0.08	0.08	0.09	0.09	0.09
	0.05	0.10	0.10	0.10	0.09	0.09	0.10	0.09	0.10	0.10	0.09	0.10	0.10	0.10	0.10	0.10	0.10	0.10	0.10	0.10	0.12
	0.10	0.11	0.11	0.11	0.11	0.11	0.11	0.11	0.11	0.11	0.11	0.11	0.11	0.12	0.11	0.11	0.12	0.13	0.13	0.16	
	0.15	0.11	0.12	0.12	0.12	0.12	0.13	0.12	0.13	0.13	0.12	0.13	0.14	0.14	0.14	0.15	0.17	0.24			
	0.20	0.13	0.13	0.14	0.14	0.13	0.14	0.14	0.14	0.14	0.15	0.15	0.15	0.17	0.18	0.20	0.27				
	0.25	0.14	0.15	0.14	0.14	0.15	0.15	0.15	0.15	0.16	0.16	0.18	0.19	0.21	0.24	0.32					
	0.30	0.16	0.16	0.16	0.16	0.17	0.17	0.18	0.17	0.20	0.20	0.22	0.23	0.27	0.34						
	0.35	0.17	0.17	0.19	0.17	0.18	0.19	0.19	0.21	0.20	0.23	0.25	0.30	0.40							
	0.40	0.18	0.19	0.20	0.21	0.21	0.23	0.22	0.24	0.25	0.26	0.32	0.39								
	0.45	0.20	0.22	0.22	0.22	0.22	0.23	0.24	0.26	0.31	0.34	0.39									
	0.50	0.23	0.24	0.23	0.26	0.24	0.27	0.27	0.31	0.36	0.38										
	0.55	0.25	0.24	0.24	0.26	0.28	0.30	0.35	0.35	0.40											
	0.60	0.26	0.28	0.26	0.27	0.31	0.32	0.34	0.41												
	0.65	0.29	0.31	0.34	0.35	0.33	0.37	0.38													
	0.70	0.29	0.29	0.32	0.34	0.37	0.40														
	0.75	0.33	0.32	0.36	0.39	0.42															
	0.80	0.34	0.34	0.39	0.42																
	0.85	0.37	0.36	0.41																	
	0.90	0.39	0.44																		
	0.95	0.38																			

Table 24: The RMSE of the POT method on ARMA-GARCH model with $\phi = \theta = 0.7$

ARIMA-GARCH		Beta																				
		0,00	0,05	0,10	0,15	0,20	0,25	0,30	0,35	0,40	0,45	0,50	0,55	0,60	0,65	0,70	0,75	0,80	0,85	0,90	0,95	
Alpha	0,00		1,21	1,29	1,31	1,39	1,45	1,50	1,49	1,59	1,63	1,64	1,90	1,96	2,06	2,30	2,41	2,78	3,24	4,01	5,48	
	0,05	1,39	1,42	1,50	1,58	1,68	1,67	1,66	1,75	1,84	2,01	2,21	2,23	2,34	2,60	2,83	3,10	3,86	4,84	7,14		
	0,10	1,61	1,60	1,65	1,84	1,84	1,93	2,07	2,13	2,30	2,41	2,54	2,72	3,07	3,45	3,93	4,80	6,78	11,51			
	0,15	1,84	1,83	1,95	2,14	2,14	2,26	2,45	2,60	2,85	3,33	3,17	3,84	4,32	5,02	6,41	8,91	19,24				
	0,20	2,18	2,26	2,31	2,45	2,63	2,82	3,07	3,37	3,62	4,10	4,58	5,21	6,60	8,60	13,33	28,69					
	0,25	2,54	2,62	2,74	2,97	3,24	3,40	3,75	4,33	4,91	5,65	6,55	8,36	11,56	17,95	45,06						
	0,30	3,04	3,15	3,45	3,82	4,12	4,57	5,06	5,86	6,69	7,88	10,64	14,76	24,03	54,87							
	0,35	3,74	3,93	4,38	4,76	5,39	6,02	7,01	8,28	9,84	12,49	18,82	29,34	67,39								
	0,40	4,66	5,37	5,47	6,02	6,95	8,19	9,58	12,34	16,14	22,68	36,35	75,01									
	0,45	5,72	6,43	7,08	8,16	9,72	11,19	14,28	18,48	26,43	42,05	84,91										
	0,50	7,38	8,33	9,60	11,32	13,50	15,63	21,61	30,86	51,16	85,72											
	0,55	9,16	10,97	12,56	15,52	19,30	24,47	34,77	50,76	101,99												
	0,60	12,00	13,93	17,31	21,36	28,75	37,52	58,39	105,99													
	0,65	15,85	19,13	25,74	31,91	43,73	63,47	99,53														
	0,70	21,29	26,19	33,79	46,45	66,41	109,79															
	0,75	28,56	36,74	50,50	68,57	99,32																
	0,80	38,38	49,52	66,44	106,02																	
	0,85	52,32	74,71	105,38																		
	0,90	70,81	105,83																			
0,95	105,02																					

Table 25: The RMSE of the BM method on ARMA-GARCH model with $\phi = \theta = 0.7$

ARIMA-GARCH		Beta																				
		0,00	0,05	0,10	0,15	0,20	0,25	0,30	0,35	0,40	0,45	0,50	0,55	0,60	0,65	0,70	0,75	0,80	0,85	0,90	0,95	
Alpha	0,00		0,80	0,81	0,83	0,83	0,84	0,90	0,96	0,96	1,04	1,12	1,09	1,22	1,31	1,32	1,56	1,73	1,91	2,32	3,27	
	0,05	0,91	0,96	0,97	0,99	0,99	1,09	1,18	1,20	1,30	1,27	1,37	1,54	1,71	1,77	2,00	2,32	2,59	3,43	5,36		
	0,10	1,07	1,21	1,23	1,25	1,29	1,36	1,41	1,52	1,61	1,80	1,86	2,18	2,27	2,51	3,09	3,87	4,75	9,72			
	0,15	1,32	1,47	1,51	1,41	1,68	1,75	1,84	2,05	2,07	2,13	2,78	2,87	3,15	4,11	4,81	7,13	16,69				
	0,20	1,64	1,70	1,92	1,85	1,91	2,11	2,44	2,54	3,07	3,08	3,48	4,19	5,23	7,05	11,00	23,16					
	0,25	2,06	2,11	2,29	2,51	2,80	2,88	3,01	3,40	3,62	4,18	4,88	6,79	8,72	13,73	40,13						
	0,30	2,77	2,72	3,00	2,90	3,32	3,72	4,20	4,85	5,56	6,52	7,77	13,86	21,97	38,74							
	0,35	3,15	2,94	3,58	4,12	4,41	4,65	5,35	6,71	7,08	9,41	15,98	23,90	52,39								
	0,40	3,63	3,57	4,34	4,70	5,59	6,55	8,08	10,44	12,23	18,28	27,95	59,45									
	0,45	4,86	5,06	6,06	6,74	9,11	8,67	10,06	13,71	20,79	33,48	73,33										
	0,50	5,84	6,26	7,59	8,22	9,67	11,67	17,34	27,07	42,12	63,13											
	0,55	7,87	7,51	9,70	12,89	16,37	17,68	25,36	39,90	68,13												
	0,60	8,30	11,44	13,17	17,46	18,71	25,62	43,71	79,70													
	0,65	12,90	15,38	21,53	26,53	41,47	37,16	69,40														
	0,70	16,81	19,08	29,54	36,81	53,84	83,11															
	0,75	21,67	27,07	45,20	47,52	69,33																
	0,80	30,02	39,20	46,97	67,47																	
	0,85	42,24	48,26	63,04																		
	0,90	38,10	68,78																			
0,95	61,65																					

Table 26: The RMSPE of the POT method on ARMA-GARCH model with $\phi = \theta = 0.7$

ARIMA-GARCH		Beta																				
		0,00	0,05	0,10	0,15	0,20	0,25	0,30	0,35	0,40	0,45	0,50	0,55	0,60	0,65	0,70	0,75	0,80	0,85	0,90	0,95	
Alpha	0,00		0,14	0,15	0,15	0,15	0,16	0,15	0,15	0,15	0,15	0,14	0,16	0,15	0,15	0,16	0,15	0,15	0,16	0,15		
	0,05	0,16	0,16	0,16	0,16	0,17	0,16	0,15	0,15	0,16	0,16	0,17	0,16	0,16	0,16	0,16	0,16	0,15	0,17	0,17		
	0,10	0,17	0,16	0,16	0,17	0,17	0,17	0,17	0,17	0,17	0,17	0,17	0,17	0,17	0,17	0,18	0,17	0,18	0,21	0,22		
	0,15	0,18	0,17	0,17	0,18	0,17	0,17	0,18	0,18	0,19	0,21	0,18	0,20	0,20	0,20	0,22	0,23	0,29				
	0,20	0,19	0,19	0,18	0,19	0,19	0,20	0,20	0,20	0,20	0,21	0,22	0,22	0,24	0,25	0,28	0,35					
	0,25	0,20	0,20	0,19	0,20	0,20	0,20	0,21	0,22	0,24	0,25	0,25	0,27	0,30	0,34	0,42						
	0,30	0,21	0,21	0,21	0,23	0,23	0,24	0,24	0,25	0,26	0,27	0,31	0,31	0,36	0,51							
	0,35	0,23	0,24	0,24	0,24	0,26	0,27	0,28	0,29	0,31	0,33	0,36	0,41	0,52								
	0,40	0,26	0,29	0,27	0,28	0,29	0,30	0,31	0,34	0,37	0,40	0,46	0,54									
	0,45	0,27	0,29	0,29	0,31	0,31	0,34	0,38	0,40	0,43	0,48	0,54										
	0,50	0,31	0,33	0,33	0,37	0,39	0,38	0,41	0,44	0,52	0,59											
	0,55	0,32	0,38	0,37	0,38	0,41	0,45	0,50	0,52	0,67												
	0,60	0,39	0,38	0,42	0,43	0,51	0,53	0,57	0,64													
	0,65	0,40	0,43	0,46	0,48	0,49	0,66	0,66														
	0,70	0,45	0,49	0,48	0,54	0,57	0,66															
	0,75	0,49	0,54	0,53	0,63	0,67																
	0,80	0,53	0,55	0,62	0,73																	
	0,85	0,56	0,69	0,76																		
	0,90	0,74	0,74																			
0,95	0,78																					

Table 27: The RMSPE of the BM method on ARMA-GARCH model with $\phi = \theta = 0.7$

ARIMA-GARCH		Beta																			
		0,00	0,05	0,10	0,15	0,20	0,25	0,30	0,35	0,40	0,45	0,50	0,55	0,60	0,65	0,70	0,75	0,80	0,85	0,90	0,95
Alpha	0,00		0,10	0,09	0,09	0,09	0,09	0,09	0,09	0,09	0,10	0,09	0,09	0,09	0,09	0,09	0,09	0,09	0,09	0,09	0,09
	0,05	0,10	0,11	0,10	0,10	0,10	0,10	0,11	0,11	0,11	0,10	0,11	0,11	0,11	0,11	0,11	0,11	0,11	0,12	0,13	
	0,10	0,11	0,12	0,12	0,12	0,12	0,12	0,12	0,12	0,12	0,13	0,12	0,13	0,13	0,13	0,14	0,15	0,14	0,18		
	0,15	0,13	0,13	0,13	0,12	0,14	0,13	0,14	0,14	0,14	0,13	0,15	0,15	0,15	0,16	0,16	0,18	0,25			
	0,20	0,14	0,14	0,15	0,14	0,14	0,15	0,16	0,15	0,17	0,16	0,17	0,17	0,19	0,20	0,23	0,29				
	0,25	0,16	0,16	0,16	0,17	0,18	0,17	0,18	0,17	0,18	0,18	0,18	0,19	0,22	0,23	0,26	0,37				
	0,30	0,19	0,18	0,19	0,18	0,19	0,19	0,20	0,21	0,21	0,22	0,23	0,29	0,33	0,36						
	0,35	0,20	0,18	0,20	0,21	0,21	0,21	0,22	0,24	0,23	0,25	0,31	0,33	0,41							
	0,40	0,20	0,19	0,21	0,21	0,23	0,24	0,26	0,28	0,28	0,32	0,36	0,43								
	0,45	0,23	0,23	0,25	0,25	0,29	0,26	0,27	0,30	0,34	0,38	0,47									
	0,50	0,25	0,25	0,26	0,27	0,28	0,29	0,33	0,38	0,42	0,44										
	0,55	0,28	0,26	0,29	0,32	0,34	0,33	0,36	0,41	0,45											
	0,60	0,27	0,31	0,32	0,35	0,33	0,36	0,43	0,48												
	0,65	0,33	0,34	0,39	0,40	0,46	0,39	0,46													
	0,70	0,35	0,36	0,42	0,43	0,47	0,50														
	0,75	0,38	0,40	0,47	0,44	0,47															
	0,80	0,41	0,44	0,44	0,46																
	0,85	0,45	0,44	0,45																	
	0,90	0,40	0,48																		
	0,95	0,46																			

Table 28: The RMSE of the POT method on ARMA-GARCH model with $\phi = \theta = 0.9$

ARIMA-GARCH		Beta																			
		0,00	0,05	0,10	0,15	0,20	0,25	0,30	0,35	0,40	0,45	0,50	0,55	0,60	0,65	0,70	0,75	0,80	0,85	0,90	0,95
Alpha	0,00		2,61	2,72	2,69	2,79	2,94	2,98	3,18	3,25	3,34	3,50	3,84	4,04	4,24	4,74	5,02	5,35	6,40	7,81	11,05
	0,05	2,77	2,75	2,87	3,12	3,04	3,21	3,33	3,42	3,56	3,95	4,08	4,44	4,76	5,42	5,94	6,50	8,05	9,90	16,04	
	0,10	3,08	3,10	3,25	3,35	3,49	3,65	3,95	4,10	4,24	4,77	4,99	5,67	5,93	6,95	8,12	9,95	13,70	25,04		
	0,15	3,40	3,51	3,69	3,91	3,98	4,32	4,49	4,77	5,37	5,58	6,40	7,37	8,54	10,51	13,20	19,71	40,32			
	0,20	3,81	4,10	4,17	4,50	4,80	5,17	5,43	6,07	6,75	7,79	8,90	10,44	13,18	16,84	29,67	60,22				
	0,25	4,56	4,66	5,15	5,35	5,94	6,47	6,80	7,71	8,91	10,38	13,85	15,60	23,16	37,37	93,74					
	0,30	5,32	5,60	6,08	6,76	7,31	8,26	8,98	10,99	12,72	16,38	20,27	29,93	49,18	108,42						
	0,35	6,51	6,80	7,78	8,41	9,93	10,46	12,82	15,07	19,30	25,81	33,34	59,10	130,03							
	0,40	8,05	9,08	10,31	10,34	13,14	15,22	18,18	23,66	29,89	48,85	81,11	137,89								
	0,45	9,87	11,27	14,15	15,22	18,02	21,03	27,60	34,79	55,58	76,12	165,97									
	0,50	12,65	15,15	18,84	21,20	26,83	29,91	38,21	56,43	94,34	209,05										
	0,55	17,39	18,91	22,44	31,45	34,59	44,39	76,55	119,53	176,25											
	0,60	23,08	28,78	31,48	42,78	52,75	80,47	107,50	176,35												
	0,65	32,72	39,62	52,31	62,20	73,35	124,33	195,08													
	0,70	45,24	55,79	69,92	81,57	113,66	184,13														
	0,75	54,97	62,59	96,19	116,74	219,18															
	0,80	76,53	88,75	128,15	195,73																
	0,85	101,73	128,14	181,51																	
	0,90	159,41	189,17																		
	0,95	170,94																			

Table 29: The RMSE of the BM method on ARMA-GARCH model with $\phi = \theta = 0.9$

ARIMA-GARCH		Beta																			
		0,00	0,05	0,10	0,15	0,20	0,25	0,30	0,35	0,40	0,45	0,50	0,55	0,60	0,65	0,70	0,75	0,80	0,85	0,90	0,95
Alpha	0,00		1,82	2,01	2,08	2,09	2,14	2,30	2,42	2,63	2,60	2,77	2,79	2,86	3,33	3,13	3,96	4,55	5,31	6,54	9,21
	0,05	2,03	2,43	2,31	2,35	2,67	2,74	2,87	2,77	3,06	3,17	3,27	3,46	3,96	4,08	4,60	5,22	5,95	8,99	13,42	
	0,10	2,37	2,47	2,64	2,65	2,88	3,22	3,15	3,25	3,71	3,80	4,03	4,41	5,23	5,82	6,88	8,19	11,89	24,46		
	0,15	2,84	2,91	3,04	2,99	3,48	3,57	3,76	4,03	4,12	4,91	5,59	5,98	6,94	9,68	12,59	19,71	40,62			
	0,20	3,42	3,34	3,65	3,93	3,86	4,29	4,84	5,07	5,51	6,27	8,00	8,86	11,91	16,34	29,34	56,19				
	0,25	3,94	4,24	4,71	4,69	5,60	6,25	6,09	6,73	7,73	9,38	14,38	14,06	22,14	36,85	99,20					
	0,30	4,58	5,16	4,97	6,04	6,45	6,77	8,33	10,53	12,19	11,76	15,67	29,25	48,35	101,42						
	0,35	6,56	6,38	6,96	7,58	9,65	9,51	11,67	13,63	17,61	26,53	29,82	58,93	137,35							
	0,40	7,65	8,37	10,52	8,72	12,21	15,00	18,35	24,52	28,75	51,04	88,56	133,98								
	0,45	9,33	10,81	14,39	14,50	18,39	20,29	28,87	33,58	58,13	61,91	168,83									
	0,50	11,55	14,26	19,70	20,99	28,72	28,08	31,61	48,65	96,13	230,15										
	0,55	17,21	16,53	20,90	33,04	34,10	41,86	79,15	128,05	183,34											
	0,60	22,79	29,45	28,41	43,26	52,37	82,09	90,46	169,69												
	0,65	33,74	40,32	56,01	58,82	66,44	126,36	176,40													
	0,70	48,83	59,90	72,10	82,70	105,08	162,71														
	0,75	56,87	53,26	95,17	101,51	230,79															
	0,80	79,39	86,54	111,04	184,27																
	0,85	100,18	125,82	135,30																	
	0,90	170,72	183,44																		
	0,95	166,16																			

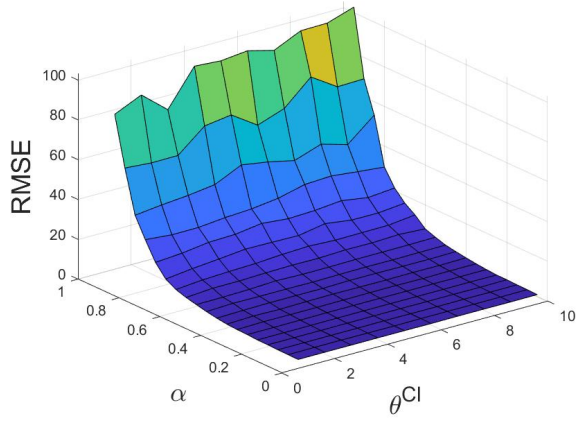
Table 30: The RMSPE of the POT method on ARMA-GARCH model with $\phi = \theta = 0.9$

ARIMA-GARCH		Beta																			
		0,00	0,05	0,10	0,15	0,20	0,25	0,30	0,35	0,40	0,45	0,50	0,55	0,60	0,65	0,70	0,75	0,80	0,85	0,90	0,95
Alpha	0,00		0,16	0,16	0,16	0,16	0,16	0,16	0,16	0,16	0,16	0,16	0,16	0,16	0,16	0,17	0,16	0,15	0,16	0,15	0,15
	0,05	0,17	0,16	0,16	0,17	0,16	0,16	0,16	0,16	0,16	0,17	0,17	0,17	0,17	0,18	0,18	0,17	0,19	0,18	0,20	0,20
	0,10	0,18	0,17	0,17	0,17	0,17	0,17	0,18	0,18	0,17	0,18	0,18	0,19	0,18	0,19	0,20	0,21	0,22	0,22	0,25	0,25
	0,15	0,18	0,18	0,18	0,19	0,18	0,19	0,19	0,19	0,19	0,20	0,19	0,20	0,21	0,22	0,23	0,24	0,26	0,32		
	0,20	0,19	0,20	0,19	0,19	0,20	0,21	0,20	0,21	0,22	0,23	0,23	0,25	0,26	0,27	0,33	0,40				
	0,25	0,21	0,20	0,21	0,21	0,22	0,22	0,22	0,23	0,25	0,25	0,28	0,28	0,32	0,37	0,46					
	0,30	0,22	0,22	0,23	0,24	0,24	0,26	0,25	0,27	0,28	0,34	0,35	0,36	0,42	0,52						
	0,35	0,24	0,24	0,26	0,26	0,27	0,28	0,30	0,32	0,34	0,36	0,40	0,45	0,53							
	0,40	0,27	0,28	0,28	0,29	0,32	0,32	0,33	0,36	0,39	0,45	0,49	0,57								
	0,45	0,29	0,30	0,33	0,34	0,35	0,37	0,39	0,42	0,47	0,56	0,59									
	0,50	0,33	0,35	0,36	0,38	0,40	0,42	0,47	0,52	0,54	0,61										
	0,55	0,37	0,39	0,40	0,43	0,44	0,47	0,54	0,58	0,61											
	0,60	0,41	0,43	0,46	0,48	0,50	0,55	0,64	0,64												
	0,65	0,46	0,48	0,50	0,55	0,57	0,61	0,70													
	0,70	0,49	0,52	0,55	0,56	0,62	0,70														
	0,75	0,52	0,58	0,60	0,66	0,66															
	0,80	0,57	0,59	0,69	0,70																
	0,85	0,62	0,64	0,80																	
	0,90	0,65	0,69																		
	0,95	0,68																			

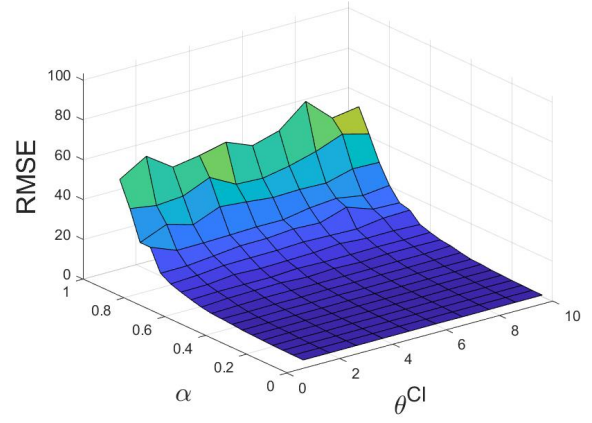
Table 31: The RMSPE of the BM method on ARMA-GARCH model with $\phi = \theta = 0.9$

ARIMA-GARCH		Beta																			
		0,00	0,05	0,10	0,15	0,20	0,25	0,30	0,35	0,40	0,45	0,50	0,55	0,60	0,65	0,70	0,75	0,80	0,85	0,90	0,95
Alpha	0,00		0,11	0,12	0,12	0,12	0,12	0,12	0,12	0,13	0,12	0,12	0,12	0,12	0,12	0,11	0,12	0,13	0,13	0,13	0,13
	0,05	0,12	0,14	0,13	0,13	0,14	0,14	0,14	0,13	0,14	0,14	0,13	0,13	0,14	0,13	0,14	0,14	0,14	0,14	0,16	0,16
	0,10	0,14	0,14	0,14	0,14	0,14	0,15	0,14	0,14	0,15	0,15	0,15	0,15	0,16	0,16	0,17	0,17	0,19	0,24		
	0,15	0,15	0,15	0,15	0,14	0,16	0,16	0,16	0,16	0,15	0,17	0,17	0,17	0,18	0,21	0,23	0,26	0,32			
	0,20	0,17	0,16	0,17	0,17	0,16	0,17	0,18	0,18	0,18	0,19	0,21	0,21	0,24	0,26	0,33	0,38				
	0,25	0,18	0,18	0,19	0,19	0,21	0,21	0,20	0,20	0,21	0,23	0,29	0,26	0,31	0,36	0,49					
	0,30	0,19	0,20	0,19	0,21	0,21	0,21	0,23	0,26	0,27	0,24	0,27	0,36	0,41	0,49						
	0,35	0,24	0,23	0,23	0,24	0,27	0,25	0,27	0,28	0,31	0,37	0,35	0,45	0,56							
	0,40	0,25	0,26	0,29	0,25	0,29	0,32	0,34	0,37	0,38	0,47	0,54	0,55								
	0,45	0,27	0,29	0,34	0,32	0,35	0,35	0,40	0,41	0,49	0,45	0,61									
	0,50	0,30	0,33	0,38	0,38	0,42	0,39	0,39	0,44	0,55	0,68										
	0,55	0,36	0,34	0,37	0,45	0,43	0,45	0,56	0,62	0,63											
	0,60	0,40	0,44	0,41	0,48	0,50	0,56	0,54	0,62												
	0,65	0,47	0,49	0,54	0,52	0,51	0,62	0,63													
	0,70	0,53	0,56	0,57	0,57	0,58	0,62														
	0,75	0,54	0,49	0,60	0,57	0,70															
	0,80	0,59	0,58	0,60	0,66																
	0,85	0,61	0,62	0,60																	
	0,90	0,70	0,67																		
	0,95	0,66																			

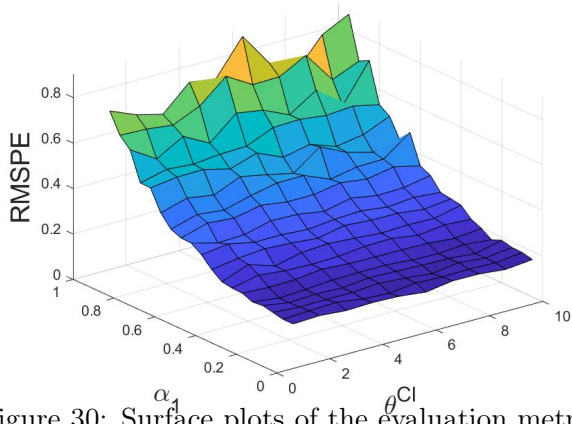
(a) RMSE - POT



(b) RMSE - BM (2)



(c) RMSPE - POT



(d) RMSPE - BM (2)

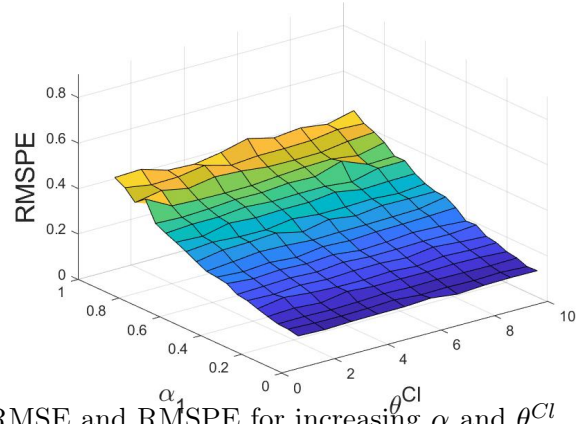
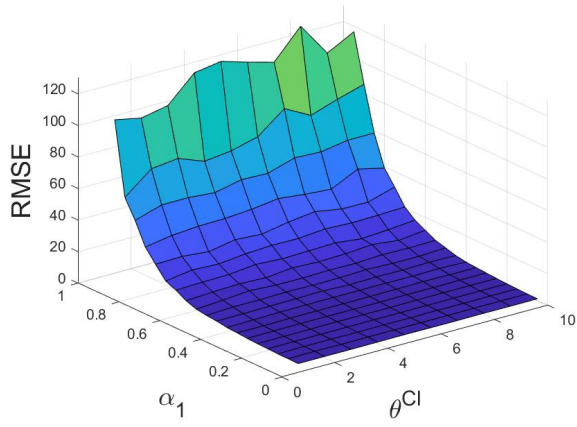
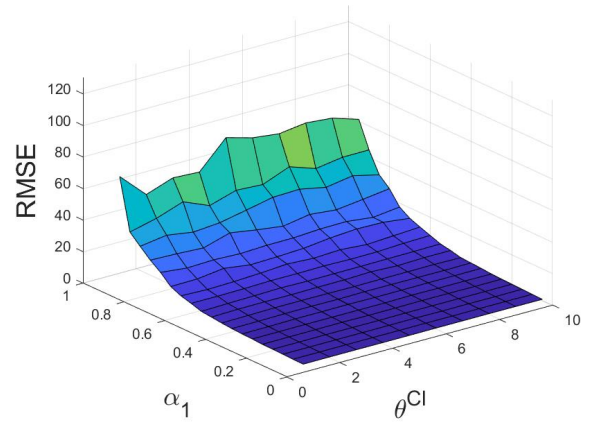


Figure 30: Surface plots of the evaluation metrics RMSE and RMSPE for increasing α and θ^{Cl} and with ϕ and θ set to 0.1.

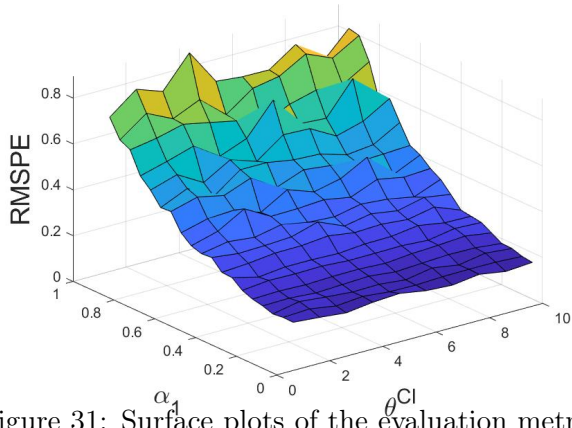
(a) RMSE - POT



(b) RMSE - BM (2)



(c) RMSPE - POT



(d) RMSPE - BM (2)

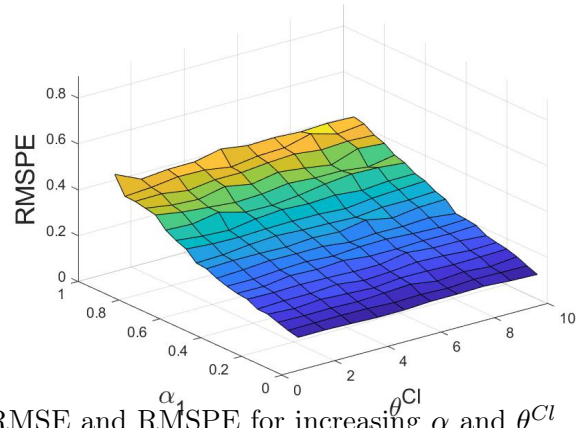
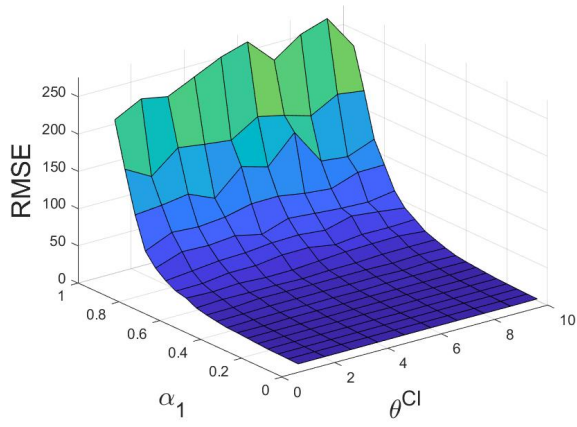
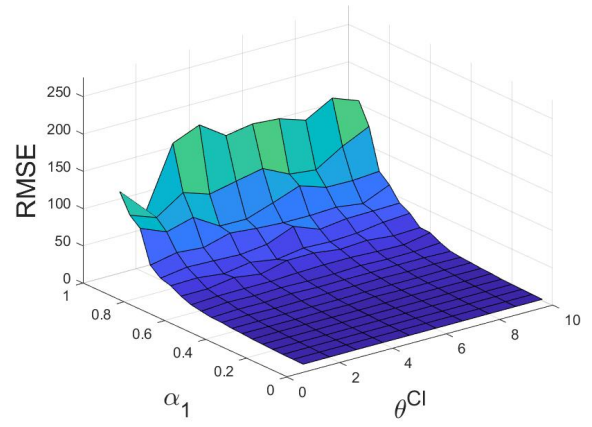


Figure 31: Surface plots of the evaluation metrics RMSE and RMSPE for increasing α and θ^{Cl} and with ϕ and θ set to 0.3.

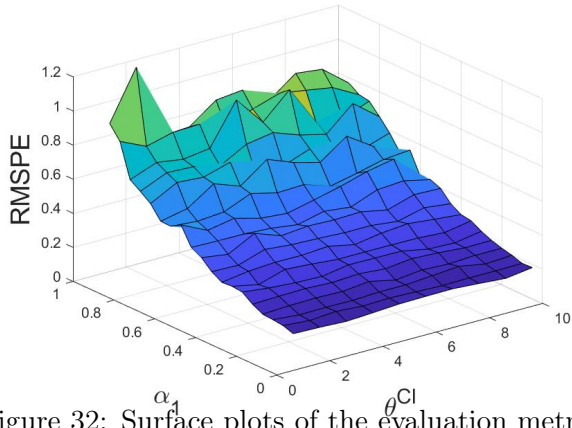
(a) RMSE - POT



(b) RMSE - BM (2)



(c) RMSPE - POT



(d) RMSPE - BM (2)

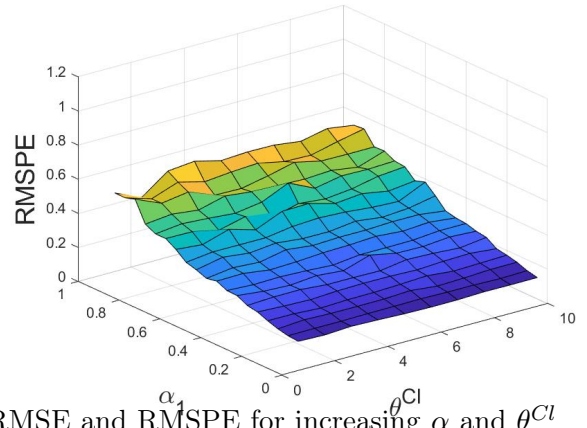
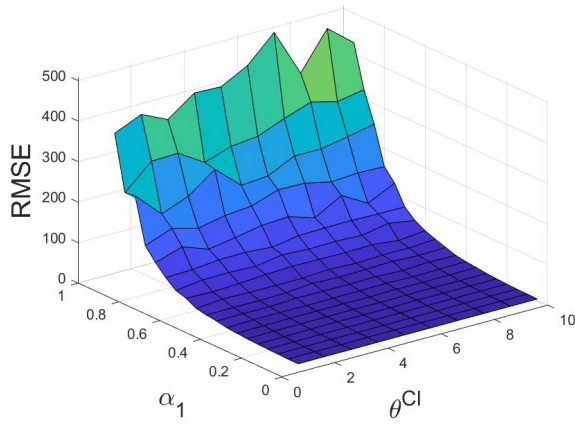
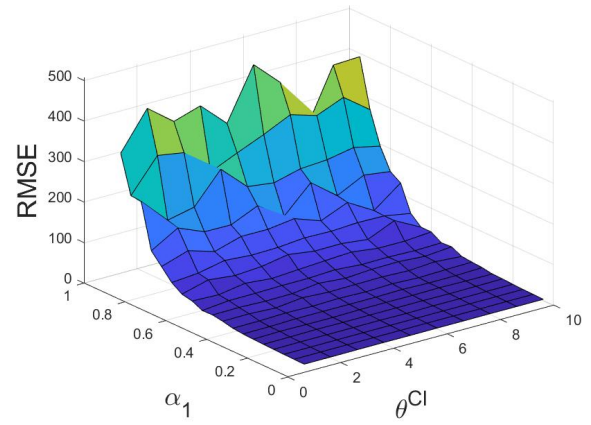


Figure 32: Surface plots of the evaluation metrics RMSE and RMSPE for increasing α and θ^{Cl} and with ϕ and θ set to 0.7.

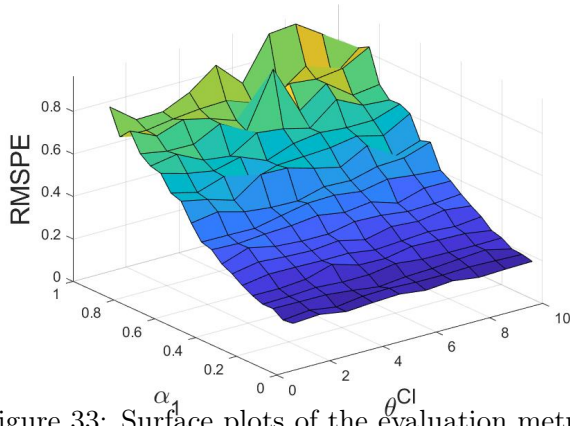
(a) RMSE - POT



(b) RMSE - BM (2)



(c) RMSPE - POT



(d) RMSPE - BM (2)

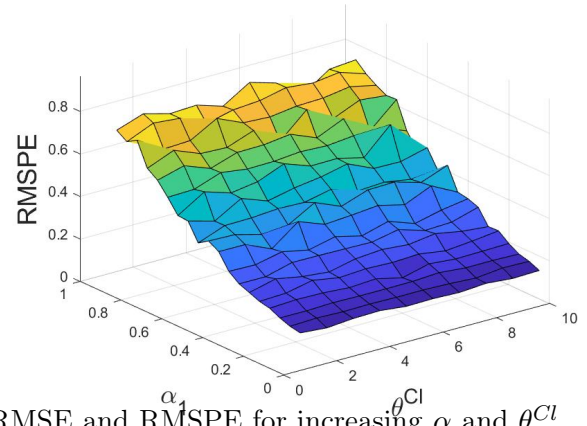


Figure 33: Surface plots of the evaluation metrics RMSE and RMSPE for increasing α and θ^{Cl} and with ϕ and θ set to 0.9.

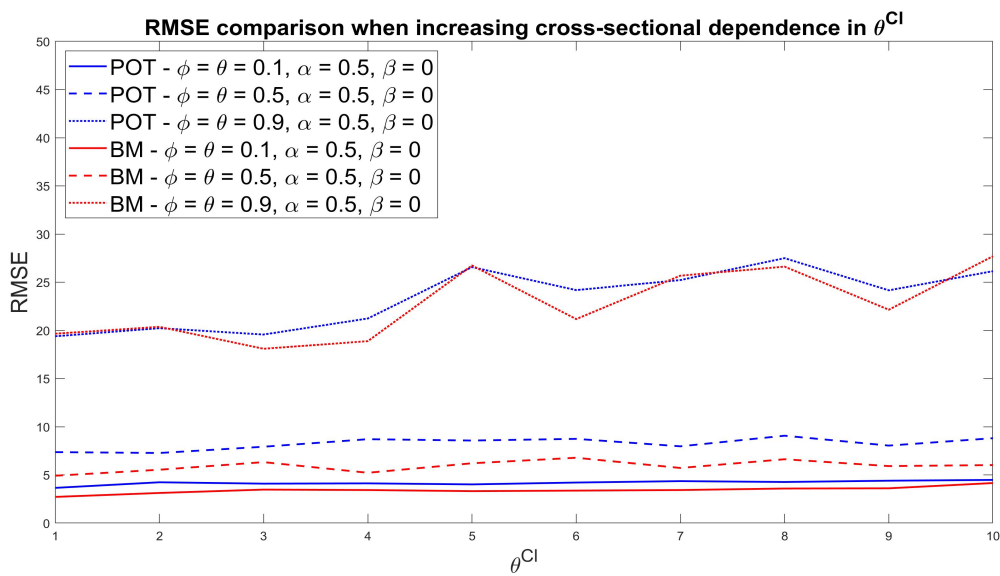


Figure 34: Comparison of the RMSE for increasing θ^{Cl} at three levels of serial dependence and $\alpha = 0.5$ and $\beta = 0$.